



## Workshop Proceedings

**French Argentinean Workshop on Heterogeneous Catalysis**  
**Santa Fe-Argentina, 11-13 April 2023**

Organized by the Instituto de Investigaciones en Catálisis y Petroquímica, “Ing. José Miguel Parera” (INCAPE, CONICET - UNL), within the framework of an international cooperation project between the groups led by Dr. Florence Epron (Institut de Chimie des Milieux et Matériaux de Poitiers, IC2MP, France) and Dr. Carlos Pieck (INCAPE, Argentina): “International Research Project, OLECAT: Catalyseurs pour la production d’olefines”.

The French-Argentinean Workshop on Heterogeneous Catalysis was declared of interest by:

The Province of Santa Fe by Decree No. 2379, 14 November 2022.

The Honorable Municipal Council of Santa Fe de la Vera Cruz, Declaration No. 5040 on 18 August, 2022.

The Chamber of Deputies of the province of Santa Fe in the Session Room on 24 November, 2022.

Of institutional interest by: the Board of Directors of the Faculty of Chemical Engineering (Resolution CD No. 423, 23 August, 2022) and of the National University of Litoral (Resolution No. 5601, 9 September, 2022).

## Organizing Committee

**Chair:** Carlos L. Pieck  
**Vice Chair:** Cristina Padró  
Sonia Bocanegra  
Silvana A. D'Ippolito  
Florence Epron  
F. Albana Marchesini  
Vanina A. Mazzieri  
M. Amparo Sánchez  
M. Ana Vicerich

## Collaborators

Adriana Ballarini  
Viviana Benitez  
Paula Brussino  
Catherine Especel  
Cristhian Fonseca

## FAWHC Proceedings editors

Silvana A. D'Ippolito  
Ramiro Olivencia

## Scientific Committee

**Chair:** Florence Epron  
Sonia Bocanegra  
Silvana A. D'Ippolito  
Catherine Especel  
F. Albana Marchesini  
Claudia Neyertz  
Cristina Padró  
Carlos L. Pieck  
M. Soledad Zanuttini

## Sponsors



**Agencia I+D+i**

Agencia Nacional de Promoción  
de la Investigación, el Desarrollo  
Tecnológico y la Innovación



**Santa Fe**  
Provincia

 **JERÁRQUICOS**



**Santa Fe**  
Capital



Diputada provincial de Santa Fe Dra. Erica Hynes  
Concejal CPN Hugo Marcucci

## Topics

**Catalyst Poisoning and Deactivation: CP**

**Catalytic Technologies for Fossil Fuels: CT**

**Catalyst Synthesis and Characterization: CS**

**Electrocatalysis and Photocatalysis: EP**

**Activation of Small Molecules (N<sub>2</sub>, CO<sub>2</sub>, CH<sub>4</sub> and others): AS**

**Environmental Catalysis: EN**

**Engineering and Catalytic Processes: EC**

**Biomass Conversion to Chemicals, Hydrogen, Syngas and Fuels: BC**

## Table of contents

### Plenary Conference

**Last advances on aromatic synthesis over zeolites**

Yannick Pouilloux

**How has research in catalysis evolved in Argentina? From the fifties to our days.**

Ulises Sedran

## Keynotes Lectures

**Oxidation reactions: from powder to structured catalysts**

Eduardo Miró

**Tuning catalytic performance by modulating the surface composition and structure**

Adrián Bonivardi

**Study by isotopic exchange of the activation of small molecules and diffusion of active species on catalytic Surface**

Nicolas Bion

**Perspectives of the production of hydrogen and its derivatives in Argentina: associated CO<sub>2</sub> emissions**

Daniel Borio

**Surface redox reactions for tuning the surface composition of bimetallic nanoparticles and their catalytic properties: the contribution of Poitiers catalysis laboratory.**

Catherine Espezel, Gwendoline Lafaye and Florence Epron

**Development of a virtual fuel testing platform**

Norberto Nigro

**Enhancing Solar Energy Conversion to H<sub>2</sub> through Photoelectrochemical Microscopy**

Dodzi Zigah

**Details of the Textural Characterization of Nanoporous Solids by Gas Adsorption**

Karim Sapag

**Zeolite-Templated Carbons: The Key Role of Zeolite Acidity**  
Thibaud Aumond, Isabelle Batonneau-Gener, Yannick Pouilloux, Annaig Le Person, Hervé Vezin, Alain Moissette and Alexander Sachse

**Second generation biofuels: glycerine esterification with fatty acids: homogeneous and heterogeneous catalyst**  
Carlos Querini

**Catalytic deoxygenation as key reactions in biomass-based chemicals production**  
Cristina Padró

**Progress on heterogeneous catalytic wet air oxidation catalysts for treatment of industrial wastewaters**  
Gwendoline Lafaye

## **Work Submitted**

---

**CP-1: Bifunctional catalysts for selective opening of decalin: thiotorance and regeneration**

Silvana A. D'Ippolito, Santiago M. Rosas, Catherine Especel, Florence Epron, María A. Vicerich, Viviana M. Benitez and Carlos L. Pieck

**CT-2: Investigation of the nickel amount on a silica-alumina support for ethylene production**

Paula Brussino, María A. Ulla and Juan P. Bortolozzi

**CS-3: Synthesis of Ni-NPs impregnated on SiO<sub>2</sub> and Ti-SiO<sub>2</sub> for the selective reduction of glycerol**  
Fernando Tuler, Raúl Comelli, Ángel Berenguer-Murcia and Diego Cazorla-Amoros

**CS-4: Cobalt oxide-based catalysts supported on zirconia fibers synthesized by Atomic Layer Deposition**  
María M. Fontanini, Sabrina A. Leonardi, Eduardo E. Miró, Juan P. Bortolozzi and Viviana G. Milt

**EN-5: Catalytic ceramic paper for soot removal**  
Sabrina A. Leonardi, Eduardo E. Miró and Viviana G. Milt

**EN-6: Reuse of eggshells for the synthesis of catalysts used in the oxidation of unburned hydrocarbons**  
M. de los Milagros Deharbe, Ramiro Serra and Alicia Boix

**EN-7: Eggshell catalysts supported on monolithic structures used in the oxidation of toluene**  
M. de los Milagros Deharbe, Alicia Boix and Ramiro Serra

**EN-8: Catalytic 3D-printed systems based on clays for oxidation reactions**  
Natalia L. Courtalón, Ezequiel D. Banús and Juan P. Bortolozzi

**AS-9: In-situ DRIFTS investigations applied to the catalytic hydrogenation and reforming processes**  
Misael Cordoba, Lina García, Juan Badano, Carolina Betti, Mónica Quiroga and Cecilia Lederhos

**EC-10: Synthesis of sulfated zirconia to obtain triethyl citrate**  
Federico L. Aguzín, Yanina M. Acuña, Cristina L. Padró and Nora B. Okulik

**EN-11: Phenol CWPO over Cu and CuFe-based structured catalysts**

Paula Brussino, María A. Ulla and Ezequiel D. Banús

**BC-12: Sorption enhanced ethanol steam reforming with K promoted Mg/Al hydrotalcites as sorbent material. The effect of Mg/Al ratio on CO<sub>2</sub> sorption capacity**

J. Fals, M. Park, R. Avendaño, S. Bocanegra, N. Amadeo and M. Laura Dieuzeide

**EN-13: Recycling of spent Ion-Li batteries: low-temperature dry reforming of methane application**

Franco I. Dubois, Florencia Volpe Giangiordano and Andrés M. Peluso

**BC-14: Catalytic Gasification of Biomass Residues at Bench Scale: Effect of reforming with recycle catalysts and Gasifying Agents**

Lina Garcia, Misael Cordoba, Liza Dosso, Carlos R. Vera, Mariana Busto and Juan M. Badano

**BC-15: Glycerol as raw material to a biorefinery**

Ezequiel H. Promancio, Leonardo A. Gusé, Fernando E. Tuler, Lisandro R. Ferrari, Diego J. García Touza, Carlos M.J. Casas and Raúl A. Comelli

**EP-16: Zinc Oxide recovered from spent alkaline batteries as photocatalyst for emergent contaminant degradation**

Maria Gallegos, Franco Dubois, Laura Damonte, Paula Caregnato and Paula I. Villabrille

**BC-17: Catalytic fast pyrolysis of tomato plants residual biomass**

Jose L. Buitrago, Juan J. Musci, Hernan Bideberripe, Mónica L. Casella, Luis R. Pizzio and Ileana D. Lick

**BC-23: 5-Hydroximethylfurfural production from fructose/Isopropanol mixture with sulfonic resins as catalysts in a continuous flow reactor**

Gabriel Pestana, Lucila Pierantoni and Javier M. Grau

**BC-24: Effect of support acidity and pore size in the synthesis of 2,5-Dimethylfuran in Pd supported over Y and L zeolites**

Gabriel Pestana, Lucila Pierantoni and Javier M. Grau

**BC-25: Valorization of glycerol by esterification reactions**

Bruno Dalla Costa, Hernán Decolatti, Maira Maquirriain, María Laura Pisarello, Lucas Tonutti and Carlos Querini

**CS-26: Synthesis and characterization of mesoporous materials with acid properties**

Lourdes Vergara, Gustavo Mendow, Carlos Querini and Bárbara Sánchez

**BC-28: Effect of ethylene glycol functionalization on a CeO<sub>2</sub>-SiO<sub>2</sub> support for Ni catalysts applied in the ethanol steam reforming**

Marcela Jaramillo-Baquero, John F. Múnera and Laura M. Cornaglia

**EC-29: Comparison of batch and continuous operating mode of the reactor for C-O hydrogenolysis of erythritol on Ir-Re catalysts**

Emanuel Virgilio, Ludmila Chorvat, Cristina L. Padró and Maria E. Sad

**EN-31: Synthesis and modification of MgO-based sorbents for the CO<sub>2</sub> capture during the water gas shift reaction at intermediates temperaturas**

Carlos F. Imbachi-Gamba, Laura Cornaglia and John Múnera

**BC-32: Gasification of cannabis waste**

Paula Saires, Melisa Bertero and Ulises Sedran

**EC-33: Oxidative dehydrogenation of propane for production of propylene using VO<sub>x</sub>/Al<sub>2</sub>O<sub>3</sub> catalysts**

Francisco J. Passamonti, Silvana A. D'Ippolito, Catherine Especel, Florence Epron, Carlos L. Pieck and Viviana M. Benitez

**BC-34: Co-processing of sugarcane bagasse pyrolytic tar and vacuum gas oil under FCC conditions**

Leandro E. Dietta, Mariana Rodriguez, Juan Rafael García, Marisa Falco and Ulises Sedran

**EN-35: Study of the sorption properties of a Li<sub>4</sub>SiO<sub>4</sub>-based sorbent in the presence of water and low CO<sub>2</sub> concentration**

Diana Peltzer, Betina Faroldi, John Múnera and Laura Cornaglia

**EP-36: Preparation of Pt-based electrocatalysts supported on hydrothermal rice husk for direct ethanol fuel cell**

María F. Azcoaga Chort, Sergio R. de Miguel, Virginia I. Rodríguez and Natalia S. Veizaga

**EN-37: CsxCu/Na-MOR coating on monoliths for co-adsorption of hydrocarbons mixture and selective catalytic reduction of NO<sub>x</sub>**

Inés Tiscornia, Leticia Gómez, Ramiro Serra, Milagros Deharbe and Alicia Boix

**BC-38: Biomass Catalytic Valorization: bio-fuel C15 molecules synthesis by hydrodeoxygenation and condensation reactions of furfural**

M. Soledad Zanuttini, Claudia Neyertz, Lucas Tonutti, Cristián Ferretti and Carlos Querini

**CS-39: Selective Hydrogenation of Fame to fatty alcohols on Ru-Sn-B/Al<sub>2</sub>O<sub>3</sub> and Rh-Sn-B/Al<sub>2</sub>O<sub>3</sub> catalysts**

Cristhian Fonseca Benitez, María Ana Vicerich, María Amparo Sánchez, Francisco J. Passamonti, Carlos L. Pieck and Vanina A. Mazzieri

**BC-40: Structured catalysts for valorization of biogas to syngas**

Francesca Bagioni, Silvia Maina, Patricia Benito, Sonia Bocanegra and Adriana Ballarini

**CT-41: Direct dehydrogenation of n-butane to n-butenes on Pt-based bimetallic catalysts supported on carbon nanotubes and vulcan carbon. Study of the promoting effect of Sn and In**

Gustavo Ramos Montero, Adriana Ballarini, Sergio de Miguel, Sonia Bocanegra and Patricia Zgolicz

**BC-42: Effect of reduction temperature on ruthenium catalysts supported on biochars from rice husk for the hydrogenation reaction of levulinic acid to γ-valerolactone**

Virginia Rodríguez, Gustavo Mendow, Bárbara Sánchez, M. Florencia Azcoaga Chort, Juan Rafael García, Richard Pujro, Sergio de Miguel and Natalia Veizaga

**BC-43: Wheat bran biorefinery. Fractionation, characterization and catalytic dehydration**

Lucas E. Retamar, Federico Piovano, Alicia V. Boix, Soledad G. Aspromonte

**CS-44: Synthesis and characterization of bimetallic catalysts for COPrOx reaction**

Leticia E. Gómez and Alicia V. Boix

**CS-45: Facile preparation of Co and Ce oxide nanoparticles by an aerosol method and their catalytic evaluation for diesel soot abatement**

María L. Godoy, Ezequiel D. Banús, Eduardo E. Miró and Viviana G. Milt

**CS-46: Zirconia-based catalysts synthesized with template-assisted sol-gel method for hydrothermal conversion of sugars**

Federico A. Piovano, Soledad G. Aspromonte and Alicia V. Boix

**EN-47: Catalytic performance of structured substrates based on synthesized Co,Ce oxide nanoparticles for particulate matter combustión**

María L. Godoy, Eduardo E. Miró, Viviana G. Milt and Ezequiel D. Banús

**CS-48: Nanostructured mixed oxide growth on alpaca and their application as microreactors for the CO oxidation**

Mayra A. Franco, Ana P. Cabello, María A. Ulla and Juan M. Zamaro

**BC-49: Catalytic transformation of biomass-derived butanol into light olefins**

Cristhian A. Fonseca and Pablo J. Luggren

**CS-50: Synthesis and characterization of Zn-modified MnCO<sub>3</sub> catalysts for application in aromatic alcohol oxidation**

Pablo J. Luggren, Juan Zelin, Hernán A. Duarte, Maria E. Sad, Verónica K. Díez and J. Isabel Di Cosimo

**BC-51: Co-processing of gas oil and pyrolysis bio-oil in the FCC process. Hydrogen transfer reactions**

Richard Pujro, Melisa Bertero, Marisa Falco and Ulises Sedran

**CS-52: Catalytic n-paraffin's dehydrogenation with metallic (Pt, PtSn, PtSnIn, PtSnGa) structured catalysts based on γ-Al<sub>2</sub>O<sub>3</sub>, MgAl<sub>2</sub>O<sub>4</sub> and ZnAl<sub>2</sub>O<sub>4</sub>**

Adriana D. Ballarini, Patricia Zgolicz, Sergio R. de Miguel and Sonia A. Bocanegra

**CS-53: Synthesis and characterization of nano-silica from rice husk ash using an alkaline method extraction process**

Carlos A. López Vargas, Laura M. Cornaglia and Betina M. Faroldi

**EN-54: Eco-friendly chitosan/alginate/carbonate adsorbent for copper and lead removal in wáter**

Jhonnys D. Guerrero and Laura B. Gutierrez

**CT-55: Development of catalysts for production of light olefins from methanol**

Francisco J. Passamonti, Viviana M. Benitez, Catherine Especel, Florence Epron, Carlos L. Pieck, Silvana A. D' Ippolito

**EN-56: Ce-based biomorphic fibers for the oxidation of soot and VOCs**

Maximiliano Rodriguez, Viviana G. Milt, Eduardo E. Miró and Eric M. Gaigneaux

**BC-57: Production of diesel-type biofuel by conversion of γ-valerolactone over noble metal-based bifunctional catalysts**

Karla G. Martínez Figueredo, Darío J. Segobia and Nicolás M. Bertero

**EC-58: Synthesis of amines from nitrile hydrogenation on Co/SiO<sub>2</sub>: Effect of the substrate structure**

Milton Agüero, Darío J. Segobia and Andrés Trasarti

**EN-59: Investigating the Impact of Preparation Method on the Nitrate Reduction and N<sub>2</sub> Selectivity of Alumina-Supported Pd,In Catalysts**

Fernanda Miranda Zoppas, Nicolás Sacco, Alejandra Devard, and F. Albana Marchesini

**EN-60: Phenol removal from water by advanced oxidation process with Cu-based catalysts**

Nicolás Sacco, Sofía Bidal, Alejandra Devard, Fernanda Zoppas and F. Albana Marchesini

**BC-61: Selective production of 1,2-propanediol by glycerol hydrogenolysis using Cu/Zn/MgAl as catalysts**

Matías G. Rinaudo, Naila Gómez González, María K. López, Luis E. Cadus, José López Nieto, Marcelo E. Domíne and María R. Morales

**BC-62: Cu/carbon xerogel catalysts for glycerol selective oxidation reaction**

Naila Gómez González, Samantha L. Flores, Ana Arenillas, Matías G. Rinaudo, Luis E. Cadus and María R. Morales

**EP-63: Oxidation advanced processes for dairy phage inactivation**

María F. Jacob, Mariángel Briggiler Marcó, Orlando M. Alfano, Andrea del Luján Quibroni and María de los Milagros Ballari

**EP-64: Kinetic Modeling of the Degradation of Water**

**Pollutants in a Photocatalytic Microreactor**

María L. Satuf, Ana L. Eusebi, Claudio L.A. Berli and Marcela V. Martin

---

**Plenary conference**

**Last advances on aromatic synthesis over zeolites**

Dr. Yannick Pouilloux

Alkylbenzenes are an important segment of the petrochemical industry for the manufacture of widely used commodities and specialty products. For decades, numerous zeolite catalysts have been synthesized, characterized and evaluated for the preparation of aromatic hydrocarbons. In particular, BTXs can be prepared by various reactions and have many applications in the chemical industry. These include the aromatization of methane, ethylene, ethane and propane, the transformation of alcohols. They can also be prepared from biomass. All these reactions are carried out on different acid catalysts based on zeolite modified or not with metals. Over the last decade, significant progress has been made in the synthesis and structure determination of new zeolites, mesoporous single crystals, hierarchical zeolites and two-dimensional zeolites. These developments have led to a better understanding of the role of zeolites (effects of structure type, morphology, acid sites, acid site accessibility, shape-selectivity factors) in the preparation of aromatic compounds. During the presentation, different examples of reactions will be given and the influence of the type of acid sites, zeolite topology and reaction conditions on the activity, selectivity and routes of these reactions will be highlighted.

**Dr. Yannick Pouilloux**

**IC2MP - Institut de Chimie des Milieux et Matériaux de Poitiers**

In 1991 he obtained PhD degree in chemistry at the University of Poitiers and then Post Doctoral at the URA CNRS 350, Poitiers - ATOCHEM, CRRA Pierre Bénite (1992). He served as director of Chemistry Department, University of Poitiers (2007-2010) and as director of Master "Analytical Chemistry and Process Quality" (2002-2007). Responsible of Master Chemistry and applications (2008-2018). From 2004 he is University Professor, section 31 CNU, University of Poitiers. Teaching: courses "Kinetics and Catalysis of Heterogeneous Chemistry" and "chromatography" in Master 1 and "Catalysis and Green Chemistry" in Master 2.

He is the director of Institut de Chimie, des Milieux et Matériaux de Poitiers, UMR 7285 CNRS since 2018. He is Member elected to Scientific Council of the University of Poitiers and to Faculty of Sciences Council of the University of Poitiers.

Main research interests: sustainable chemistry and heterogeneous catalysis. Developments of new porous materials such as zeolites and mesoporous solids used in the transformation of organic compounds ( $\text{CO}_2$ , ethylene, glycerol and fatty esters). Development of model reaction to characterize catalytic materials.

#### **How has research in catalysis evolved in Argentina? From the fifties to our days**

**Dr. Ulises Sedran**

The visible roots of research in catalysis in our country can be traced to the mid-fifties. Afterwards, a steady road, however winding, has been outlined by researchers at universities and, particularly

from the seventies onwards, by researchers at CONICET, based on the institution's double-dependency-institute creation policy. Although research in catalysis in our country can be regarded as the applied type of research, fundamental studies are also performed. Given that funding has been granted from state sources mainly, the development of the area has been severely conditioned by both economic and political factors. However, some examples of cooperation with private companies are worth to be mentioned. In recent years, the number of projects associated to the valorization of residual biomass has increased significantly and the discovery of large new sources of oil and gas has opened the door to new opportunities.

**Dr. Ulises Sedran**

**INCAPE - Instituto de Investigaciones en Catálisis y Petroquímica**

Dr. Ulises Sedran graduated as a Chemical Engineer (1980) and got his Ph.D. degree at National University of Littoral (1985), Argentina. He was a postdoctoral fellow and became a Professor at the University of Western Ontario, Canadá (1989-1991).

He was the Director of Scientific Technological Center CONICET Santa Fe (2016-2020) and presently he is the Director of the Institute of Research on Catalysis and Petrochemistry at Santa Fe, Argentina, since 2013. He is the head of a research group devoted to refining processes, particularly the catalytic cracking of hydrocarbons FCC, the evaluation of commercial catalysts and feedstocks, the environmental impact of processes and products, and the use of nonconventional resources in refining (waste plastics,

biomass, shale and heavy oils). Since 1987 he is a Researcher at CONICET, now with the position of Superior Researcher.

He is a Full Professor at National University of Littoral in the area of Chemical Reaction Engineering. He teaches courses at the graduate and postgraduate levels. He is the advisor of doctorate students and cooperates with companies in the oil refining and petrochemical areas.

## **Keynotes Lectures**

---

### **Oxidation reactions: from powder to structured catalysts**

**Dr. Eduardo Miró**

The benefits of using structured catalysts in oxidation reactions, both for environmental and uses, are discussed in terms of kinetics and characterization studies. Monoliths, fibers, and microreactors applications are described for pollutants deep oxidation reactions and for oxidative dehydrogenation reactions and industrial uses.

### **Tuning catalytic performance by modulating the surface composition and structure**

**Dr. Adrián Bonivardi**

A deep understanding of a reaction mechanism is a must for the rational design of catalysts in order to improve their catalytic performance. The use of *in situ* and *operando* IR measurements combined with calculation based on density functional theory is crucial to reach that goal. Two examples are presented: (i) Synthesis of methanol from CO<sub>2</sub> on palladium-based catalysts. The

hydrogenation of CO<sub>2</sub> to methanol over PdGa alloy supported catalysts is compared to a bench top Cu-ZnO catalyst; and (ii) Steam reforming of ethanol for H<sub>2</sub> production by non-noble metal. Two alternatives were tested to achieve this improvement: by doping ceria with gallium and by controlling the support shape.

### **Study by isotopic exchange of the activation of small molecules and diffusion of active species on catalytic surface**

**Dr. Nicolas Bion**

The utilization of isotopic tracers is very efficient to develop mechanistic insights into heterogeneous catalysis and implement strategies for the development of active and selective catalysts. Kinetic Isotopic effect (KIE), Steady State Isotopic Transient Kinetic Analysis (SSITKA), Temporal Analysis of Product (TAP) are among the most powerful techniques which contributed to improve the understanding of crucial catalytic reactions for industry like ammonia synthesis, selective catalytic reduction of NO<sub>x</sub>, methane steam reforming. The technique of isotopic exchange to study the interactions between gas phase labeled molecules and solid catalysts is also particularly interesting to investigate the activation and diffusion of active species on the surface and in the bulk of the catalytic material. In such studies, two general reaction types have been investigated: (i) homomolecular exchange in which a mixture of labeled molecules is scrambled over a surface, and (ii) heterolytic exchange in which a labeled molecule is scrambled with the lattice atoms of the catalyst. In the talk, some illustrations of the role of oxygen mobility for total oxidation reaction (specifically CH<sub>4</sub> combustion) will be given on simple and mixed oxides. The activity of simple oxides is often linked to the presence of M<sup>n+</sup>/M<sup>(n+1)+</sup> ion pairs associated with oxygen vacancies. M<sub>1</sub>M<sub>2</sub>O<sub>x</sub> mixed oxides

generally have superior performance due to the presence of highly active  $M1^{n+}/M2^{(n+1)+}$  ion pairs. In some mixed oxides, the metal M1, non-reducible and inactive in itself, is able to induce a partial reduction of M2: the active site is the  $M2^{n+}/M2^{(n+1)+}$  ion pair stabilized by the presence of M1. The perovskites  $\text{LaMnO}_3$  and  $\text{LaCoO}_3$  are outstanding examples of this class of materials. The behavior of yttria-stabilised zirconia (YSZ) mixed oxide is specific by the absence of reducible elements and the intrinsic existence of oxygen vacancies due to the partial substitution of  $\text{Y}^{3+}$  for  $\text{Zr}^{4+}$ . The association of perovskite and YSZ oxides may have a beneficial impact on methane conversion via catalytic partial oxidation and combustion reactions. Relationships will be established with the behavior of Solid Oxide Cells composed of perovskite-based electrode and YSZ electrolyte. Another illustration will be the investigation of  $\text{N}_2$  activation and lattice N mobility on nitride catalysts for ammonia synthesis at low pressure and temperature. In this collaborative work with Hargreaves' group in Glasgow we have established that  $^{15}\text{N}/^{14}\text{N}$  exchange pathways involving reaction of lattice nitrogen within ternary interstitial nitride like  $\text{Co}_3\text{Mo}_3\text{N}$ ,  $\text{Ni}_2\text{Mo}_3\text{N}$  occurred. On this basis, the proposal can be made that ammonia synthesis over this material involves the Mars-van Krevelen mechanism in which it is the lattice N itself which is hydrogenated to yield  $\text{NH}_3$  with the transient vacancy being replenished by  $\text{N}_2$  from the gas-phase. Electride-like intermetallic phases initially developed to store hydrogen in the form of hydrides (type  $\text{LaScSi}$ ) combined with Ru are also studied for ammonia synthesis. As demonstrated by  $^{15}\text{N}_2/^{14}\text{N}_2$  homomolecular exchange reactions, these materials have the ability to enrich the electron density of ruthenium (Ru) nanoparticles deposited on their surface to promote the cleavage of  $\text{N}_2$  bond and thus overcome the limiting step of this reaction. The hydrogen, also dissociatively activated on

the ruthenium, migrates into the interstitial sites of the intermetallic phase and releases the surface for the activation of the  $\text{N}_2$ , thus avoiding any poisoning phenomenon.

### **Perspectives of the production of hydrogen and its derivatives in Argentina: associated $\text{CO}_2$ emissions**

**Dr. Daniel Borio**

During the last decades, the global demand of  $\text{H}_2$  has grown steadily. Around 70 MM ton  $\text{H}_2/\text{yr}$  are produced around the world as pure  $\text{H}_2$  and used mainly in petroleum refining and ammonia synthesis (fertilizers). Other 45 MM ton  $\text{H}_2/\text{yr}$  come mixed with other gases ( $\text{CO}$ ,  $\text{CO}_2$ ). More than 4 MM ton  $\text{H}_2$  are produced annually in Latin America, mostly from natural gas ( $\text{CH}_4$ ), and used in oil refining, synthesis of ammonia and methanol and Direct Reduction of Iron Oxides (DRI). Some of these processes include (partial) Carbon Capture and Utilization (CCU), particularly the  $\text{NH}_3/\text{urea}$  plants. An important point is the share of Latin America in the global  $\text{CO}_2$  emissions. The contribution of each Latin American country to the global carbon emissions is low or very low. For example, the share of Argentina in the global  $\text{CO}_2$  emissions is between 0.6 to 0.9%. Within it, industry contributes only around 15%. The production of  $\text{H}_2$  from natural gas, in the context of Vaca Muerta and other non-conventional gas resources, is analyzed. Carbon capture, storage and utilization (CCSU) is discussed. The Carbon Intensity (CI) of different technologies for the production of blue  $\text{H}_2$  is compared. The perspectives of green  $\text{H}_2$  in Argentina are also discussed, focused on production costs and regulatory aspects. The

production of NH<sub>3</sub> and some derivatives is analyzed, together with the trade balance of nitrogenous fertilizers within the period 2010-19. In the near future, Argentina should produce additional amounts of NH<sub>3</sub>, to be used both as raw material for the production of fertilizers (substitution of imports) and as carrier for H<sub>2</sub> exports. This would reduce the frequent shortage of dollars in our economy as well as generate added value and local jobs. Liquefied NH<sub>3</sub> appears as an effective option to export H<sub>2</sub> with higher energy density. The local chemical industry should therefore react to this opportunity in the global market by developing improved decarbonization strategies. The new technologies for H<sub>2</sub> production from natural gas (e.g. ATR), with much lower Carbon Intensity, make it possible to think of a steady growth in the production of blue H<sub>2</sub> in the coming decades. The expected increase in the production of green H<sub>2</sub> could contribute to the valorization of captured CO<sub>2</sub>, by using it to produce synthetic fuels or chemicals (Power to X).

### **Surface redox reactions for tuning the surface composition of bimetallic nanoparticles and their catalytic properties: the contribution of Poitiers catalysis laboratory.**

**Dr. Catherine Especel**

Bimetallic catalysts have emerged as an important class of heterogeneous catalysts since they have played a significant role in petroleum refineries, especially in enhancing the octane number of gasoline. After this discovery, a number of bimetallic catalysts have been reported for a range of reactions including oxidation, hydrogenation, hydrogenolysis, and reforming reactions. The

properties of bimetallic catalysts are significantly different from their monometallic analogues. Indeed, the modification of a monometallic catalyst by the addition of a second metal is an important approach for tailoring the electronic and geometric structures of the nanoparticles to enhance their catalytic activity and selectivity. In many cases, bimetallic nanoparticles have higher catalytic efficiencies than their monometallic counterparts, owing to strong synergy between the metals. Nowadays, many research activities are devoted to the development of new bimetallic catalysts, because of the tremendous demand for high-performance catalysts for various practical applications. Because of the presence of a second metal component, the complexity in preparing these materials increases, and in many cases, it is the method of preparation which determines the final structure, and hence properties, of these materials. This presentation will highlight the preparation methods of supported bimetallic systems by the surface redox reactions developed in our research group since the 1990s. The preparation of bimetallic M1-M2 catalysts by surface redox reactions occurs at the surface of the monometallic M1 nanoparticles and an oxidized form of the M2 modifier and is governed by the electrochemical potential of the species implied in the reaction. This process can be direct (direct redox reaction or galvanic replacement) or may involve an intermediate reducing agent activated at the surface of M1, as H<sub>2</sub>, for reducing the oxidized form of the M2 modifier (refilling or catalytic reduction). Two examples of bimetallic systems will be described: 1) Co-Re/TiO<sub>2</sub> catalysts prepared by direct redox reaction for the selective hydrogenation of citral towards unsaturated alcohols, 2) Pd-Re/TiO<sub>2</sub> catalysts prepared by catalytic reduction for the transformation of succinic acid towards butanediol. For more

than thirty years, the Poitiers catalysis laboratory has been studying the preparation of supported bimetallic catalysts by surface redox reactions, largely contributing to offering high-performance bimetallic formulations for applications in the fields of biomass valorization, energy and environment.

### **Development of a virtual fuel testing platform**

**Dr. Norberto Nigro**

The importance of the efficient use of fuels in general applications and particularly in automotive transport is well known. Its impact in geopolitical and environmental terms is undeniable, motivating studies to focus on improving consumption and a significant reduction in emissions, always maintaining the performance of the engine that uses it. To date, most of the published studies analyze a fuel through laboratory tests using only the fuel. In the case of gasoline, these are qualified based on their antiknock power measured in terms of RON and MON. In the case of Diesel cycle engines, one of the required tests is that of the cetane number, which estimates the ignition delay of the fuel by compression. Other thermophysical parameters that are measured are calorific value, density, viscosity, surface tension, among others. Although all these indicators have made it possible to design the engines we use today, we believe that with modern calculation techniques it is possible to predict in advance how that fuel will behave when applied to a real engine. Our development is aimed precisely at being able to simulate this behavior but on a virtual engine, a mathematical and computational model that predicts the engine curves as if they were

tested on a test bench. The engine model takes into account the non-stationary 3D character of the problem, solving the gas flow from its entry into the combustion chamber through the intake system to its exit through the exhaust system. In particular, combustion is solved using a model that is a hybrid between a simplified chemistry model and a detailed one. For the naphthas on the market, a substitute fuel is characterized for the real fuel mixture, but which performs similarly to the real one in terms of combustion dynamics. Comparative results with market fuels are presented to identify the effectiveness of the developed tool.

### **Enhancing Solar Energy Conversion to H<sub>2</sub> through Photoelectrochemical Microscopy**

**Dr. Dodzi Zigah**

Photoelectrochemical cells use semiconductors to convert solar energy into chemical energy. Effective photoelectrodes must satisfy multiple criteria, such as strong absorption across the solar spectrum, efficient transport of charge carriers, ability to catalyze reactions, and low-cost. Scanning photoelectrochemical microscopy (SPECM) is a technique that allows for the characterization of photoelectrochemical materials at the microscale. It combines local irradiation of the sample with a microelectrode probe for localized electrochemical analysis of the surface. SPECM can provide information about the local photocurrent generated at the sample under irradiation and detect the photoelectrocatalytically generated Oxygen/Hydrogen at the microelectrode. It has been used to study the development of potential photocatalysts, evaluate the electron-

transfer processes involved in photocurrent generation, and screen the photoelectrochemical activities of various materials. The technique can be used to improve the understanding of fundamental processes involved in light-induced water splitting. We will discuss about the use of electrochemical microscopy for the rapid screening of different materials and for studying intermediate species adsorbed at the surface of photoelectrodes during the water oxidation reaction. The technique allows for quick analysis and characterization of materials and enables the detection and quantification of intermediate species that play a crucial role in the electrocatalytic process. By using photoelectrochemical microscopy, we obtained a better understanding of the mechanism and kinetics of the electrochemical reactions and optimized the performance of the materials for energy conversion applications. The semiconductor material studied is TiO<sub>2</sub>, was prepared by anodizing a titanium surface in an ethylene glycol solution in the presence of ammonium fluoride. The anodization process resulted in the formation of TiO<sub>2</sub> nanotubes of varying lengths, which were screened using photoelectrochemical microscopy with a homemade optoelectrode that combined an optical fiber and an optoelectrode. SPECM it is an effective tool for the detection and quantification of adsorbed hydroxyl radicals on a nanostructured TiO<sub>2</sub> substrate electrode. The technique provides valuable information about the saturation coverage and decay kinetics of the adsorbate. Moreover, electrochemical microscopy in combination with a microcapillary and an ultramicroelectrode has been used to generate arrays of TiO<sub>2</sub> with different properties, and combined with an optical fiber-ultramicroelectrode (OF-UME) allows for rapid mapping of TiO<sub>2</sub> array properties on a single surface. In addition, the new approach

for fast investigation of the influence of TiO<sub>2</sub> nanotube length, grown on a single titanium electrode, is an efficient method for tuning the length of the nanotubes and determining the optimal length for photoelectrochemical application. A new approach is presented for growing aligned TiO<sub>2</sub> nanotubes on a single electrode with the length of the nanotubes. The photocurrent measurements obtained using scanning photoelectrochemical microscopy (SPECM) indicated a maximum photocurrent for nanotubes with a length of 4300 nm. The study also shows that the surface interrogation mode of scanning electrochemical microscopy (SI-SECM) is useful in characterizing photoelectrochemical reactions on semiconductors, providing a new method for the extraction of quantitative information from the formation and decay of adsorbed species at a representative photocatalyst.

#### **Details of the Textural Characterization of Nanoporous Solids by Gas Adsorption**

**Dr. Karim Sapag**

In the field of Materials Science, materials with pores of the order of nanometers (pores up to 100 nm in size) play an important role due to their various applications, mainly in the field of Energy and the Environment. One of its fundamental characteristics is texture, which refers to its specific surface area, pore volume, and pore size distribution. The most widely used technique to characterize these properties is gas adsorption, particularly nitrogen adsorption at 77K, although other gases such as argon at 87K and carbon dioxide at 273K can be also used. In the study of textural characterization, an

adsorption isotherm is obtained experimentally that deserves special attention, since its shape can be used to obtain enriching information. From the experimental data, models are used and geometries are assumed, which specifically depend on the characteristics of the samples and the analysis regions. Therefore, many studies have been carried out to find out which are the most suitable models/methods for different materials. In this talk, important details of the technique will be highlighted, specifying the experimental aspects to obtain reproducible results and as precise as the experiment allows, highlighting the most accepted and applicable models to various nanoporous materials, following what is proposed by the IUPAC.

### **Zeolite-Templated Carbons: The Key Role of Zeolite Acidity**

**Dr. Alexander Sachse**

Zeolite Tempered Carbons (ZTCs) feature defined micropore topologies, which make them unique components of the extended carbon materials family. ZTCs allow bridging the gap between activated carbons and 2D graphene sheets; coined as 3D microporous graphenes and claimed to be true carbon Schwarzes. Due to their unparalleled properties ZTCs are very promising in a number of fields and especially in the development of energy storage and transformation devices. ZTCs are achieved through the use of carbon precursors, which diffuse and condense in the porosity of a zeolite that acts as sacrificial scaffold. Various parameters of the ZTC synthesis have been studied, such as the nature of the carbon precursor and the zeolite structure. Zeolites are

microporous silicoaluminates, which present conspicuous textural and chemical properties. Acidity is one of the most striking features of zeolites and is a key function exploited in numerous industrial catalytic hydrocarbon transformation processes, in combination with hydrothermal stability and shape selectivity. Surprisingly, rather little has been reported on the real impact on textural and electrical conductive properties that zeolite acidity has on the formation of ZTCs. The ZTCs are presented as electrocatalysts and electrodes in supercapacitors very promising, electrical conductivity should be considered as essential parameter for the identification of high quality ZTCs. Zeolite acidity plays a fundamental role in the achievement of ZTCs with high electrical conductivity.

### **Second generation biofuels: glycerine esterification with fatty acids: homogeneous and heterogeneous catalyst**

**Dr. Carlos Querini**

Second generation biofuels, and products obtained from waste renewable materials are key components towards environmental recovery and protection. The use of glycerine obtained as a by-product in the biodiesel industry, and free fatty acids obtained either in the vegetable oil treatment or in the glycerine purification processes can be used to obtain valuable products, such as glycerides, biodiesel and monoglycerides. In this work the reaction between glycerine and free fatty acids is used to synthesize second generation vegetable oil. The reaction occurs in a biphasic system in the presence of an acid catalyst. Both, liquid and solid acid have been studied. Sulphuric, methanesulfonic, and p-toluensulphonic

acids were used, as well as SBA-15 functionalized with propylsulfonic groups, modifying also the hydrophobicity of the surface. The effects of the free fatty acid/glycerine ratio, temperature, catalyst concentration, and pressure, were addressed. Kinetic parameters were also obtained.

### **Catalytic deoxygenation as key reactions in biomass-based chemicals production**

**Dr. Cristina Padró**

In recent decades, the development of new processes from biomass derivatives has been promoted to replace the traditional synthesis of numerous chemicals that usually involves sources of fossil origin. Substrates that originate from biomass often contain high O/C ratio that must be selectively reduced to yield valuable chemicals or fuels. In this sense, C-O hydrogenolysis and dehydration are key deoxygenation reactions in the conversion of polyols and sugars into platform molecules, since they allow the number of carbon atoms of the starting molecule to be maintained. The aim of this work is the development of heterogeneous catalysts for the selective conversion of polyols. Particularly, the required characteristics of the catalysts to lead the reactions towards the desired products are investigated in two reactions: C-O hydrogenolysis of erythritol (polyol of C4) catalyzed by supported noble metals and dehydration of butanediol on solids with controlled acidity.

### **Progress on heterogeneous catalytic wet air oxidation catalysts for treatment of industrial wastewaters**

**Dr. Gwendoline Lafaye**

Around the world, industrial processes generate a wide variety of wastewaters containing organic pollutants with negative impact for ecosystems. The preservation of the water resource is a major target for the coming decades. Catalytic Wet Air Oxidation (CWAO) is an efficient and promising oxidative pollution removal process that has made many achievements in the research of wastewater treatment. It is known as a green process whose powerfulness is based on the combination of high temperature (130-300°C) and oxygen or air pressure (5-60 bar) together with a catalyst. This latter must be highly active, selective and stable as well as easily recoverable and reusable. Supported noble metal on oxides or carbon materials are the most widely used heterogeneous catalysts since they meet these criteria. The key factor for CWAO process to achieve wider industrial applications is the catalyst. Indeed, for a perennial process, this latter must be ecologically and economically acceptable, that is a catalyst without the presence of noble metals, stable in the CWAO operating conditions, inexpensive and abundant in nature. This is a very challenging task. The advances in the research on wastewater treatment by CWAO process will be summarized in aspect of non-noble metal catalyst development.

## Bifunctional catalysts for selective opening of decalin: thiotolerance and regeneration

Silvana A. D'Ippolito<sup>1</sup>, Santiago M. Rosas<sup>1</sup>, Catherine Espeel<sup>2</sup>, Florence Epron<sup>2</sup>, María A. Vicerich<sup>1</sup>, Viviana M. Benitez<sup>1</sup>, Carlos L. Pieck<sup>1\*</sup>

<sup>1</sup>INCAPE, Colectora Ruta Nac. N° 168 - Paraje El Pozo, Santa Fe 3000 (Argentina),

<sup>2</sup>Institut de Chimie des Milieux et Matériaux de Poitiers (IC2MP), Université de Poitiers, CNRS, 4 rue Michel Brunet, TSA51106, 86073 Poitiers Cedex 9, (France)

\*pieck@fiq.unl.edu.ar

### Introduction

The selective ring opening (SRO) is a viable technology to enhance the light cycle oil (LCO) fraction and thus contribute to meet the growing demand for diesel fuel. LCO products can be hydrogenated and then opened by SRO to obtain linear or mono-branched paraffins leading to an improved cetane index for diesel fuel application. Moreover, the sulphur content of the LCO fractions is about 0.2 wt% to 2 wt% and the industrial fractions must be hydrotreated in a first stage to decrease the S content between 6 ppm to 16 ppm.

In this work, the activity and S-tolerance of monometallic and bimetallic catalysts supported on  $\text{SiO}_2\text{-Al}_2\text{O}_3$  and zeolite HY are studied in the hydroconversion of decalin (model molecule of hydrogenated aromatics of the LCO fraction), as well as the regeneration of the most promising catalysts.

### Materials and Methods

A stainless-steel autoclave reactor was used in the reaction of decalin. The reaction conditions were as follows: volume of decalin = 25 cm<sup>3</sup> doped with thiophene (S = 10 and 20 ppm) temperature = 350 °C, hydrogen pressure = 3 MPa, catalyst loading = 1 g and stirring rate = 1360 rpm. It was checked that diffusional limitations due to mass transfer were negligible in these reaction conditions. The samples were analyzed at the end of the reaction (6 hours) by gas chromatography (Thermo Scientific Trace 1300, Phenomenex ZB-5 capillary column). Catalysts with a total metallic content of 2 %wt supported on  $\text{SiO}_2\text{-Al}_2\text{O}_3$  (70 % $\text{SiO}_2$ ) and zeolite HY, monometallics Pt, Ir, Rh and bimetallics with a unitary.

The samples previously used in the decalin reaction were regenerated in a fixed bed reactor at 450 °C (10 °C min<sup>-1</sup>). The samples were first heated in nitrogen until the target temperature was reached. Then the gas flow was changed to a O<sub>2</sub>/N<sub>2</sub> mixture (5% O<sub>2</sub> 40 cm<sup>3</sup> min<sup>-1</sup>). This regeneration treatment was performed for 0.5, 1 and 2 h.

### Results and Discussion

Ring opening proceeds more effectively on bifunctional catalysts. In the development of catalysts for opening the decalin ring, the influence of the support (modification of the acid function), the metallic composition, the preparation method and other variables under different reaction conditions were studied. The different combinations of the variables shown in Figure 1 and an exhaustive characterization allowed to optimize the catalytic formulations.

Supports	Metal function	Preparation method	Catalytic evaluation
$\text{Al}_2\text{O}_3$ , $\text{SiO}_2$ $\text{TiO}_2$ , Zeolite HY, $\text{Nb}_2\text{O}_5$ $\text{SiO}_2\text{-Al}_2\text{O}_3$ (5, 20, 30, 40, 60, 70, 80 % $\text{SiO}_2$ ) Modified by: Mg, Cl and Na	Monometallics Pt, Ir, Rh, Pd, Ru Bimetallics Pt-Ir, Ru-Pt, Rh-Pd, Rh-Pt	Impregnation Catalytic reduction Coimpregnation Successive impregnations Activation treatment: calcination and reduction temperature	$T_{\text{reaction}}=300$ , 325 and 350 °C With and without S (10, 15 and 20 ppm)

Figure 1. Variables studied in the optimization of catalytic formulations for SRO of decalin.

In Figure 2 (a) it can be seen that in the absence of sulfur, with bimetallic catalysts less yield is reached to decalin ring opening products compared to the iridium and rhodium monometallic catalysts. However, they 2Ir-Pt catalysts exhibited a greater tolerance to thiophene poisoning mainly the one supported on  $\text{SiO}_2\text{-Al}_2\text{O}_3$ . The addition of sulfur not significantly modify the yield to ring opening products using zeolite HY as support, since the acid function predominates in the decalin ring opening mechanism. The regenerated 2Ir-Pt catalysts were evaluated again in the decalin reaction. Figure 2 (b) shows that the regeneration process is more effective in the 2Ir-Pt catalyst supported on  $\text{SiO}_2\text{-Al}_2\text{O}_3$ .

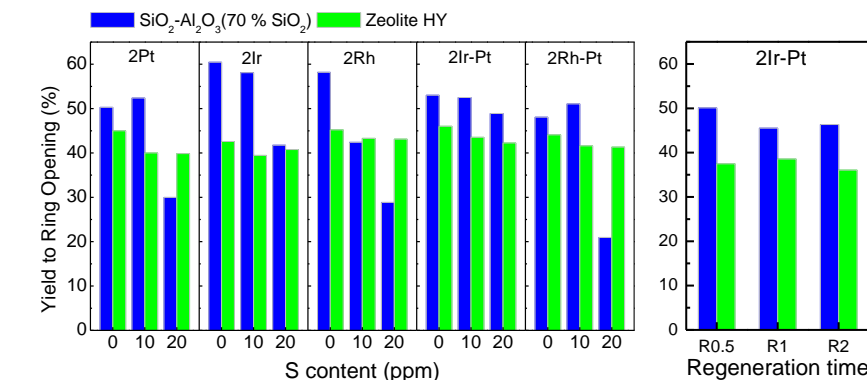


Figure 2. Yields to decalin opening products obtained: (a) as a function of the S content in the feed (b) regenerated at t=0.5, 1 and 2 h indicated R0.5, R1 and R2 respectively.

### Main Conclusions

Bifunctional catalysts supported on  $\text{SiO}_2\text{-Al}_2\text{O}_3$  present significant advantages over those supported on zeolite HY in terms of the opening of naphthenic rings, as well as thiotolerance and regeneration.

## Investigation of the nickel amount on a silica-alumina support for ethylene production

Paula Brussino\*, María A. Ulla and Juan P. Bortolozzi  
INCAPE (UNL-CONICET), Santiago del Estero 2829, Santa Fe 3000 (Argentina)  
\*pbrussino@fiq.unl.edu.ar

### Introduction

Around 160 million tons of ethylene are produced annually [1]. This olefin is known worldwide as one of the most important chemicals since it is used in chemical industries as a feedstock in the production of a wide variety of compounds, ending up in the every-day consumer goods. Its globally-established production is the steam cracking of naphtha or ethane, a process for which the energy consumption for the production of 1 kg of ethylene ranges from 15 to 27 MJ/kg [2]. Also, the carbon footprint is estimated at 1.6 metric tons of CO<sub>2</sub> per ton of produced ethylene. A greener alternative route for its production is the Oxidative Dehydrogenation of Ethane (ODE) reaction, because with an adequate catalyst it can be operated at lower temperatures (T<500 °C) and high ethylene yields could be achieved.

NiO-based supported catalysts are among the most studied materials for this reaction since nickel is relatively cheap and the catalytic performance is associated to the NiO-support interactions. By achieving strong NiO-support interactions, high ethylene selectivity can be obtained. Nevertheless, ethane conversion is generally low. Therefore, in this work several Ni loadings incorporated to a commercial silica-alumina support [3] were analyzed, with the aim to investigate the influence of the amount of Ni on both the NiO generated species and the catalytic performance.

### Materials and Methods

The catalysts were prepared by wet impregnation of nickel nitrate on a commercial support (SIRAL40®) that was previously calcined in air flux at 500 °C for 4 h. The formed pastes were dried in a stove and calcined at 500 °C for 2 h. The obtained catalysts were named Nix, where x indicates the nickel amount with respect to the support mass: 20, 30, 40, 50, 60 and 80 wt.% Ni, and characterized by N<sub>2</sub> desorption, TEM-EDS, LRS, XRD, TPR and XPS. In addition, they were tested in the ODE reaction at 300–450 °C and W/F = 0.6 g s/cm<sup>3</sup>.

### Results and Discussion

The main characteristics of the catalysts are shown in **Table 1**. The Ni/Al+Si ratios obtained with TEM and XPS were similar to the corresponding nominal ratios for Ni amounts up to 50 wt. %. At higher Ni contents, marked NiO accumulations which highly overcame the nominal values were seen in the TEM mappings of Ni60 and Ni80, and in XPS for Ni80. This was also seen in the TEM micrographs (**Figure 1**), where nickel was found mostly well-spread for Ni20, with the exception of some small crystals (inset). For Ni80, NiO was regularly loose in the form of big crystals, although some NiO was also deposited on the support (not shown).

**Table 1. Main properties of the catalysts and catalytic performance at 450 °C.**

Catalyst	Nominal Ni/Al+Si	TEM Ni/Al+Si	XPS Ni/Al+Si	BE (eV)	S <sub>BET</sub> (m <sup>2</sup> /g)	X <sub>C<sub>2</sub>H<sub>6</sub></sub> (%)	S <sub>C<sub>2</sub>H<sub>4</sub></sub> (%)
Ni20	0.18	0.21	0.14	855.7	244	28.1	74.5
Ni30	0.27	n. a.	0.26	855.4	220	30.7	71.0
Ni40	0.37	0.28	0.43	855.0	262	34.8	70.2
Ni50	0.46	0.40	0.42	854.5 / 856.5	221	38.4	68.0
Ni60	0.55	n. d.	0.60	854.3 / 856.3	158	41.3	63.5
Ni80	0.73	n. d.	0.97	854.1 / 856.2	108	42.5	60.1

n. a. = not available, n. d. = not determined.

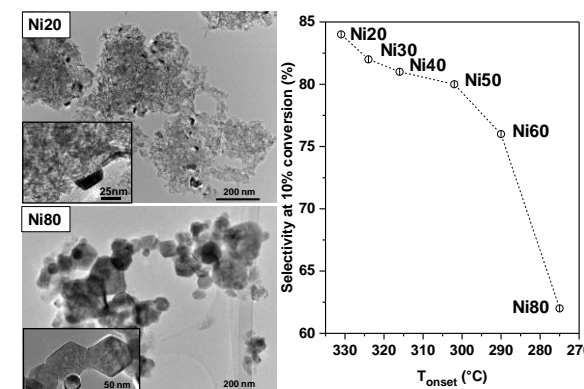


**Figure 1.** Left: TEM micrographs of Ni20 and Ni80, right: ethylene selectivity at 10% ethane conversion vs. the onset temperature of the TPR profiles.

Some differences were also seen in the reduction profiles (TPR) and at a surface level (XPS). From 50 wt.% of Ni, Ni<sup>2+</sup> species with higher reducibility and bulk tendency appeared. These had an impact mostly on ethane conversion, but for Ni60 and Ni80 the ethylene selectivity was the main affected parameter. A marked drop in the selectivity was present for this last catalyst due to the presence of many NiO big particles with properties similar to those of bulk NiO (Figure 1).

### Main Conclusions

Different Ni amounts (<80 wt.%) were incorporated to a silica-alumina support to conform a suitable catalyst for the ODE reaction. Both ethane conversion and ethylene selectivity were modified. The Ni species formed in the catalysts with lower loadings were characterized by stronger NiO-support interactions and lower reducibility, favoring ethylene selectivity.

### References

- [1] [www.synbiobeta.com/read/lanzatech-produces-ethylene-from-co2-changing-the-way-we-make-products-today](http://www.synbiobeta.com/read/lanzatech-produces-ethylene-from-co2-changing-the-way-we-make-products-today) (Accessed 01-02-2023).
- [2] O. Mynko, I. Amghizar, D. J. Brown et.al; J. Clean. Prod. 362 (2022) 132127.
- [3] P. Brussino, E. L. Mehring, M. A. Ulla, J. P. Bortolozzi; Catal. Today 394-396 (2022) 133-142.



## Synthesis of Ni-NPs impregnated on $\text{SiO}_2$ and $\text{Ti-SiO}_2$ for the selective reduction of glycerol

Fernando Tuler<sup>1\*</sup>, Raúl Comelli<sup>1</sup>, Ángel Berenguer-Murcia<sup>2</sup>, Diego Cazorla-Amoros<sup>2</sup>

<sup>1</sup>INCAPE, Colectora Ruta Nac. 168, km 0, Paraje El Pozo, Santa Fe 3000 (Argentina)

<sup>2</sup>Materials Science Institute and Inorganic Chemistry Department, Univ. of Alicante, Spain

\*ftuler@fiq.unl.edu.ar

### Introduction

This work is part of a project for the valorization of glycerol (the “co-product” of biodiesel production) in a biorefinery environment. The continuous increase in biodiesel production generates a simultaneous increase in the availability of glycerol. It motivates scientific researches to use the glycerol as a raw material to produce add-value and energetic compounds. An interesting compound for Argentinean industry is ethylene glycol (EG), due to its high demand and there are no producers in our country. In a previous work, studying different catalysts for the selective reduction of glycerol to obtain EG in gas phase, very good results were obtained with the  $\text{Ni/SiO}_2$  system prepared by the incipient wet impregnation, which allowed filing patent application and subsequently granted in February 2022 [1]. The aim of this work is to synthesize catalysts by more advanced techniques such as Ni nanoparticle synthesis (Ni-NPs), as well as colloidal Ni-NPs suspensions to impregnate supports, such as  $\text{SiO}_2$ ,  $\text{Ni/SiO}_2$  nanocomposite and synthesis of mesoporous silica and titanosilicates ( $\text{Ti-SiO}_2$ ) type supports, which are then impregnate with the Ni active phase. In this way, the objective is to optimize catalytic performance, controlling Ni dispersion, morphology, particle size, and separation between them in the preparation.

### Materials and Methods

Nickel nitrate ( $\text{Ni}(\text{NO}_3)_2 \cdot 6\text{H}_2\text{O}$ , Sigma-Aldrich),  $\text{SiO}_2$  (Aerosil® 380), titanium (IV) ethoxide (Sigma-Aldrich), tetramethylorthosilicate (Sigma-Aldrich), were used.

Ni-NPs were prepared following a chemical method [2]. The effect of solvent (water, EG, and ethanol) on the Ni-NPs morphology was investigated. These Ni-NPs were taken from each procedure and suspended in water by ultrasound, and then  $\text{SiO}_2$  was added to each suspension under agitation. After that, they were dried in an oven overnight.

The  $\text{Ni/SiO}_2$  nanocomposite catalysts were prepared as in the previous case of Ni-NPs, where in the same solution that the NPs are synthesized, silica was added, so that the NPs are deposited directly on the support during the preparation.

Synthesis of supports: mesoporous  $\text{SiO}_2$  and  $\text{Ti-SiO}_2$  have been prepared adapting a synthetic protocol described elsewhere [3]. Obtained supports were impregnated with different Ni loadings (0.5, 1.0, 2.5, and 5.0 Ni wt.%) by the technique described in [4].

All the prepared catalysts have been characterized by Transmission Electron Microscopy (TEM) with a JEOL JEM-2010. High Resolution Transmission/Scanning (SEM) with a FEI Titan Themis. Supports and catalysts based on  $\text{Ti-SiO}_2$  were analyzed using an Ultraviolet-Visible-Near-Infrared (UVVisible-NIR, V-670, JASCO).

### Results and Discussion

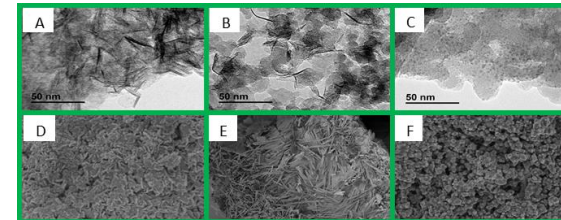


**Fig. 1.** TEM and SEM images for Ni-NPs (A and D, respectively), Ni-NPs impregnated on  $\text{SiO}_2$  (B and E), and  $\text{Ni/SiO}_2$  nanocomposite (C and F).

As can be seen in Fig. 1-A and D, the Ni-NPs have fiber shape (~24 nm long and 1 nm wide), using water and ethanol as solvent, while using EG the particles are spherical of about 3 nm (not shown). The same morphology were observed for the catalysts impregnated with the Ni-NPs to the  $\text{SiO}_2$  (Fig. 1-B and E), this images reveal fiber particles on granular support ( $\text{SiO}_2$ ), except for the catalyst synthesized with EG (not shown) which presents spherical particles. However, for  $\text{Ni/SiO}_2$ nanocomposites, where support and  $\text{Ni}(\text{NO}_3)_2$ mixed together in the preparation (Fig. 1-C and F),  $\text{SiO}_2$  was homogeneously impregnated by spherical NPs, regardless of the solvent used.

The UV-Vis analysis, not shown, revealed that Ti is incorporated as single sites into the silica framework, mainly in tetrahedral coordination, even though a small fraction of Ti in octahedral coordination is obtained in all samples. An increase in the band at 380 nm is observed as the Ni loading increases from 0.5 to 5.0 Ni wt%.

### Significance or Main Conclusions

Ni-NPs were obtained by a simple synthesis method. The synthesized NPs present fibers shapes, and when suspended it and impregnated supports maintain the same morphology. However,  $\text{Ni/SiO}_2$  nanocomposite presents a homogeneous distribution of spherical NPs on the surface of the supports. Finally, the synthesis of titanosilicate allowed the incorporation of Ti into the silica framework in a mostly tetrahedral coordination; it would mean a high dispersion of Ti. Then Ni was impregnated to this support, with which it is expected to have a much more controlled impregnation of Ni in  $\text{Ti-SiO}_2$ , where the Ni sites are anchored to Ti in the support. It remains to complement the characterization and evaluate all catalysts in the selective reduction reaction of glycerol to compare the catalytic behavior with the synthesis and catalytic systems obtained.

### References

- [1] R. Comelli and F. Tuler Arg. Pat. P20180103864 (02/2022).
- [2] M. Ali, N. Remalli, V. Gedela, B. Padya, P. K. Jain, A. Al-Fatesh, U. Rana, V. Srikanth, Solid State Sciences 64 (2017)
- [3] J. García-A., M. Navlani-G., Á. Berenguer-M., K. Mori, Y. Kuwahara, H. Yamashita, D. Cazorla-A., RSC Adv. 6 (2016) 91768.
- [4] J. García-A., J. Fernández-C., J. Juan-J., I. Such-B., L.E. Chinchilla C, J.J. Calvino-G., D. Cazorla-A., Á. Berenguer-M., Journal of Catalysis 386 (2020) 94–105.



## Cobalt oxide-based catalysts supported on zirconia fibers synthesized by Atomic Layer Deposition

María M. Fontanini\*, Sabrina A. Leonardi, Eduardo E. Miró, Juan P. Bortolozzi, Viviana G. Milt.

*Instituto de Investigaciones en Catálisis y Petroquímica, INCAPe (FIQ, UNL-CONICET),  
Santiago del Estero 2829, Santa Fe, 3000, (Argentina)*

\*mfontanini@fiq.unl.edu.ar

### Introduction

Atomic Layer Deposition (ALD) is an advanced technique for preparing catalysts at atomic level. It provides the ability to synthesize supported catalysts and it is based on self-limiting chemical reactions of alternate doses of precursors that saturate the surface, separated by an inert gas purge. ALD provides some advantages such as large-area uniformity and excellent conformability [1].

Within this frame of reference, this work is focused on the synthesis of cobalt oxide grown onto zirconia fibers by the ALD technique. These catalysts were tested in the CO oxidation, which is considered a model reaction for environmental concern [2].

### Materials and Methods

The deposition of the cobalt precursor was carried out in a quartz reactor with a flow rate of  $N_2 = 70 \text{ ml} \cdot \text{min}^{-1}$  and a pressure  $P \approx 10 \text{ torr}$ . The deposition was carried out in cycles of four stages: (I) Pretreatment: support were heated at  $250^\circ\text{C}$  and the  $\text{Co(acac)}_3$  at  $110^\circ\text{C}$  in a  $N_2$  flow for 1 h; (II) Deposition: the support and the precursor were heated at  $155^\circ\text{C}$  for 15 min (III) Purge:  $N_2$  flow for 30 min to eliminate the precursor not anchored to the support and (IV) Calcination: air flow ( $60 \text{ ml} \cdot \text{min}^{-1}$ ) at  $500^\circ\text{C}$  for 1 h [3]. One, two and four ALD deposition cycles were performed in order to obtain different cobalt contents. The samples so obtained were named as  $\text{Co}(x) \text{ ZrO}_2\text{-f}$ , where "x" indicates the number of ALD cycles performed and "f" refers to fiber. Synthesized catalysts were characterized by Scanning Electron Microscopy (SEM), Energy-dispersive of X-ray Analysis (EDX) and X-Ray Photoelectron Spectroscopy (XPS) and they were tested in the CO oxidation reaction. For this purpose, 50 mg of the samples were heated from room temperature up to  $600^\circ\text{C}$  ( $4^\circ\text{C} \cdot \text{min}^{-1}$ ) in  $O_2$  (2%) + CO (1%) diluted in He (total flow  $30 \text{ ml} \cdot \text{min}^{-1}$ ) in a flow system.

### Results and Discussion

Images of the zirconia support and the catalysts prepared were obtained by SEM. Fiber bundles (100  $\mu\text{m}$  in length and 8  $\mu\text{m}$  in diameter approximately) formed by a few fibers of 2  $\mu\text{m}$  in diameter, with a furrowed surface, are observed. No differences were detected between the bare support and the supports on which the active phase was deposited. Cobalt was dispersed homogeneously along the fibers and its content was low in all samples (<1.2 %at.).(Figure 1.a).This indicates a good distribution of the active phase on the fibers.

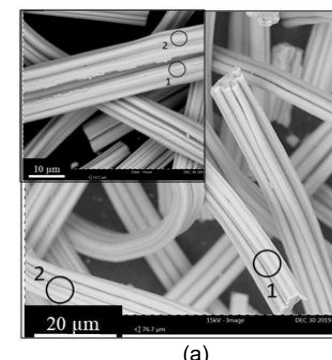
The amounts of cobalt incorporated in each reaction cycle were obtained by EDX analysis and its relative abundance respect to zirconium was calculated from XPS characterization results (Table I). As expected, the cobalt amount increased with the number of ALD cycles. While the number of cycles increased from 1 to 4, the relative

abundance of cobalt to zirconium (Co/Zr ratio) raised linearly from 0.08 to 0.37, thus indicating that the synthesis route proceeded successfully.

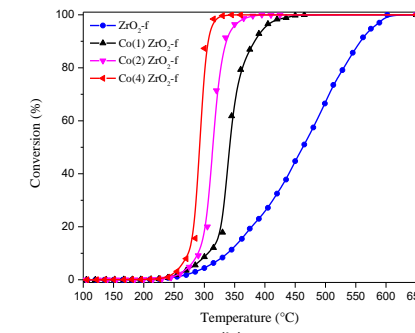
Table 1. Atomic surface ratios obtained by XPS.

Catalyst	Co loading (at.%) <sub>EDX</sub>	Co/Zr) <sub>XPS</sub>
$\text{Co}(1)\text{ZrO}_2\text{-f}$	0.37	0.08
$\text{Co}(2)\text{ZrO}_2\text{-f}$	0.61	0.18
$\text{Co}(4)\text{ZrO}_2\text{-f}$	1.24	0.37

Catalytic activity of the zirconia fibers with cobalt deposited by the ALD technique is shown in Figure 1.b. The conversion of carbon monoxide as a function of temperature is displayed. The bare zirconia fibers showed the lowest catalytic activity ( $T_{50} = 460^\circ\text{C}$ ). For the catalyst with one ALD cycle this temperature shifted 120  $^\circ\text{C}$  to lower values. The sample with two ALD cycles shows better activity ( $T_{50} = 310^\circ\text{C}$ ), while the catalyst with four cycles of depositions displayed a  $T_{50}$  value of 290  $^\circ\text{C}$ . Characterization techniques (LRS, XPS) along with kinetic results indicated that cobalt oxide is the active phase and that its amount influences the catalytic behavior.



(a)



(b)

Figure 1.a: SEM image of  $\text{Co}(4)\text{ZrO}_2\text{-f}$  catalyst. Inset: bare  $\text{ZrO}_2$  fibers. b: Catalytic activity of the catalysts prepared by ALD.

### Main Conclusions

Cobalt oxide catalysts supported on zirconia fibers were successfully prepared by the ALD technique. The amount of the catalytic element increased with the number of ALD cycles and so did the catalytic activity, which indicates that the preparation technique allows increasing the number of active sites when loading low amounts of catalyst.

### References

- [1] H.L. Lu, G.Scarel, X. L. Li, M. Fanciulli, J. Cryst. Growth 310 (2008) 5464–5468.
- [2] P.H. Ho, M. Ambrosetti, G. Groppi, E. Tronconi, R. Palkovits, G. Fornasari, A. Vaccari, P. Benito, Stud. Surf. Sci. Catal. 178 (2019) 303–327.
- [3] S.A. Leonardi, V.G. Milt, M.M. Fontanini, E.E. Miró, J.P. Bortolozzi, Mater. Chem. Phys. 294 (2023) 127043.

## Catalytic ceramic papers for soot removal

Sabrina A. Leonardi<sup>1\*</sup>, Eduardo E Miró<sup>1</sup> and Viviana G. Milt<sup>1</sup>

<sup>1</sup> Instituto de Investigaciones en Catálisis y Petroquímica, (INCAPE), UNL, CONICET,  
Facultad de Ingeniería Química, Santiago del Estero 2829 - 3000, Santa Fe, Argentina.

\* sleonardi@fiq.unl.edu.ar

### Introduction

Carbonaceous particles emitted into the atmosphere come from different combustion processes in industries, power plants and means of transport. Soot particles are carriers of harmful organic compounds, and can cause various diseases [1]. Diesel engines are considered one of the main sources of soot, being important not only the mass emitted, but also the size of the particles, since the smaller the size, the greater the penetration into the lungs. Until now, diesel particulate filters have been the most effective way to remove soot particles. They have the capacity to retain the particles by filtration and then burn them in situ with the action of an incorporated catalyst, taking advantage of the high temperatures generated in the exhaust pipes. In this framework, the elaboration of particulate filters from flexible materials such as ceramic papers was proposed, with the addition of active phases, Co,Ce or Co,Ba,K, for the combustion of different types of diesel soot.

### Materials and Methods

Ceramic papers were prepared using a standard papermaking method described by SCAN-C 26:76 and SCAN-M 5:76, with some modifications to adapt it to the use of ceramic fibers. The method consists of three steps: (i) preparation of ceramic paper discs, partially replacing cellulosic fibers with ceramic fibers and incorporating polyelectrolytes and binder, (ii) calcination treatment at 600 °C for 2 h and (iii) incorporation of active phases (Co,Ce or Co,Ba,K) by dripping of precursor solutions followed by another calcination treatment until 5% w/w of total active phase is obtained. The steps are described in detail in a previous work [2]. The ceramic papers thus obtained were named PN (ceramic paper without catalyst) and Co,Ce-PN and Co,Ba,K-PN, for catalytic ceramic papers. Catalytic ceramic papers were carefully characterized by Scanning Electron Microscopy (SEM), Laser Raman Spectroscopy (LRS) and Temperature Programmed Reduction (TPR) (not shown). The catalytic activity was evaluated by Temperature Programmed Oxidation (TPO) experiments for three types of soot, one obtained in the laboratory (LabSoot), another obtained in a test bench (BenchSoot) and the last one is a commercial soot model (Printex U). The evaluation conditions described by Leonardi et al. [2] were followed.

### Results and Discussion

Figure 1 shows images of ceramic papers prepared as discs 160 mm in diameter and 2.5 mm thick (Fig. 1a,b). The flexibility of the structure can be seen in Fig. 6c, while Fig. 6d shows how the ceramic discs can be easily cut into pieces. The ceramic papers are composed of ceramic fibers resistant to high temperatures (up to 900 °C). The intertwining of these cylindrical fibers (SEM image, Fig. 1e) provides a tortuous structure throughout the thickness of the disc that allows soot particles to be retained. X-ray tomography revealed a high porosity

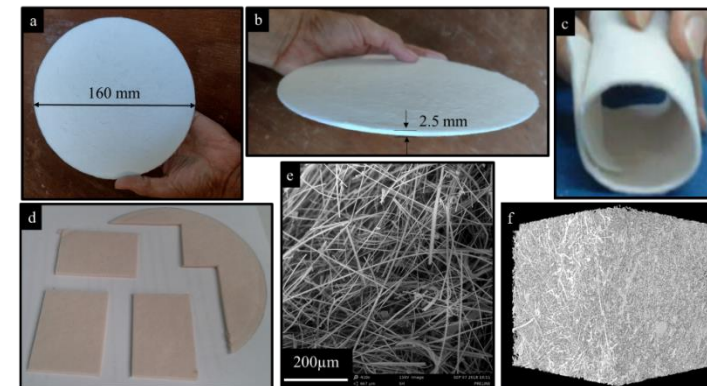


**Figure 1:** Ceramic paper discs a-d) photographs, e) SEM image and f) X- ray tomography.

of the ceramic paper structure, 75%, with an average pore size of 25.8 μm. Additionally, mechanical properties (elastic modulus: 0.76 MPa and tensile index: 0.05 N.m.g<sup>-1</sup>) indicated a flexible structure, consistent with photos shown in Fig. 1 c,d).

Table 1 lists the maximum combustion rate temperatures ( $T_M$ ) obtained in the different TPO experiments. For BenchSoot and LabSoot, a decrease in  $T_M$  is only observed when adding Co,Ba,K. However, only small differences are observed between the  $T_M$  values of Co,Ce-PN samples compared to PN samples. This behavior may be related to the distribution of the catalyst over the ceramic structure, since in the samples containing Co,Ba,K, the molten salts of K help to improve the distribution of the active phases and to enhance the soot-catalyst contact during TPO evaluations.

Moreover, the presence of the BaCoO<sub>3-y</sub> perovskite detected by TPR could contribute to the high catalytic activity obtained for Co,Ba,K-PN, as this mixed oxide helps to trap and release NO<sub>x</sub> and thus benefit soot combustion.

**Table 1:** Catalytic and non-catalytic soot combustion

Catalyst	Maximum combustion rate temperature (°C) ( $T_M$ )		
	LabSoot	BenchSoot	Printex U
PN	491	476	492
Co,Ce-PN	480	472	425
Co,Ba,K-PN	390	427	390

### Significance or Main Conclusions

The ceramic papers developed here constitute a suitable substrate for catalyst deposition as they have good thermal and mechanical resistance and are easily adaptable to different reactor geometries. In this work we showed results of catalytic activity for diesel soot removal that are favorable for the development of particulate filters.

### References

- [1] S. Hama, I. Ouchen, K. Wyche, R. Cordell, P. Monks; Atmos. Res. 274 (2022) 106180.
- [2] S. Leonardi, E. Miró, V. Milt; Catalysts 12 (2022) 885.

## Reuse of eggshells for the synthesis of catalysts used in the oxidation of unburned hydrocarbons.

M. de los Milagros Deharbe<sup>1\*</sup>, Ramiro Serra<sup>1</sup>, and Alicia Boix<sup>1</sup>  
<sup>1</sup>INCAPE, Santiago del Estero 2829, Santa Fe 3000 (Argentina)  
\*mdeharbe@fiq.unl.edu.ar

### Introduction

The management and reuse of waste to produce new materials is a methodology used to reduce environmental damage. Eggshells are a waste from the food industry that is normally discarded without prior treatment. For this reason, it is important to study the use of eggshells, for example, as a source of  $\text{CaCO}_3$  [1]. Catalytic processes are used to reduce air pollution that represents a threat to human health and the environment. The main polluting gases are  $\text{CO}_x$ ,  $\text{NO}_x$ ,  $\text{VOC}_s$ , unburned hydrocarbons, among others. Some of the catalytic processes used are: catalytic reduction, catalytic oxidation, and adsorption processes. In the present work, the catalytic oxidation of hydrocarbons is studied using toluene as a test molecule.

The most widely studied materials for these processes are metal oxides and noble metals. Among the transition metals, cobalt is the most promising for hydrocarbon oxidation. Cobalt oxides have very good activity as well as being a low-cost and relatively non-toxic alternative, mainly spinel  $\text{Co}_3\text{O}_4$ , which exhibits redox chemical properties[2].

### Materials and Methods

The preparation of catalysts from chicken eggshells (C) requires a series of steps (Fig. 1a): shell cleaning, grinding, the addition of cobalt by wet impregnation (CoC), oven drying, and calcination at different temperatures, 450, 550, 700, and 900 °C (C-450, CoC-450, CoC-550, CoC-700, and CoC-900).

The catalytic evaluation was carried out in a continuous flow system coupled to a gas chromatograph. The feed stream contained 1000 ppm toluene in excess of oxygen (10%) and diluted in helium.

### Results and Discussion

The catalysts, CoC-450, CoC-550, CoC-700, and CoC-900, and supports, uncalcined shell (C) and C-450, were evaluated for the toluene oxidation reaction. Figure 1a shows the conversion of toluene as a function of temperature.

The toluene conversion curves as a function of temperature show that eggshell without heat treatment and C-450 present low catalytic activity reaching 550°C with a conversion of only 40%. On the other hand, it was observed that, the addition of 16% cobalt promoted toluene oxidation in all catalysts (CoC-900, CoC-700, CoC-550, and CoC-450).

In the catalytic materials, CoC, the influence of the calcination temperature of the samples was analyzed. The CoC-450 catalyst presented its activation temperature,  $T_{20\%}$  (the temperature at which 20% conversion is reached), at 200°C and a rapid conversion reaching 90% conversion ( $T_{90\%}$ ) at 270°C. In turn, the CoC-550 catalyst achieved a  $T_{20\%}=240^\circ\text{C}$  quickly reaching a  $T_{90\%}=290^\circ\text{C}$ . The materials, CoC-700 and CoC-900, presented lower conversion reaching a  $T_{90\%}$  at 360°C and 425°C respectively.

Comparing the performance in toluene oxidation the four catalysts follow the following order: CoC-450 >CoC-550 >CoC-700 >CoC-900.

The  $\text{Co}_3\text{O}_4$  spinel present in the catalysts calcined at 450 °C and 550 °C would be the active species. However, calcination at higher temperatures, 700 °C, and 900 °C, promoted the formation of mixed Ca and Co oxides which have lower catalytic activity. These species were determined by XRD (not shown).

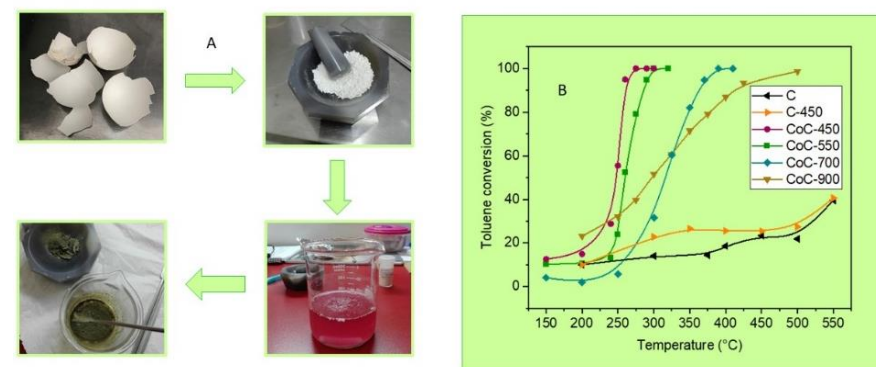


**Figure 1.** (A) Methodology of preparation of catalytic materials. (B) Toluene conversion as a function of temperature: eggshell and catalysts CoC.

### Significance or Main Conclusions

It was possible to use waste eggshells in conjunction with cobalt to develop catalysts that showed very good results in the oxidation of toluene. The best catalytic performance was obtained by the cobalt catalyst supported on eggshell and calcined at the lowest temperature, CoC-450. This could be due to the presence of the cobalt spinel in its structure which is active for the reaction.

### References

- [1] Waheed, M.; Yousaf, M.; Shehzad, A.; Inam-Ur-Raheem, M.; Khan, M.K.I.; Khan, M.R.; Ahmad, N.; Abdullah; Aadil, R.M. *Trends Food Sci. Technol.* (2020), 106, 78–90.
- [2] Ren, Q.; Mo, S.; Peng, R.; Feng, Z.; Zhang, M.; Chen, L.; Fu, M.; Wu, J.; Ye, D. *J. Mater. Chem. A* (2018), 6, 498–509



## Eggshell catalysts supported on monolithic structures used in the oxidation of toluene

M. de los Milagros Deharbe<sup>\*</sup> Alicia Boix<sup>1</sup> and Ramiro Serra<sup>1</sup>  
<sup>1</sup>INCAPE, Santiago de Estero 2829, Santa Fe 3000 (Argentina)  
<sup>\*</sup>mdeharbel@fiq.unl.edu.ar

### Introduction

The presence of hydrocarbons in industrial processes as well as their emission to the atmosphere is a problem that can be treated by catalytic oxidation processes.

The developed catalysts are usually produced in powder form but are difficult to use in real conditions due to the high flow rates that generate pressure drop problems. To minimize this problem, monolithic structures are used in which the active material is deposited. These structured materials also have the advantages of better heat transfer and greater chemical and mechanical stability.

In addition, the use of waste to produce new materials is an alternative to reduce the environmental impact.

In this work, cobalt catalysts were developed using eggshell supported monolithic structures, and their performance in the oxidation of toluene under different concentrations of reagents in the feed stream was studied.

### Materials and Methods

Powder catalysts: Eggshell was used as a support for the catalytic material. It was washed, dried, and ground. Then, cobalt was incorporated by wet impregnation with solutions of different concentrations of cobalt acetate. ( $\text{Co}_8\text{C}$ ,  $\text{Co}_{12}\text{C}$  and  $\text{Co}_{16}\text{C}$ ).

Structured catalysts were prepared by washcoating [1] and then calcined in a muffle at 450°C for 8 hours (M-Co<sub>8</sub>C-450, M-Co<sub>12</sub>C-450, and M-Co<sub>16</sub>C-450).

The catalytic behavior was studied in a continuous flow system coupled to a gas chromatograph. The operating conditions, toluene and oxygen concentration, were varied.

### Results and Discussion

Toluene conversion was studied using the catalysts M-Co<sub>8</sub>C-450, M-Co<sub>12</sub>C-450, and M-Co<sub>16</sub>C-450 whose cobalt loadings were determined by ICP, resulting in 8, 12, and 16% respectively. In this order, the catalytic conversion at 240 °C was 60, 76 y 100% (Table 1). This effect could be due to the presence of a higher number of cobalt active sites. On the other hand, the catalyst, M-Co<sub>16</sub>C-450, was used to analyze the effect of varying the concentration of the reactants on the oxidation of toluene. Figure 1 shows the toluene conversion at 230°C. It was observed that at the same O<sub>2</sub> concentration (15%), the increase in toluene concentration decreased the conversion, which could be due to a limitation of the active catalyst sites. In addition, when the percentage of oxygen is increased at the same concentration of toluene (1000 ppm) the conversion increases. This result is consistent with the Mars-Van Krevelen mechanism through which the hydrocarbon oxidation reaction takes place [2] where the reactant molecules are oxidized by the lattice oxygen of the catalyst and this lattice oxygen is

replaced with oxygen from the gas phase, so a higher percentage of oxygen in the gas phase would result in a higher conversion

**Table 1. Catalytic Results**

Catalyst	Co (%)	Toluene conversion (%)
M-Co <sub>16</sub> C-450	16	100
M-Co <sub>12</sub> C-450	12	76
M-Co <sub>8</sub> C-450	8	60

Reaction condition:  $T=240^\circ\text{C}$ , toluene concentration 1000 ppm and oxygen concentration 15%

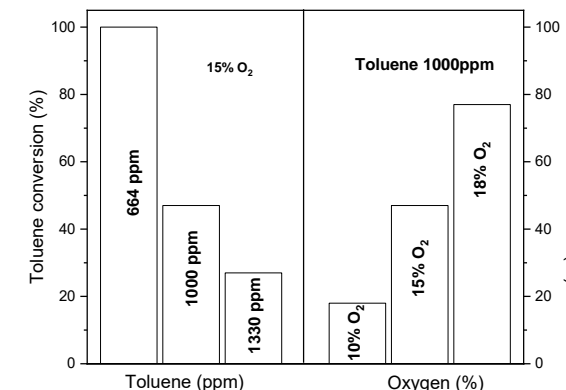


**Figure 1.** Toluene conversion at 230°C of catalyst M-Co<sub>16</sub>C-450, variation in the concentration of the reactants (toluene and oxygen concentration).

### Significance or Main Conclusions

Structured catalysts were successfully developed using a residue such as eggshell. The catalyst with the best catalytic performance was the one with higher cobalt content, M-Co<sub>16</sub>C-450, which could be due to a higher number of active sites. On the other hand, a higher concentration of oxygen in the feed stream resulted in higher conversion, while when the concentration of toluene was increased, competition for active sites resulted in a decrease in conversion.

### References

- [1] B.M. Sollier, L.E. Gómez, A. V. Boix, E.E. Miró, *Appl. Catal. A Gen.* 550 (2018) 113–121.
- [2] J. Zhong, Y. Zeng, M. Zhang, W. Feng, D. Xiao, J. Wu, P. Chen, M. Fu, D. Ye, *Chem. Eng. J.* 397 (2020) 125375.



## Catalytic 3D-printed systems based on clays for oxidation reactions

Natalia L. Courtalón<sup>1\*</sup>, Ezequiel D. Banús<sup>1</sup> and Juan P. Bortolozzi<sup>1</sup>

<sup>1</sup> INCAPe, Santiago del Estero 2829, Santa Fe 3000 (Argentina),

\*ncourtalon@fiq.unl.edu.ar

### Introduction

Atmospheric pollution impacts in public health causing many diseases and contributing to climate change. Two of the major pollutants are carbon monoxide (CO) and soot or particulate matter (PM). These compounds are emitted from internal combustion engines [1] and they can be removed from the gas exhaust by oxidation reactions.

In the last decade, additive manufacturing had a wide spread given by the accessibility of the 3D-printers. This technique enables to obtain objects by piling two-dimensional layers with a specific shape. Currently, a wide variety of different 3D-printing technologies could be found. Among them, “robocasting” or “direct ink writing” is of particular interest, since it makes possible to print materials such as gels and pastes [2]. Heterogeneous catalysts could be improved by 3D printing [3] since it allows to obtain structured systems with complex and controlled geometry.

In this context, the aim of this work is to develop a low-cost heterogeneous catalytic system by robocasting, active in the CO oxidation and soot combustion. These systems are based on a commercial clay adapted to be 3D printed, being Co and Ce the active elements.

### Materials and Methods

Commercial 3D-printable clay was employed as support of the catalysts. Two different types of heterogeneous catalysts using the clay were made. Firstly, a set of supported powder catalysts were made in order to perform a catalytic activity screening in the reactions of interest (total metal loading: 2 mmol/g<sub>clay</sub> and variable Co/Ce proportion). These catalysts were obtained by wet impregnation of Co and/or Ce nitrate precursors on the calcined clay powder, followed by a calcination stage (600°C, 2 h). On the other hand, structured catalysts were prepared with an equivalent composition to those powders with the best catalytic performance. Thereby, monolithic clay substrates were 3D-printed in a wood-pile configuration by robocasting. The active phase was incorporated to the structures by impregnation and subsequent calcination, until metal loadings up to 0.5 mmol/g were achieved. The prepared systems were characterized by X-ray Diffraction (XRD), X-ray Fluorescence (XRF), Thermogravimetric Analysis (TGA) and Specific Surface Area (BET) and Laser Raman Spectroscopy (LRS).

The catalytic performances of both powder and structured catalysts were evaluated in a flow system through temperature-programmed tests. For the PM combustion, soot was incorporated to the powder catalyst in a 20:1 ratio in tight contact while for the structured catalysts this addition was through impregnation from a soot-hexane suspension (600 ppm).

### Results and Discussion

Clay characterization (XRD) indicated that it is composed of kaolinite, halloysite, calcite and quartz. This is in agreement with the elemental composition obtained by XRF. BET analysis indicated a specific area of 16.3 m<sup>2</sup>/g and TGA profiles showed that the material has

suitable properties (thermal and mechanical stability) after treatment at 750°C (2 h). According to XRD and LRS results, CeO<sub>2</sub> and Co<sub>3</sub>O<sub>4</sub> oxides were found in the catalysts.

The results of the catalytic activity of the prepared powders in the CO oxidation are listed in Table 1. Temperatures corresponding to 50% (T<sub>50</sub>) and 90% (T<sub>90</sub>) of CO conversion are shown. The Co catalyst and all the Co:Ce catalysts had a similar performance, with a slight tendency to increase the T<sub>50</sub> when the Ce proportion rises up. Ce catalyst showed the highest T<sub>50</sub> of the series. This indicates that the presence of Ce in these systems did not improve its performance in the CO oxidation. The structured catalysts showed similar behavior as its powder counterpart.

Table 1. Catalytic results in the CO oxidation for the powder catalysts.

Catalyst	Co	Co90Ce10	Co75Ce25	Co50Ce50	Co25Ce75	Ce
Co:Ce ratio	100:0	90:10	75:25	50:50	25:75	0:100
T <sub>50</sub> [°C]	198	201	205	210	217	354
T <sub>90</sub> [°C]	228	221	232	237	253	406

Reaction conditions: Tight contact, W/F = 0.1 g s / cm<sup>3</sup>

On the contrary, for PM combustion the results indicated there is an optimum Co:Ce ratio. From the prepared powder catalyst set, the best performance was exhibited by the powder catalyst with Co:Ce 90:10 ratio. This solid showed a temperature of maximum combustion rate (T<sub>max</sub>) of 340°C in tight contact, whereas this value was 460°C for the Co and the Ce catalysts (Figure 1). In this case, the corresponding structured catalyst exhibited a T<sub>max</sub> = 440°C. These results were expected since in the structured systems the contact between the catalyst and soot is loose, making more difficult to catalyze the solid-gas reaction, thus increasing the T<sub>max</sub> values.

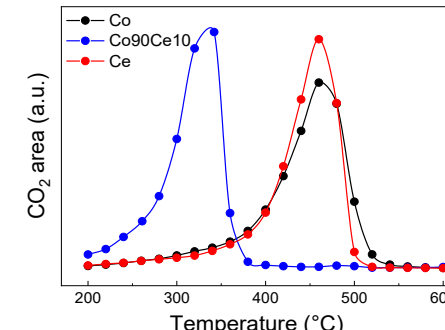


Figure 1: Soot combustion of powder catalysts.

### Significance

A novel methodology that allows obtaining 3D-printed structured catalysts with specific geometries was successfully implemented. The prepared systems were active in CO oxidation and soot combustion, showing a synergy between Co and Ce in the last one. The results found constitute a starting point to optimize the manufacture of these catalysts.

### References

- [1] I.A. Reşitoğlu, K. Altınışik, A. Keskin, Clean Technol. Environ. Policy 17 (2015) 15–27.
- [2] S.B. Balanı, S.H. Ghaffar, M. Chougan, E. Pei, E. Şahin, Results Eng. 11 (2021).
- [3] C. Parra-Cabrera, C. Achille, S. Kuhn, R. Ameloot, Chem. Soc. Rev. 47 (2018) 209–230.

## In-situ DRIFTS investigations applied to the catalytic hydrogenation and reforming processes

Misael Cordoba<sup>1,2\*</sup>, Lina García<sup>1</sup>, Juan Badano<sup>1</sup>, Carolina Betti<sup>1</sup>, Mónica Quiroga<sup>1</sup>, Cecilia Lederhos<sup>1</sup>

<sup>1</sup>INCAPE, Colectora Ruta Nacional 168 Km 0, Santa Fe 3000 (Argentina)

<sup>2</sup>Grupo de Investigación en Catálisis, Universidad del Cauca, calle 5 No. 4-70, Popayán 1100 (Colombia)

\*mcordoba@fiq.uni.edu.ar

### Introduction

The initial and decisive step to carry out a catalytic process consists of developing an appropriate catalyst for the reaction of interest. The current trend is to approach rational design and optimization, making use of recent instrumental and theoretical advances. In the last decade Diffuse Reflectance Infrared Fourier Transform Spectroscopy (DRIFTS) has become a very popular method for the characterization of catalysts and it has been applied quite extensively to the identification of all adsorbed species on the surface, and consequently may contribute in the identification of reaction intermediates. Recent works of catalytic systems using infrared absorption spectroscopy to study the adsorption of alkynes and alkenes over supported metal catalysts and single crystals, have been published [1]. On the other hand, in the latest works the catalytic reforming of tar model compounds of a gasification stream of agroforestry residues with in-situ DRIFTS was studied [2]. The interaction between the catalyst, tar model compounds and the main carbon species present in the syngas ( $\text{CH}_4$ ,  $\text{CO}_2$ , and CO) were evaluated [3]. In this work, the 1-pentyne selective hydrogenation and toluene catalytic reforming were carried out over different catalysts using a DRIFTS cell. The adsorption, hydrogenation of pure 1-pentyne and reforming of syngas and toluene/syngas mixture were monitored by in situ DRIFTS.

### Materials and Methods

The catalysts were provided by work group. The processes were performed in a Shimadzu Affinity-1S FTIR equipment, coupled to a DRIFTS thermal cell with a ZnSe mirror. For each analysis ~ 30 mg of each catalyst was reduced in-situ 30 min in  $\text{H}_2$  flow, then subjected to vacuum or flushed with  $\text{N}_2$  and cooled to analysis temperature. The background of the samples was recorded and the experiments were carried out, passing through the saturator  $\text{N}_2$  or  $\text{H}_2$  with pure 1-pentyne for adsorption/ hydrogenation, while mixture of syngas ( $\text{H}_2$  17%, CO 18%,  $\text{CO}_2$  14%,  $\text{CH}_4$  5%,  $\text{N}_2$  46%) and toluene/syngas for catalytic reforming to 1 atm. The analysis were performed every 2 min during 30 min in transmittance mode with a resolution of  $4 \text{ cm}^{-1}$  and 64 scans. The spectra were processed using the Kubelka-Munk method. The noncondensable syngas was analyzed in a Shimadzu 2014 gas chromatograph equipped with a TCD detector.

### Results and Discussion

Figure 1 shows the in-situ DRIFTS tests of 1-pentyne adsorbed on Ag-supported catalysts and syngas reforming on  $\text{NiMo}/\text{Al}_2\text{O}_3$ , Fe/AC, dolomite, pyrolysis residue catalysts. In Figure

1 (a) vibration bands of formation of intermediate species of alkyne on the surface of Ag-supported catalysts with different intensity are observed. Intermediate 1-pentyne di- $\pi$  bond species are observed on the surface of all catalysts at ~ 1597, 1433, 1392 and 1257  $\text{cm}^{-1}$ , while alkene di- $\sigma$  bound species with bond vibrations  $\nu(-\text{C}=\text{C}-)$  at ~ 3076, 1650, 1000 and 950  $\text{cm}^{-1}$ . On the other hand, changes in the intensity ratio of bands between  $I_a(1500 \text{ cm}^{-1}) / I_b(1200 \text{ cm}^{-1})$ , and also in the intensity vibration bands of the alkynyl bond  $\nu(\text{H}-\text{C}\equiv)$  at 3330 and 628  $\text{cm}^{-1}$  are observed on surface of Ag catalysts [1]. The adsorbed intermediate species could indicate possible routes for the selective hydrogenation of 1-pentyne. Figure 1 (b) shows IR peaks of carbon species present in the syngas ( $\text{CH}_4$ ,  $\text{CO}_2$ , and CO) during the catalytic reforming at 600°C. For  $\text{NiMo}/\text{Al}_2\text{O}_3$  and pyrolysis residue catalysts a peak negative at 2366  $\text{cm}^{-1}$  and 3016  $\text{cm}^{-1}$  associated to  $\text{CO}_2$  and  $\text{CH}_4$ , respectively, were observed. This could indicate that the methanation reaction is promoted ( $\text{CO}_2 + 4\text{H}_2 \leftrightarrow \text{CH}_4 + 2\text{H}_2\text{O}$ ). While Dolomite and Fe/AC show the interaction between  $\text{CH}_4$ ,  $\text{CO}_2$ , CO and the catalytic surface. The peaks at 3010, 2358, 2180, 2100, 1500 and 750  $\text{cm}^{-1}$  are associated with the adsorption of  $\text{CH}_x$ , O-C-O carbonates, CO adsorbed, carbonate and formate ( $\text{HCOO}$ ) species, respectively. The mentioned peaks and the hydroxyl signals (band centered at 3300  $\text{cm}^{-1}$ ) could indicate that the methanation, dry reforming and Water Gas Shift reactions in these catalysts are promoted.

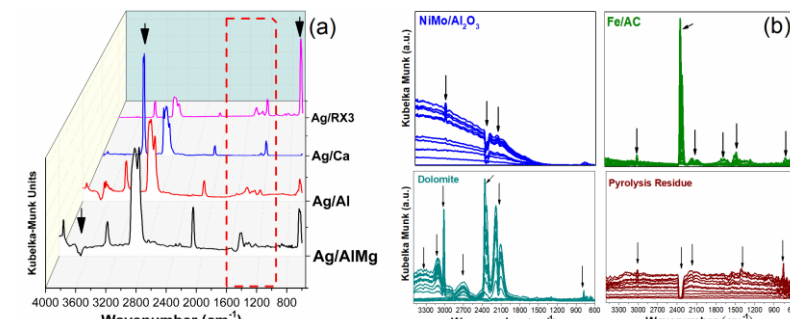


Figure 1. In-situ DRIFTS analysis (a) 1-pentyne adsorbed on Ag-supported catalysts (b) syngas reforming over  $\text{NiMo}/\text{Al}_2\text{O}_3$ , Fe/AC, Dolomite and pyrolysis residue catalysts.

### Conclusion

The In-situ DRIFTS adsorption analysis of the alkyne allowed to identify some surface species over each catalyst that may favor the high selectivity of the evaluated Ag-supported. The experiments of in-situ DRIFTS during catalytic reforming of syngas and toluene allowed to evaluate the performance of the low-cost catalysts and their possible mechanisms during reforming.

### References

- [1] M. Cordoba et al. Topics in Catalysis 65 (2022) 1347–1360.
- [2] S. Wang et al. ACS Catalysis 10 (2020) 2046–2059.
- [3] E. Quiroga et al. Waste Management 147 (2022) 48–59.

## Synthesis of sulfated zirconia to obtain triethyl citrate

Federico L. Aguzín<sup>1\*</sup>, Yanina M. Acuña<sup>1</sup>, Cristina L. Padró<sup>2</sup>, Nora B. Okulik<sup>1</sup>

<sup>1</sup>INIPTA, Comandante Fernández 755 (3700), Pres. Roque Sáenz Peña, Chaco (Argentina)

<sup>2</sup>INCAPE, UNL-CONICET, RN168 km 0, Paraje "El Pozo" (3000), Santa Fe (Argentina)

\*federicoaguzin@uncaus.edu.ar

### Introduction

The current paradigms of chemical engineering contemplate the integral use of the renewable sources of our planet for the sustainable development of societies, seeking to save biodiversity and the quality of life of people. In this sense, the aim of this work is to replace plasticizers based on petrochemical phthalates, which have low biodegradability and considerable toxicity, by others obtainable from renewable sources. Esters of carboxylic acids and alcohols that can be obtained by biomass fermentation, such as citric acid (CA) and ethanol (EtOH), constitute a sustainable alternative. The esterification to obtain triethyl citrate (TEC) proceeds sequentially through **Scheme 1** and involves the formation of the intermediate products monoethyl citrate (MEC) and diethyl citrate (DEC). This reaction requires the use of catalysts to achieve good yields.

SBA-15 is a nanostructured mesoporous silica material with high surface area and pore volume [1], which by incorporating heteroatoms (such as Al, Ga, Ti, and Zr) and treatment with mineral acids generates Brønsted and Lewis acid sites, making it of interest in catalysis [2]. In particular, sulfated zirconia shows high activity in numerous reactions, among which several esterifications can be mentioned [3]. This abstract reports the synthesis of a sulfated zirconia catalyst supported on SBA-15 (SZ-10) to obtain TEC by esterification of CA with EtOH. The properties of the material were evaluated by different techniques and its reaction activity was compared with that of the commercial resin Amberlyst 36 (A36).



**Scheme 1.** Esterification of CA with EtOH to obtain MEC, DEC and TEC.

### Materials and Methods

The SBA-15 mesoporous siliceous material was synthesized by hydrothermal treatment in an acidic medium according to Valles *et al.* [2] by using the triblock copolymer Pluronic 123 (P123, Sigma-Aldrich) as template and tetraethyl orthosilicate (TEOS, 98 %, Sigma-Aldrich) as source of silicon, with a molar gel composition of 1TEOS:158 H<sub>2</sub>O:6HCl:1.6·10<sup>-2</sup> P123. The ZrO<sub>2</sub> was incorporated with a Si/Zr molar ratio of 10 by wet impregnation method with a solution of hydrated zirconium oxychloride (99.99 % Sigma-Aldrich). Sulfation was carried out by stirring a suspension of Zr-SBA-15 in a 10 vol% aqueous solution of H<sub>2</sub>SO<sub>4</sub>. The material obtained was named as SZ-10. A commercial resin, namely Amberlyst 36 wet (Sigma-Aldrich), was also used as catalyst. The SZ-10 catalyst was characterized by physisorption of N<sub>2</sub>, XRD, EDXRF, FTIR and potentiometric titration.

The activity of the catalyst SZ-10 and A36 was evaluated in the liquid phase for the esterification of CA (Sigma-Aldrich) with EtOH (Biopack) in a Parr 4561 reactor. Reaction

conditions: 110 °C, 1wt % catalyst, 1/20 SA/EtOH, 800 rpm. Samples were analyzed by HPLC in gradient mode at a wavelength of 210 nm.

### Results and Discussion

The N<sub>2</sub> adsorption-desorption isotherm for SZ-10 allowed estimating a specific surface area of 264 m<sup>2</sup>/g and a pore size of 5 nm. The low angle diffraction pattern indicated that the pore structure of the support was preserved. While at extended angle the pattern did not show signs that could be attributed to any of the crystalline phases of ZrO<sub>2</sub>, which suggests a good dispersion on the surface. The EDXRF study confirmed the Si/Zr molar ratio of 10 used in the synthesis. The absorption bands in the FTIR spectrum were associated with the presence of bonds with the species with S, Zr, Si and O. The FTIR spectrum of the pyridine showed the presence of both Brønsted and Lewis acid sites. Potentiometric titration indicated that in aqueous solution this material has high concentration of acid sites, although lower than A36.

Catalytic tests showed that catalyst SZ-10 is more active than A36. On SZ-10 complete CA conversion was achieved at 150 minutes of reaction while the selectivity to TEC at the end of the reaction was 47 % on SZ-10 and 14 % on A36 (See **Figure 1**).

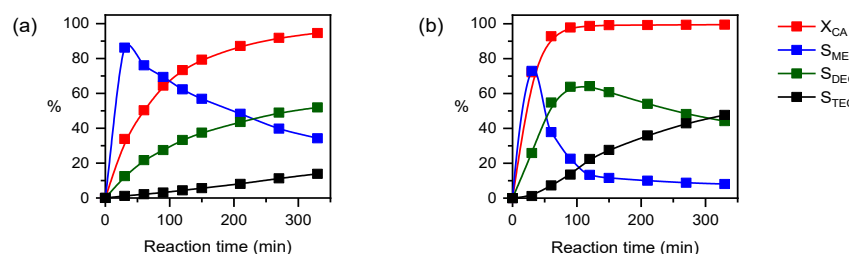


**Figure 1.** CA conversion and selectivities to MEC, DEC and TEC in the esterification of CA with EtOH using (a) A36 and (b) SZ-10 as catalyst. Reaction conditions: 110 °C, 1wt % catalyst, 1/20 SA/EtOH, 800 rpm.

### Conclusions

The synthesis of the bio-plasticizer TEC was possible by heterogeneous catalysis using SZ-10 and A36. SZ-10 was shown to be more active and selective to TEC than A36. The superlative behavior of SZ-10 was attributed to a synergistic Brønsted-Lewis acid effect.

### Acknowledgment

We thank Andrea Beltramone and María L. Martínez for their contribution in SZ-10 synthesis.

### References

- [1] D. Zhao, J. Feng, Q. Huo, et al., Science 1998, 279 (5350), 548-552.
- [2] V. Valles, Y. Sa-ngasaeng, M. Martínez, et al., Fuel 240 (2019) 138-152.
- [3] V. Mutlu, S. Yilmaz, Appl. Catal. A Gen. 522 (2016) 194-200.

## Phenol CWPO over Cu and CuFe-based structured catalysts

Paula Brussino\*, María A. Ulla and Ezequiel D. Banús  
INCAPE (UNL-CONICET), Santiago del Estero 2829, Santa Fe 3000 (Argentina)  
\*pbrussino@fiq.unl.edu.ar

### Introduction

Phenol and its derivates are present in several industries effluents. These compounds are highly toxic and not biodegradable [1]. Its degradation to carbon dioxide via the Catalytic Wet Peroxide Oxidation (CWPO) is an interesting alternative to eliminate them from these effluents since low temperatures and atmospheric pressure can be applied by using an adequate catalyst. Copper and iron-based catalysts are amongst the most studied catalysts for this reaction due to their good catalytic performance. Nevertheless, Cu and Fe leaching to the reaction media generated by the drop of pH is still an issue to be solved [2]. Structured catalysts have advantages over powder ones, associated to the versatility in their design and, in liquid-phase reactions related to the simplicity of the catalyst removal from the reaction media. In a previous work of our group we found that the iron from wire-meshes used as substrates prevented Cu leaching [3]. Considering these aspects, the objective of this work is to analyze the effect of Fe as a co-active phase in Cu-based catalysts supported on alumina and not supported using a substrate that is not composed by iron: cordierite monoliths.

### Materials and Methods

Alumina supported structured catalysts (Cu-Al-M and CuFe-Al-M) and un-supported structured catalysts (Cu-M and CuFe-M) were prepared by alumina washcoating followed by immersion in copper and copper-iron nitrates solution in the first case, and immersion in copper and copper-iron nitrates solution in the second case. When Fe was present, a Cu/Fe ratio of 0.35 was used. Once the desired load was achieved, 20 mg Cu, these were calcined at 900 °C for 2 h. All the structured catalysts were characterized by SEM/EDS, XRD, LRS, and XPS, and tested in the CWPO of phenol for 3 h. Cu and Fe leaching, pH and phenol conversion were monitored during the reactions and the final TOC concentration was measured.

### Results and Discussion

In general, the catalysts presented similar atomic ratios to the nominal ones, but the supported catalysts presented some heterogeneity (**Table 1**). XRD and XPS showed the presence of CuO, Fe<sub>2</sub>O<sub>3</sub> and Fe<sub>3</sub>O<sub>4</sub>. With the exception of CuFe-M, the catalysts achieved 100% phenol conversion at different times: 20 min for the supported catalysts and 90 min for Cu-M. These results were associated to the TOC conversions and leaching values. The supported catalysts exhibited high Cu and Fe leaching (**Figure 1.b**) and therefore, high TOC conversion, whereas for the un-supported catalysts these results depended on the presence of iron. When iron was present practically no leaching occurred, although some Cu was leached (0.142 mg/L), affecting phenol and TOC conversions. These results are consistent with the reduced copper to oxidized copper ratios obtained by XPS: those catalysts with more reducible copper were the ones with the highest copper leachings and TOC conversions.

**Table 1. Main properties of the catalysts and catalytic performance data.**

Structured Catalyst	Atomic ratio <sup>a</sup>	Cu/Fe	Cu 2p <sub>3/2</sub> BE (eV)	Fe 2p <sub>3/2</sub> BE (eV)	$\frac{Cu^r}{Cu^{ox}}$	X(%) /t(min)	X <sub>TOC</sub> (%)
Cu-M	0.01 ± 0.00	-	934.6 933.2	-	1.7	100/90	72.5
CuFe-M	0.01 ± 0.00	0.40 ± 0.11	933.8 933.0	712.0 710.2	0.3	69/180	4.6
Cu-Al-M	0.02 ± 0.00	-	935.0 932.3	-	7.4	100/20	76.6
CuFe-Al-M	0.01 ± 0.01	0.09 ± 0.02	934.4 932.6	712.9 710.8	4.5	100/20	71.5

<sup>a</sup> Cu/Al+Mg+Si for the un-supported catalysts (nominal= 0.01), and Cu/Al for supported catalysts (nominal=0.04), obtained by SEM/EDS; <sup>b</sup> reduced copper to oxidized copper ratio from XPS.

Iron affected copper reducibility in both supported and un-supported catalysts, more markedly in the last ones, practically preventing its leaching.

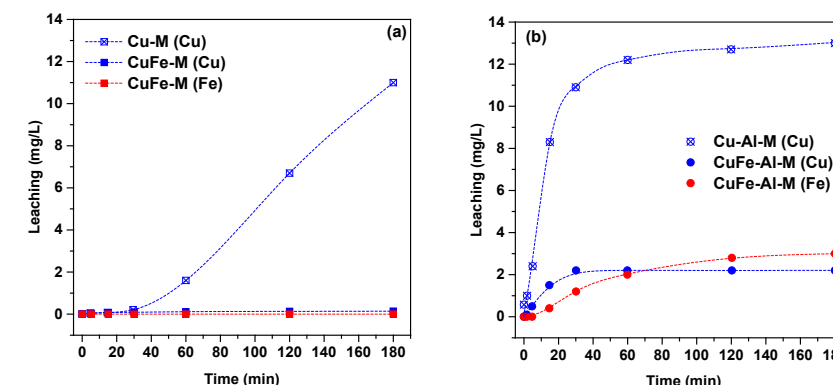


**Figure 1.** Copper and/or iron leaching during the reaction for the un-supported (a) and supported structured catalysts (b).

### Significance or Main Conclusions

Iron added as a co-active phase minimized or prevented metal leaching, depending on whether the active phase was supported or not. Cu and Fe species are more reducible when supported, leading to high phenol and TOC conversions but also high leaching.

### References

- [1] G. Busca, S. Berardinelli, C. Resini; L. Arrighi; J. Hazard. Mater. 160 (2008) 265–288.
- [2] S. Jiang, Z. Zhao, K. Cui; et.al; Chem. Eng. J. 430 (2022) 132787.
- [3] P. Brussino, M. S. Gross, E. D. Banús; M. A. Ula, Chem. Eng. Process: Process Intensification 146 (2019) 107686.



## Sorption enhanced ethanol steam reforming with K promoted Mg/Al hydrotalcites as sorbent material. The effect of Mg/Al ratio on CO<sub>2</sub> sorption capacity.

J. Fals<sup>1</sup>, M. Park<sup>1</sup>, R. Avendaño<sup>1</sup>, S. Bocanegra<sup>2</sup>, N. Amadeo<sup>1</sup> and M. Laura Dieuzeide<sup>1\*</sup>.

<sup>1</sup> Laboratorio de Proceso Catalíticos. Instituto de Tecnologías del Hidrógeno y Energías Sostenibles (ITHES), UBA-CONICET. Facultad de Ingeniería. Pabellón de Industrias. Ciudad Universitaria. Ciudad Autónoma de Buenos Aires. <sup>2</sup> Instituto en Catálisis y Petroquímica "Ing. Jose Miguel Parera" (INCAPE) Centro Científico Tecnológico CONICET. Santa Fe (CCT-Sant Fe) Argentina. \*ldieuzeide@fi.uba.ar

### Introduction

The main advantage of sorption enhanced ethanol steam reforming (SE-ESR), is the intensification of the process, reducing energy consumption while producing H<sub>2</sub> with low concentrations of carbon oxides [1,2]. To improve feasibility on SE-ESR, it must be operated in multicyclic sorption-regeneration scheme, so it becomes important the use of materials that work under ethanol steam reforming conditions (atmospheric pressure, 500-600°C). In this context Mg/Al based hydrotalcites are a promising material, since they have high CO<sub>2</sub> sorption capacity in this temperature range, but they can also be regenerated at the same temperature under an inert stream.

In a previous work the effect of potassium loading has been analyzed, and it was proved that potassium loadings between 15 and 20wt.% significantly enhanced the de CO<sub>2</sub> sorption capacity under SEESR conditions [2]. Moreover, Macedo et. al [3] have concluded that exists an optimum Mg/Al ratio that enhances hydrotalcites CO<sub>2</sub> sorption capacities.

Therefore, based on these results and on the ones reported by Macedo et. al [3], in this study, sorption-enhanced ethanol steam reforming (SEESR) is investigated using a Ni-based catalyst in the presence of CO<sub>2</sub> sorbents based on Mg/Al hydrotalcites with different Mg/Al (1.0, 2.5, 4.0, and 5.0) ratio and promoted with potassium (15wt.%). The aim is to evaluate in first instance, the effect of Mg/Al ratio on hydrotalcites CO<sub>2</sub> sorption capacity, and then their performance in SE-ESR, to produce high H<sub>2</sub> purity at mild temperatures (500°C).

### Materials and Methods

The catalyst used is a Ni-Mg-Al hydrotalcite-type solid previously developed by our research group, with molar ratio Mg/Ni = 4 and the molar ratio [Ni(II) + Mg(II)]/Al (III) = 3. The sorbents used in this work are hydrotalcites with different Mg/Al molar ratios (Mg/Al = 1.0, 2.5, 4.0 and 5.0), synthesized by homogeneous precipitation method. These solids were modified with a potassium load of 15wt% by means of excess wetness impregnation method. Before and after impregnation, the synthetic hydrotalcites were sieved to a particle size between 177-297 µm and calcined at 500°C for 4h. The hydrotalcites were named 15KHT-1.0, 15KHT-2.5, 15KHT-4.0 and 15KHT-5.0, respectively, in concordance with their Mg/Al ratio.

The synthesized and promoted sorbents were studied by XRD, ICP, BET, CO<sub>2</sub>-TPD, and CO<sub>2</sub> sorption – desorption tests. SE-ESR tests are carried out in a fixed-bed reactor. The reactor packing consists in a homogeneous mixture of 0.5g of catalyst and 2.5g of sorbent

inside a tubular stainless-steel reactor.

### Results and Discussion

Results indicates there is a linear dependence between BET surface area and hydrotalcites Mg/Al ratio, up to a Mg/Al ratio of 5, accompanied by an increase in mean pore size and there upon an enhancement in CO<sub>2</sub> sorption capacity. The CO<sub>2</sub>-TPD profiles show that the total amount of basic sites increases for the potassium promoted samples compared to the unpromoted ones and between the impregnated samples, HTK-4.0 presents the higher proportion of strongest basic sites that are mainly responsible for CO<sub>2</sub> sorption capacity. Based on CO<sub>2</sub> sorption profiles (Figure 1) there is an optimum Mg/Al ratio that enhance CO<sub>2</sub> sorption capacity. HTK-4.0 presents the highest CO<sub>2</sub> sorption capacity, being 2.9 mol CO<sub>2</sub>/kg<sub>sorbent</sub>. SEESR preliminary results with HTK-4.0, show that H<sub>2</sub> purities higher than 90% (75% correspond to conventional ethanol reforming) can be obtained up to 10 minutes, with CO purities minor than 2%.

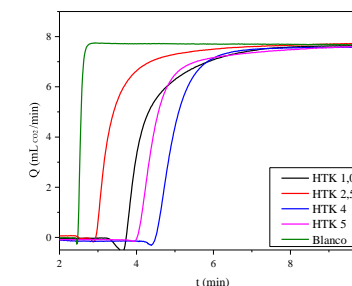


**Figure 1.** CO<sub>2</sub> sorption profiles for hydrotalcites with different Mg/Al ratio, promoted with 15wt.% of potassium.

### Significance or Main Conclusions

It has been proven that hydrotalcites Mg/Al ratio influence its CO<sub>2</sub> sorption capacity and that the best performance was obtained with hydrotalcite with Mg/Al=4. Additionally, it was confirmed that with these sorbent H<sub>2</sub> purities around 90% were obtained under SE-ESR. These are promising results regarding the application of these solids in the reaction system, although it is necessary to carry out cyclic operation studies to confirm the effect of the Mg/Al ratio.

### References

- [1] R. Avendaño, M.L. Dieuzeide, P. Bonelli, N. Amadeo, Lat. Am. Appl. Res. 50 (2020) 121-126.
- [2] R. Avendaño, J. Fals, S. Bocanegra, M.L. Dieuzeide, N. Amadeo, Int. J. Hydrogen Energy, 2023, In press.
- [3] M. S. Macedo, M.A. Soria, L.M. Madeira, Chem. Eng. J. 420 (2021) 129731.



## Recycling of spent Ion-Li batteries: low-temperature dry reforming of methane application

Franco I. Dubois<sup>1\*</sup>, Florencia Volpe Giangiordano<sup>1</sup>, Andrés M. Peluso<sup>1,2</sup>

<sup>1</sup>CINDECA (CONICET-UNLP), 47 st, 257, La Plata (Argentina)

<sup>2</sup>UPL (CICPBA-UNLP), Manuel B. Gonnet (Argentina),

\*francodubois13@gmail.com

### Introduction

In the context of searching for alternative synthetic fuels to replace the conventional ones obtained from oil, the production of synthesis gas (or syngas) gained renewed interest from both the scientific community and technological developers. Syngas consists of H<sub>2</sub> and CO in various proportions. For methanol synthesis or the Fischer-Tropsch process, it is necessary to have syngas with H<sub>2</sub>/CO ratio of at least 1. The dry reforming of methane (DRM, equation (1)) is an important reaction that treat two major greenhouse gases, CH<sub>4</sub> and CO<sub>2</sub>, present in biogas and natural gas [1].



This reaction is extremely endothermic and requires high operating temperatures, usually in the range of 600-1000°C to achieve desirable conversion levels. This condition and the rapid carbon formation due to secondary reactions, eventually leads to catalyst deactivation. Transition metals like Ni and Co are preferred for the catalyst in terms of cost and availability. Also it has been of interest working at low temperatures (500-600°C) for energetic costs and possible benefits in the catalyst performance [2].

Ion-lithium batteries (ion-Li) are the most preferred for small devices and their increasing worldwide use poses a challenge for the waste management [3]. The general cathode material of this batteries consist in a complex oxide mixture of Li, Ni, Mn and Co metals. The negative impact of wrong disposal of the batteries and the cost of their treatment makes necessary to consider the recycling as an opportunity to recover and revalue these type of materials. In this sense, recycling of the Ni, Co and Mn could be interesting as precursors metals for catalyst in the DRM. In this work we compare the characteristics of recycled catalysts with similar commercial salt preparations and their performance in the DRM reaction at low temperature (600°C).

### Materials and Methods

The hydrometallurgical procedure used for the recovery of metals present in depleted ion-Li batteries was described elsewhere by our investigation group at CINDECA [4]. The leached solution containing Ni, Co, Mn and Li was used with the incipient wetness co-impregnation method, with γ-Al<sub>2</sub>O<sub>3</sub> as support. The solid obtained was dried at 105°C for 24 h and calcined at 600°C for 4 h in air. This procedure was repeated to obtain two solids with increase metal concentration, and two more solids with commercial salts Ni(NO<sub>3</sub>)<sub>2</sub>.6H<sub>2</sub>O (Aldrich, 99,999%), Co(NO<sub>3</sub>)<sub>2</sub>.6H<sub>2</sub>O (Aldrich, 99,999%) and Mn(NO<sub>3</sub>)<sub>2</sub> (Aldrich, 50% wt. solution in dilute nitric acid) for comparing. All solids were characterized by SBET, DRX, SEM, TPR and XPS.

The DRM reaction was evaluated in a fixed bed reactor with 30 mg of catalyst. All catalyst were reduced at 600°C for 1.5 h with H<sub>2</sub> (70 ml.min<sup>-1</sup>) and balanced with Ar. The reactant gases consisted in a mixture of CH<sub>4</sub>/CO<sub>2</sub>/N<sub>2</sub> (relation 1:1:8) and GHSV of 200 L.h<sup>-1</sup>.g<sup>-1</sup>. The reactants and products were on-line analyzed with Shimadzu GC-8A and a TCD detector.

### Results and Discussion

In Table 1 are depicted some characterizations results of the catalysts and their activity for the DRM. The catalyst impregnated with the batteries lixiviate with increasing concentration are named "LX1" and "LX2", respectively. "NiCo" and "NiCoMn" are the solids made from commercial salts (nitrates) of the metals, impregnated in γ-Al<sub>2</sub>O<sub>3</sub>. The performance for DRM was comparable with that of the commercial catalysts, with a decrease in conversion for the lixiviate ones, possibly related with the decrease in S<sub>g</sub> and with differences in coordination of the metals such as Mn and Co in the structure. The incorporation of Mn has a positive effect in the conversions and H<sub>2</sub>/CO relation. Increasing the metal %w/w on the solids made from lixiviate has a counter effect in the performance. A stability test was runned and after 30 h reaction showed for LX1 and NiCoMn similar conversion and H<sub>2</sub>/CO relation. Future test aim for studying the atomic environment of the metal species such as Ni, Li and their role in the reaction.

Table 1. Characterizations and Catalytic Performance

Catalyst	Metals Concentration <sup>1</sup> %w/w	S <sub>g</sub> (m <sup>2</sup> /g)	Catalytic Performance <sup>2</sup>		
			X <sub>CH4</sub> %	X <sub>CO2</sub> %	H <sub>2</sub> /CO
γ-Al <sub>2</sub> O <sub>3</sub>	-	189.8	-	-	-
NiCo	Ni 4% ; Co 4%	175.4	48.7	53.3	0.93
NiCoMn	Ni 4% Co 1% Mn 2%	195.3	61.0	55.8	1.08
LX1	Ni 3% Co 1% Mn 1%	138.7	47.5	53.1	1.23
LX2	Ni 6% Co 1% Mn 3%	120.2	46.1	43.8	0.91

1- Measured by ICP. 2- Reaction Conditions: 600°C, atmospheric pressure, measured at 3 h.

### Significance or Main Conclusions

In the aim for a circular economy, the recovery and revalue of materials of ión-Li spent batteries, the metals present in cathode material like Ni, Co and Mn can be recycled and used for the synthesis of catalytic materials with applications in the DRM reaction, giving performances comparable to commercial catalysts for this reaction at relative low temperature.

### References

- [1] I.V. Yentekakis, P. Panagiotopoulou, G. Artemakis; Appl. Catal. B: Environmental 296 (2021) 120210.
- [2] Y. Zhang, R. Zeng, Y. Zu et al.; Chinese Journal of Chemical Engineering 48 (2022) 76-90.
- [3] K.M. Winslow, S.J. Laux, T.G. Townsend; Resources, Conservation and Recycling 129 (2018) 263-277.
- [4] C.G. Marcoccia, M.A. Peluso, J. E. Sambeth; Molecular Catalysis 481 (2020) 110223.

## Catalytic Gasification of Biomass Residues at Bench Scale: Effect of reforming with recycle catalysts and Gasifying Agents

Lina Garcia<sup>1,2</sup>, Misael Cordoba<sup>1</sup>, Liza Dosso<sup>1</sup>, Carlos R. Vera<sup>1</sup>, Mariana Bustos<sup>1</sup>, Juan M. Badano<sup>1</sup>

<sup>1</sup>INCAPE, Colectora Ruta Nacional 168 Km 0, Santa Fe 3000 (Argentina)

<sup>2</sup>Grupo de Investigación (GCISA), Universidad del Cauca, calle 5 No. 4-70, Popayán 1100, (Colombia)

\* lgarcia@fiq.unl.edu.ar

### Introduction

The use of biomass residue as a resource of renewable energy has increased in the last years. The main residues used are the lignocellulosic such as of wood and different cereals (sorghum and rice) [1]. The catalytic gasification technology is based on incomplete combustion process, where the biomass and the gasifying agent generate a syngas. It is compound of H<sub>2</sub>, CH<sub>4</sub>, CO, CO<sub>2</sub> and light or heavy hydrocarbons, known as tar [2]. This last one presents a negative effect to the syngas applications. An alternative to eliminate them is the catalytic thermal method, which uses catalysts that transform tar at lower temperatures, with higher gas yields and better quality. These catalysts can be used directly in the gasifier or downstream in a reformer. The most commonly used catalysts in gasification are natural minerals and downstream of the gasifier in the reforming are supported transition and noble metals [3]. The quality of the syngas depends on the biomass and operating conditions such as the use of catalysts and gasifying agents. An optimal gas for energy applications [4] must have a tar content <0.5 g/Nm<sup>3</sup>, H<sub>2</sub>:CO ratio ≥ 1 and a lower heating power (LHV) ≥ 5 kJ/L. The aim of this work is to study the catalytic gasification of biomass thought of parameters as total tar (g/Nm<sup>3</sup>), H<sub>2</sub>:CO ratio and lower heating value (LHV) of syngas. The effect of the catalysts in the reforming (recycled catalysts) as also of the gasifying agents (air, steam, O<sub>2</sub> and mixture) were evaluated to generate a gas with potential for energy applications.

### Materials and Methods

The pine sawdust (residue) was used to the gasification. Previously, it was sieved between 0.50-0.85 mm and dried at 120°C for 48 h. The catalyst used as fluidizing material and catalyst in the gasifier was Dolomite (Dol). While in the reforming a pyrolysis residue (RP) and Ni-Mo on alumina (NiMo/Al) were used. Dol was supplied by José Luis Calvo Explotación Minera (Argentina). Prior to use, Dol was calcined in air at 700°C for 24 h. RP was supplied by Wenten SRL (Argentina) and came from pyrolysis (550 °C, 32 h) of polyethylene (10.8%), laminated plastic, polyethylene, polypropylene and polystyrene (41.6%), spent oil (45.4%) and truck tyres (2.2%) and NiMo/Al was a spent catalyst discharged from a hydrodesulfurization (HDS) unit. This last one was calcined in air at 600°C for 20 h to eliminate carbon and sulfur compounds. These catalysts were conditioned prior to the test, it were reduced in a flow of H<sub>2</sub> (100 mL/min) at 600°C (reforming temperature) for 1 h, the gasification tests were carried out with a feed flow (biomass) of 0.840 kg/h in the gasifier with catalytic reformer coupled downstream. The gasifying agents were air, steam, O<sub>2</sub> and mixture of them. With the same equivalent ratio (ER) of 0.45 and steam /biomass ratio (SB) of 0, condition (1) and 0.006, condition (2).

### Results and Discussion

Figure 1 shows the total tar (g/Nm<sup>3</sup>), LHV (kJ/L) and H<sub>2</sub>:CO ratio of syngas in the conditions evaluated during catalytic gasifying with Dol (catalyst/biomass ratio: C/B of 0.16) and reforming with the recycled catalysts NiMo/Al and RP (space velocity: WHSV of 6 h<sup>-1</sup>) at 600°C, with ER:0.45 (air and mixture O<sub>2</sub>-air). Without steam (1) SB:0 and with steam (2) SB:0.006. It was evident that steam contribution increases the H<sub>2</sub>:CO ratio and decreases of tar content, this effect was marked in the gasification and reforming with both catalysts due to the steam favor reactions such as Water Gas Shift that promote the generation of H<sub>2</sub> and a tar less refractory. For the other hand, the use of the mixture O<sub>2</sub>-air and O<sub>2</sub> as gasifying agents instead of air improved the LHV, reaching the highest value with O<sub>2</sub> (~9 kJ/L) due to the syngas is not dilute with the N<sub>2</sub> of air. The recycled catalysts used in the reforming (NiMo/Al and RP) presented catalytic good activity on the reduction of tar with values < 1 g/Nm<sup>3</sup> and H<sub>2</sub>:CO ratio >1 showing the benefit of employing the catalytic reformer. The recycled catalysts NiMo/Al and RP presented good performance, which is attractive from the environmental and economic point

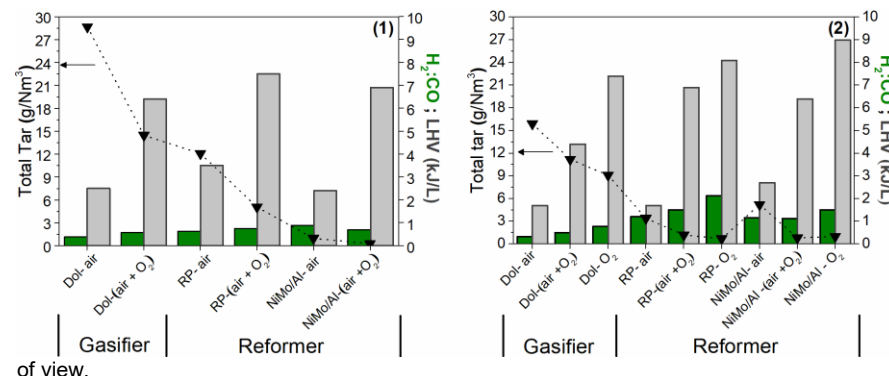


**Figure 1.** Catalytic gasification and reforming with ER: 0.45 and different AG (1) SB: 0 and (2) SB: 0.006. Total tar (▼), LHV (kJ/L) (■) and H<sub>2</sub>:CO ratio (▲).

### Conclusions

The gasifying agents and recycled catalysts (RP and NiMo/Al) showed a positive effect on the quality of the syngas. The autothermal and catalytic gasification at bench scale with downstream catalytic reforming was used to obtain syngas with quality promising for energy applications from agroforestry residues such as pine sawdust.

### References

- [1] A. Akbarian et al. Bioresource Technology 362 (2022) 127774.
- [2] A. Molino, S. Chianese, D. Musmarra; Journal of Energy Chemistry 25 (2016) 10-25.
- [3] L. Garcia et al. Topics in Catalysis 65 (2022) 1382–1393.
- [4] M. Valderrama et al. Biomass and Bioenergy 108 (2018) 345-370.



## Glycerol as raw material to a biorefinery

Ezequiel H. Promancio<sup>1</sup>, Leonardo A. Gusé<sup>1</sup>, Fernando E. Tuler<sup>1</sup>, Lisandro R. Ferrari<sup>1,2</sup>,  
Diego J. García Touza<sup>2</sup>, Carlos M.J. Casas<sup>2</sup>, and Raúl A. Comelli<sup>1\*</sup>  
<sup>1</sup> INCAPe (UNL – CONICET). CCT-CONICET-Santa Fe. Santa Fe 3000 (Argentina)  
<sup>2</sup> Varteco Química Puntana S.A. Villa Lynch (Pcia. de Buenos Aires) 1672 (Argentina)  
\* rcomelli@fiq.unl.edu.ar

### Introduction

Argentine has an installed capacity of 4.0 Mt/y of biodiesel, being 82% located in the Province of Santa Fe. The biodiesel process also produces glycerol, about 10wt.% of the total product; consequently, 0.4 Mt/y of glycerol would be available, being 0.2 Mt/y the USP grade glycerol capacity which is mainly to export. Glycerol can be considered as the “co-product” in the biodiesel process, and it could be fed as raw material to a biorefinery.

Selective oxidations of glycerol in liquid phase to dihydroxyacetone (DHA) and lactic acid, selective reductions of glycerol in gas phase to propylene glycol (PG) and/or ethylene glycol (EG), and the steam reforming of glycerol to hydrogen ( $H_2$ ) or syngas (hydrogen plus carbon monoxide), were studied to produce those added-value chemicals and energetic compounds and also to show a possible integration of processes into a biorefinery framework.

### Materials and Methods

Details of catalyst preparations, techniques and equipments for their characterizations, and systems to measure their catalytic performances, were previously published [1].

### Results and Discussion

Selective oxidations of glycerol in liquid phase produced: *i*) DHA on Pt/K-FER, being the first active and selective monometallic catalyst in this reaction, improving catalytic behavior using Pt-Bi/K-FER, reaching 75.9% conversion and 93.9% selectivity to DHA [2]; and *ii*) lactic acid on Cu/Al<sub>2</sub>O<sub>3</sub>, obtaining 99.8% conversion and 86.5% selectivity to lactic acid. Selective reductions of glycerol in gas phase produced: *i*) PG on Cu-Ce/Al<sub>2</sub>O<sub>3</sub>, reaching 99.8% conversion and 83.2% selectivity to PG [3]; and *ii*) EG on Ni/SiO<sub>2</sub>, achieving 100% conversion and 91% selectivity to EG in the liquid fraction [4]. These reduction reactions demand  $H_2$ , which can be obtained by steam reforming of glycerol using Ni/Al<sub>2</sub>O<sub>3</sub> promoted by adding compounds such as Ce, Co, Mg, and Zr; this steam reforming also produced carbon oxides and methane, being possible to use the syngas ( $H_2$  plus carbon monoxide) and methane as energetic compounds and carbon dioxide to carbonylation reactions.

From the strong link with the productive sector, two pilot plants are in the final building step, one to produce 100 t/y of PG from glycerol but versatile to also obtain acetol (intermediate product in the reaction to PG) and/or EG, and another one for reforming glycerol to produce the  $H_2$  demanded for the previous reduction processes. Consequently, glycerol was converted to DHA, lactic acid, PG, acetol, EG,  $H_2$ , syngas, carbon dioxide, and methane; then, the possible integration of the corresponding processes allows consider the co-product of biodiesel as an example to apply the concept of biorefinery [1]. In 2021, the project "GLYCEROL as Raw Material for BIREFINERY" received the Technological

Innovation Award from the ACADEMIA NACIONAL de CIENCIAS EXACTAS, FÍSICAS y NATURALES – ANCEFN of Argentine. Nowadays, a new project is starting being its objective to design and build an integrated platform to validate in a bench scale, catalytic processes which taking place in both liquid and gas phase, adding value to the oleochemical chain, using initially glycerol as raw material.

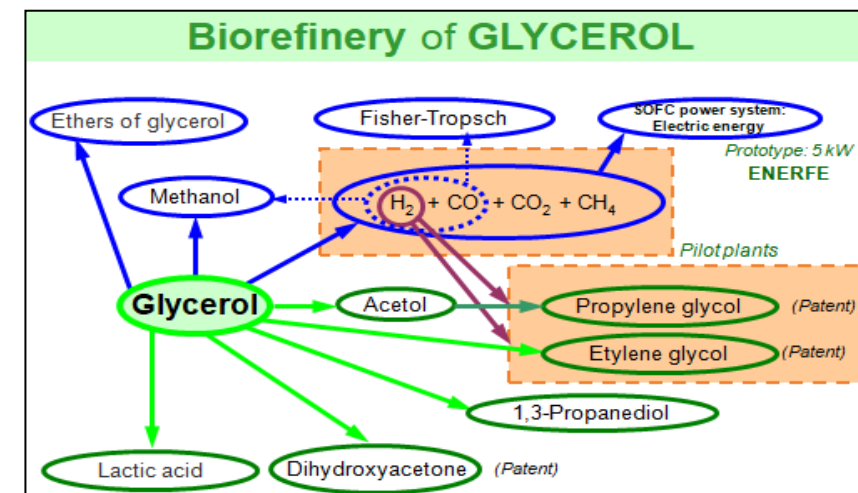


Figure 1. Added-value chemicals and energetic compounds from glycerol.

### Significance or Main Conclusions

The original obtained results allowed their protection and their transfer to the productive sector. From the strong link with this sector, two pilot plants are in the final building step, one to produce 100 t/y of PG from glycerol but versatile to also obtain acetol and/or EG, and another one for reforming glycerol to produce the  $H_2$  needed for these reduction processes.

### References

- [1] L.R. Ferrari, F.E. Tuler, E. Promancio, L. Gusé, D. García Touza, C. Casas, R.A. Comelli; Catalysis Today 394-396 (2022) 247-255.
- [2] R.A. Comelli, S. Antuña; Un Catalizador de oxidación selectiva de glicerol a dihidroxiacetona y un proceso para su elaboración: AR 078267 B1 (2016).
- [3] R.A. Comelli, L.R. Ferrari; Catalytic process for the production of propylene glycol from glycerol in the presence of a cerium and copper catalyst: EP 3 235 566 B1 (2019); US 10,857,522 B2 (2020); BR 112017012993-0 (2021); and AR 098779 B1 (2021).
- [4] R.A. Comelli, F.E. Tuler; Un proceso de obtención de etilenglicol a partir de glicerol y un catalizador de Ni para este proceso: AR 114944 B1 (2022).



## Zinc Oxide recovered from spent alkaline batteries as photocatalyst for emergent contaminant degradation

Maria Gallegos<sup>1\*</sup>, Franco Dubois<sup>1</sup>, Laura Damonte<sup>2</sup>, Paula Caregnato<sup>3</sup>, Paula I. Villabril<sup>1</sup>,

<sup>1</sup>CINDECA (UNLP - CONICET - CIC), calle 47 n°257, La Plata 1900 (Bs. As.,Argentina)

<sup>2</sup>IFLP (UNLP- CONICET) Diagonal 113 y 64, La Plata 1900 (Bs. As.,Argentina)

<sup>3</sup>INIFTA (UNLP - CONICET), Diagonal 113 y 64, La Plata 1900 (Bs. As.,Argentina)

\*mvgallegos@quimica.unlp.edu.ar

### Introduction

Carbamazepine (CBZ) is an antiepileptic and psychiatric drug, belonging to the group of emerging contaminants (EC) [1]. The world consumption of this drug is around 1,000 tons per year. It is very persistent and resistant to biodegradation [2]. On the other hand, battery consumption is also an environmental problem due to its final disposal. Zinc, one of the main pollutants, can be released by the attack of climatic agents, leaching through soils to reach surface water courses and aquifers, contaminating the environment [3]. To avoid this harmful action, it is possible to obtain ZnO from spent batteries [4] whose versatility and its possible use in advanced oxidation processes for the effective removal of EC is widely known.

Therefore, in this work, we propose to prepare two ZnO-based materials from battery waste, characterize them, and evaluate their performance in the photocatalytic degradation of CBZ.

### Materials and Methods

Two solids were prepared from solutions obtained from the leaching of anodic paste from spent alkaline batteries. The leaching process was previously described by Gallegos et al [4]. The scheme shown in Figure 1 shows the steps followed to obtain the materials. XRD, SEM, TEM, Raman, and DRS techniques were used to characterize the materials. Photocatalytic experiments were carried out in a glass reactor at 25°C, in air, and with continuous magnetic stirring. A Rayonet RPR-100 photochemical reactor with eight interchangeable UV-A ( $\lambda_{\text{max}} 365$  nm) or vis ( $\lambda_{\text{max}} 575$  nm) lamps was used. The quantification of CBZ at different irradiation times was determined by high-performance liquid chromatography at 200 nm wavelength.

### Results and Discussion

The characterizations evidenced the effect of the counterion's nature present in the solutions on the observed structural and morphological properties. In both solids, the presence of the wurtzite phase was detected, however, a second phase of Zn(SO<sub>4</sub>) was observed in the NPS-ZS material.

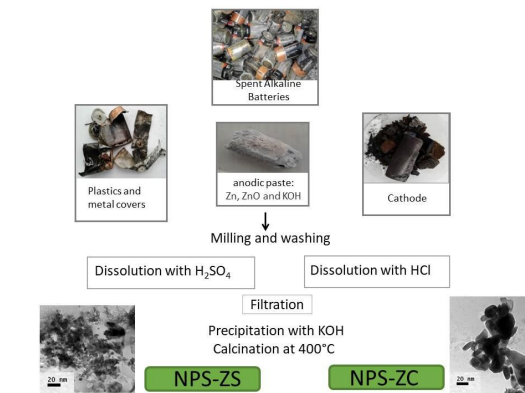


Figure 1. Flow- sheet of the preparation of ZnO from spent alkaline batteries

Control results showed neither significant adsorption of CBZ on the materials nor direct photolysis of CBZ with UV or vis light. Regarding the photocatalytic activity, the NPS-ZC catalyst showed a better performance than the NPS-ZS for CBZ degradation with UV lamps. The percentage of degradation of CBZ was 93% after 3 h. using UV irradiation (see Table 1).

Table 1. Photocatalytic Results

	% CBZ degradation	
	UV irradiation	vis irradiation
NPS-ZS	74±6	6±5
NPS-ZC	93±5	12±5

Reaction conditions:  $[CBZ]_0 = 15 \text{ ppm}$ , 1 g/L catalyst,  $V = 80 \text{ mL}$ , 25 °C, 3 h.

### Significance or Main Conclusions

This study demonstrates that it is possible to prepare photocatalysts using metals recovered from spent alkaline batteries as raw materials and that they can be used to efficiently degrade contaminants of concern, such as pharmaceuticals. This work is framed within the principles of Green Chemistry since it introduces a valorization of environmentally hazardous waste.

### References

- [1] C. Peña-Guzmán, S. Ulloa-Sánchez, K. Mora, et al.; J. Environ. Manage. 237 (2019) 408–423.
- [2] R. Meribout, Y. Zuo, A.A. Khodja, et al.; J. Photochem. Photobiol. A: Chem. 328 (2016) 105–113.
- [3] E.M. Melchor-Martínez, R. Macías-Garbett, A. Malacara-Becerra, et al.; Chem. Environ. Eng. 3 (2021) 100104
- [4] M.V. Gallegos, F. Aparicio, M. Peluso, et al; Mater. Res. Bull 103 (2018) 158-16



## Catalytic fast pyrolysis of tomato plants residual biomass

Jose L. Buitrago<sup>1</sup>, Juan J. Musci<sup>2</sup>, Hernan Bideberripe<sup>1</sup>, Mónica L. Casella<sup>1</sup>, Luis R. Pizzio<sup>1</sup> and Illeana D. Lick<sup>1\*</sup>

<sup>1</sup> CINDECA (CONICET – UNLP-CIC), 47 N° 257, La Plata 1900, Argentina.

<sup>2</sup> CITNOBA (UNNOBA-UNSA-CONICET), Monteagudo 2772, 2700, Pergamino, Argentina

\*ilick@quimica.unlp.edu.ar

### Introduction

Catalytic biomass pyrolysis is a promising technology for using residual biomass to produce value-added products with a wide range of applications. However, there is a challenge in developing catalysts that can efficiently produce profitable pyrolysis products [1-4]. The catalytic and non-catalytic pyrolysis of tomato residual biomass from La Plata and El Gran La Plata plantations were performed using acid catalysts. The catalysts were synthesized from the immobilization of tungstophosphoric acid (TPA), a heteropolyacid with a Keggin structure, in zirconia with a multimodal porous structure created by adding macro- and mesoporous templates ( $\text{ZrO}_2\text{-SiO}_2\text{-P123-TPA}$ ) and they were thoroughly characterized. The presence of catalysts during the fast pyrolysis experiments modified the bioliquid composition. The results showed an increase in the production of furan derivatives when the pyrolysis was carried out in presence of the  $\text{ZrO}_2\text{-SiO}_2\text{-P123-TPA}$  catalyst, as well as a decrease in the number of products obtained compared to the non-catalyzed tests.

### Materials and Methods

The catalysts were synthesized by immobilizing TPA on micro-mesoporous and mesomacroporous zirconium oxide ( $\text{ZrO}_2\text{-TPA}$  and  $\text{ZrO}_2\text{-SiO}_2\text{-P123-TPA}$  respectively). The  $\text{ZrO}_2\text{-SiO}_2$  was generated by the hydrolysis of zirconium n-propoxide and the addition of silica nanospheres (230–300 nm) synthesized by a modified Stöber method [2] and Pluronic P123 (Sigma Aldrich), as mesoporous macro- and mesoporous formers, respectively. In the case of  $\text{ZrO}_2$  the synthesis was performed without the template addition. The template removal was conducted through sodium hydroxide washing under ultrasonic treatment. The catalysts were obtained by wet impregnation of the synthesized support with a TPA ethanol solution. The concentration solution was chosen to obtain 25% TPA content in the final material. The materials were calcined at 450°C during 2 h. The solid characterization was performed using several techniques such as, Fourier Transform Infrared spectroscopy (FT-IR), scanning electron microscopy (SEM),  $\text{N}_2$  adsorption-desorption analysis, potentiometric titration with nbutyl amine and thermogravimetric analysis (TGA). The catalytic pyrolysis experiments were performed in a fixed-bed tubular reactor. The reactor was loaded with 1 g of biomass, keeping a 2:1 ratio of biomass and catalyst for the catalytic test, and with only biomass for the noncatalytic tests. The tests were carried out at 450°C and with a nitrogen flow rate of 200 mL/min for 5 min. The condenser was maintained at  $0 \pm 1^\circ\text{C}$ . The bio-liquid produced was then weighed, extracted, and analyzed using a Shimadzu GCMS-QP2010SE gas chromatograph mass spectrometry (GC-MS) system.

### Results and Discussion

The study aimed to investigate the impact of catalytic and non-catalytic conditions on the product distribution of the liquid fraction obtained from pyrolysis. SEM micrographs and textural results showed that the addition of pore-formers resulted in changes in the morphology and pore size distribution, increased  $S_{\text{BET}}$  and  $d_p$  of the solids. This increase is attributed to a greater mesopores formation during the synthesis process, associated with the addition of Pluronic. It is worth mentioning that the  $\text{ZrO}_2\text{-SiO}_2\text{-P123-TPA}$  catalyst also contains macropores, generated by the  $\text{SiO}_2$  nanospheres. However, the area ascribed to their presence cannot be measured by  $\text{N}_2$  adsorption. FT-IR analysis indicated that the pore-formers were successfully eliminated by NaOH-and ultrasonic treatment, while potentiometric titration showed that the number of acid sites and their strength decreased in the order  $\text{ZrO}_2\text{-TPA} > \text{ZrO}_2\text{-SiO}_2\text{-P123-TPA}$ . Results showed that the yield of the liquid fraction was in the range of 35–38% for both conditions and, also was found that the presence of catalysts hindering the formation of some products. The comparison of the catalytic performance of the catalyst showed that  $\text{ZrO}_2\text{-SiO}_2\text{-P123-TPA}$  catalyst exhibits superior performance in terms of furfural yield. This fact can be attributed to its increased surface area and moderate acidic sites. These findings suggest that incorporating pore-formers in catalyst synthesis could be a strategy for optimizing catalytic processes [3,4].

**Table 1. Physicochemical properties and catalytic results**

Catalyst	Products of pyrolysis (%)				Physicochemical properties				
	P1	P2	P3	P4	Acid site number*	Ei (U/mV)	$S_{\text{BET}}$ ( $\text{m}^2 \text{g}^{-1}$ )	$V_p$ ( $\text{cm}^3 \text{g}^{-1}$ )	$d_p$ (nm)
Non-catalytic	8.1	13.0	7.6	16.5	n.d	n.d	n.d	n.d	n.d
$\text{ZrO}_2\text{-TPA}$	12.1	13.0	7.6	16.5	185	684	159	0.1	3.0
$\text{ZrO}_2\text{-SiO}_2\text{-P123TPA}$	15.8	16.1	7.6	14.5	77	122	191	0.2	3.7

P1:Furfural, P2:Acetol, P3: 2,3 Furanone, P4:Acetic Acid

### Main Conclusions

The results showed that the  $\text{ZrO}_2\text{-SiO}_2\text{-P123-TPA}$  and  $\text{ZrO}_2\text{-TPA}$  catalysts, acid and multiporous material, displayed very good performance for the fast pyrolysis processes in terms of reaction selectivity and directed the reaction towards the formation of furanic compounds.

### References

- [1] J.L. Buitrago, I.D. Lick, L.R. Pizzio, et al. ANAIS Do 28o Congresso Ibero Americano de Catálise. Campinas: Galoá. (2022).
- [2] P.M. Arnal, C. Weidenthaler, F. Schüth, Chemistry of Materials 18 (2006) 2733– 2739.
- [3] X. Bai, J. Li, C. Jia, et al. H. Chen, Fuel 258 (2019) 116089.
- [4] Y.Y. Chong, S. Thangalazhy-Gopakumar, H. K. Ng, S. Gan, L.Y. Lee, P.B. Ganesan; Clean Technol Environ Policy 21 (2019) 1629–1643.

## 5-Hydroxymethylfurfural production from fructose/isopropanol mixture with sulfonic resins as a catalyst in a continuous flow reactor

Gabriel Pestana, Lucila Pierantoni and Javier M. Grau\*

INCAPE, CCT-CONICET, Rn 168, Km 0, Santa Fe, 3000, (Argentina), \*jgrau@fiq.unl.edu.ar

### Introduction

The 5-hydroxymethylfurfural (HMF) it's a platform compound for the synthesis of liquid biofuels like 2,5-Dimethylfuran (DMF) or 5-Etoximethylfurfural (EMF) [1]. Biomass is the only renewable and plenty available sustainable carbon resource. Glucose from lignocellulosic biomass can be easily isomerized to fructose whose dehydration produces HMF using acid catalysts [2]. A wide variety of acid catalysts have been studied for these reactions in biphasic water/organic solvent systems and in batch reactors [3,4]. Although some authors propose continuous reactors, they do not consider the feasibility of a future industrial scale-up due to the costs and toxicity of catalysts and solvents [5]. Besides, in an aqueous acid environment, carbohydrates and their derivatives produce a wide range of by-products that diminish the yield and selectivity of products. In this work, we compare the behavior of two simple cationic ion exchange resins in a continuous flow reactor with a WHSV of  $3.1 \text{ h}^{-1}$  at  $120^\circ\text{C}$  using  $45 \text{ g L}^{-1}$  fructose in isopropanol for 240 min. The best of them holds a yield and selectivity to HMF up to 57.6% and 62.2% respectively at steady state, with a fructose conversion of 99.7%.

### Materials and Methods

**Materials:** IONAC® cation ion exchange resins has been used, the Mesoporous CFP110 (RII/M)-H<sup>+</sup> and the gel type C267 (RII/G)-H<sup>+</sup>. Both were activated by ionic exchange with HCl (1N), 30 min at (1:3 ratio v/v), washed with deionized water until neutral pH was reached and dried for 12 h at  $100^\circ\text{C}$ . The acid strength and the total number of acid sites were determined by potentiometric titration with butyl amine (0.01N) in acetonitrile.

**Catalytic evaluation:** The reaction was carried out in a continuous tubular reactor at 10 bar of N<sub>2</sub>. 0.35 g of catalyst was loaded with carborundum above and below forming a fixed bed in the middle of the reactor. The fructose was diluted in isopropanol/water (9:1 ratio v/v), and an HPLC pump feeds the fructose solution at a rate of  $0.4 \text{ ml min}^{-1}$  setting a WHSV of  $3.1 \text{ h}^{-1}$ . The reaction temperature was fixed at  $120^\circ\text{C}$  with a rate of heating of  $4^\circ\text{C min}^{-1}$ , and the catalytic run was carried out for 240 min, taking liquid samples in a collector every 30 min. The liquid samples were analyzed to quantify the fructose and products by HPLC with a YL9100 equipped with a U.V detector measuring simultaneously at 190 and 284 nm. An AMINEX HPX-87H Biorad column using 5mM H<sub>2</sub>SO<sub>4</sub> as a carrier at 50 bar, 0.65 ml/min, and  $65^\circ\text{C}$ .

### Results and Discussion

Table 1. shows resin properties. The (RII/G)-H<sup>+</sup> showed higher acid strength (higher  $EI^\circ$ ) [6], and higher concentration of total acid sites than the (RII/M)-H<sup>+</sup>. The total amount of acid sites has been related to the %DVB and surface area as reported in [3], this might be attributed to the localization and availability of the acid sites in the porous or reticular structure. Fructose conversion and selectivity to HMF are shown in Figure 1.A. Both resins show a high conversion: (RII/M)-H<sup>+</sup> showed a very stable behavior, with a fructose conversion of 92-96%

**Table 1.** Resins properties and acidity characterization (acid strength and total acid sites).

Resin	Sg ( $\text{m}^2\text{g}^{-1}$ )	DVB (%)	EI° (mV)	Total acidity (Equiv H <sup>+</sup> g <sup>-1</sup> )
(RII/M)-H <sup>+</sup>	35.0	20.0	500	0.1
(RII/G)-H <sup>+</sup>	1.0	8.0	550	0.6

and HMF selectivity of 55-62%. The (RII/G)-H<sup>+</sup> shows a slight deactivation with a conversion drop from 99-85% and selectivity to HMF from 49-44%. The characterization suggests that the unsteadiness of (RII/G)-H<sup>+</sup> could be attributed to its higher acidity [7]. Similarly, it is shown in Figure 1.B, that both resins were active in the production of HMF but (RII/M)-H<sup>+</sup> achieved a higher HMF yield than (RII/G)-H<sup>+</sup> under reaction conditions throughout the period time, (on average 57.6% higher than 39.6% respectively). In addition, (RII/M)-H<sup>+</sup> has reached a more stable production of HMF than (RII/G)-H<sup>+</sup>, which could be attributed to the possible deactivation of (RII/G)-H<sup>+</sup> during the experiment. Since higher acidity could promote secondary reactions, producing alkoxides, levulinates [1], and humins [2,4] which can polymerize and deposit as carbon produced by the degradation of those by-products or even the degradation of fructose and HMF [2,3,5,7]. In both cases, no etherification product was observed, confirming the stability of isopropanol under the reaction conditions.

### Significance or Main Conclusions

High acidity in the resin can produce deactivation by degradation of fructose, HMF, or by-products by deposition of humins, decreasing the yield of HMF. The (RII/M)-H<sup>+</sup> resin has shown the highest production of HMF and a stable behavior over time due to its adequate acidity. Isopropanol is a suitable solvent to stabilize the reaction product. This resin/solvent system will be used to optimize operating conditions looking for a scale-up of the process.

### References

- [1] E. Ramírez, R. Bringue, C. Fité, et al; J Chem Technol Biotechnol 92 (2017) 2775-2786.
- [2] B. Torres, I. Fuñez, C. García, J. Cecilia, R. Moreno, et al; Chem. Proc. 2 (2020) 34-39.
- [3] F. Richter, K. Pupovac, R. Palkovitz, F. Schüth, et al; ACS Catal. 3 (2013) 123-127.
- [4] S. Pyo, M Sayed, R. Hatti-Kaul; Org. Process Res. Dev. 23 (2019) 952-960.
- [5] C. Tempelman, U. Jacobs, T. Hut, E. Pereira, et al; App Cat A, Gen. 588 (2019) 117-267.
- [6] A. Sosa, M. Gorsd, M. Blanco, L. Pizzio; J Sol-Gel Sci-Tec 83 (2017) 355-364.
- [7] R. Karinen, K. Vilonen, M. Niemela; ChemSusChem 4 (2011) 1002-1016.

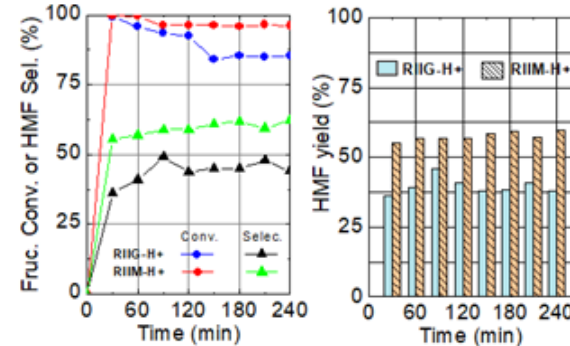


**Figure 1.A)** Fructose conversion and HMF selectivity. **B)** HMF yield.



## Effect of support acidity and pore size in the synthesis of 2,5-Dimethylfuran in Pd supported over Y and L zeolites

Gabriel Pestana, Lucila Pierantoni and Javier M. Grau\*

INCAPE, CCT-CONICET, Rn 168, Km 0, Santa Fe, 3000, (Argentina), \*jgrau@fiq.unl.edu.ar

### Introduction

In the context of biorefineries, 2,5-Dimethylfuran (DMF) is a promising biofuel that can replace petroleum-derived octane boosters (MTBE) due to its excellent properties similar to naphtha [1]. The method to obtain DMF is mainly by reduction of the formyl and hydroxyl groups of 5-Hydroxymethylfuran (HMF) using supported metal catalysts in organic solvents such as alcohols. Some authors proposed a system to obtain DMF in good yield (79%) by hydrogenation of HMF over a Cu-Ru/C catalyst using butanol as solvent [1]. Several works have been published on this reaction testing metals supported on different materials and solvents, for example, Pt/C with acetonitrile as a solvent [2]. Our work analyzes the effect of the acidity and pore size of two commercial zeolites, the dispersion, and particle size of Pd selected as hydrogenating metal over the overall reaction performance and selectivity to DMF.

### Materials and Methods

**Materials:** Two commercial zeolites: K-LTL (Lynde Type L, Union Carbide SK-45, Si/Al=3) and NaY (Faujasite Type Y, UOP-Y54, Si/Al=2.4), were used in the preparation of the catalysts. Both were stabilized in air for 4 h at 450°C, to obtain Bronsted acidity; then were exchanged with (1M) NH<sub>4</sub>NO<sub>3</sub> solution under stirring for 6 h at 90°C; the solid was washed, dried, and calcined again at the same previous conditions, this ensures the ion exchange between Na<sup>+</sup>/K<sup>+</sup> cations and NH<sub>4</sub><sup>+</sup>. During calcination, NH<sub>4</sub><sup>+</sup> decompose into H<sup>+</sup> and then NH<sub>3</sub> was released. Subsequently, Pd was added as active phase by the incipient wet impregnation method. An aqueous solution of PdCl<sub>2</sub> was impregnated on the supports with enough concentration to achieve 1% wt of Pd (verified by ICP). The catalysts were dried, calcined in air for 4 h at 450°C, and reduced for 1 h to 500°C in H<sub>2</sub> flow (50 mL min<sup>-1</sup>). The catalysts were identified (with and without exchange with NH<sub>4</sub><sup>+</sup>) as PdHL, PdHY, and PdKL, PdNaY.

**Characterization:** The porous texture of the catalysts was studied in an ASAP 2020 by N<sub>2</sub> adsorption-desorption at -196 °C; all the samples were previously outgassed for 6 h at 200 °C under vacuum (10<sup>-6</sup> Torr), the BET and t-plot methods were used to calculate the specific surface area (Sg) and micropore volume (V<sub>p</sub><sup>MIC</sup>), and total pore volume was quantified by the N<sub>2</sub> at P/P<sub>0</sub> = 0.99 (V<sub>p</sub><sup>TOT</sup>). The acidity of the catalysts was analyzed by NH<sub>3</sub>-TPD; 0.19 g of catalyst was saturated with 25 mL min<sup>-1</sup> of 5% NH<sub>3</sub>/He at 100 °C, then the NH<sub>3</sub> was desorbed by increasing the temperature up to 940 °C (10 °C min<sup>-1</sup>) and monitored with a TDC. The mean Pd particle size MPS<sub>Pd</sub>, and metallic dispersion %D, were measured by TEM.

**Catalytic evaluation:** In a batch reactor, 0.25 g of reduced catalyst was loaded with 25 mL of a solution (20 g/L) of HMF in Butanol, and then pressurized under 15 bar of H<sub>2</sub>. The reactor was heated up to 180°C; the reaction was carried out for 2 h, stirred at 1500 RPM. To stop the reaction, the reactor was cooled with water. The liquid samples were analyzed in a Shimadzu GC-8A with a shin carbon Restek micro pack column with an FID to measure the DMF and an HPLC YL9100 equipped with a U.V detector at 284 nm, an AMINEX HPX-87H Biorad column, 5 mM H<sub>2</sub>SO<sub>4</sub> as mobile phase at 0.65 mL min<sup>-1</sup>, 50 bar, and 65°C to measure the HMF.

### Results and Discussion

Table 1 shows the properties of the catalysts. The lowest Sg and V<sub>p</sub><sub>(TOT and MIC)</sub> obtained by ASAP, the lowest MPS<sub>Pd</sub>, and the higher %D obtained by TEM are shown by the PdHL catalyst. Likewise, the acidity obtained for PdHL is intermediate between the series of catalysts studied.

**Table 1.** Properties of the Catalysts.

Catalyst	Sg (m <sup>2</sup> g <sup>-1</sup> )	V <sub>p</sub> <sup>TOT</sup> (mLg <sup>-1</sup> )	V <sub>p</sub> <sup>MIC</sup> (mLg <sup>-1</sup> )	NH <sub>3</sub> -TPD (mmolg <sup>-1</sup> )	MPS <sub>Pd</sub> (nm)	D (%)
PdKL	145	0.109	0.075	0.37	6.3	18
PdNaY	342	0.287	0.177	1.49	4.2	26
PdHL	98	0.094	0.043	1.75	1.4	79
PdHY	174	0.186	0.164	1.96	2.3	48

HMF conversion, DMF yield, and selectivity are shown in table 2. Both protonic zeolites showed higher conversion, selectivity, and yield than their cationic (Na<sup>+</sup>/K<sup>+</sup>) forms, these results confirm that H<sup>+</sup> acid sites are required for HMF hydrogenation to DMF [3]. The PdHL catalyst showed the highest HMF conversion (98.4%), DMF yield (94.7%), and selectivity (96.5%). Although PdHY and PdNaY showed high HMF conversion too, they showed lower DMF yield and selectivity than the PdHL catalyst. This drop in the yield and selectivity could be attributed due to the deactivation by oxidation, leaching or syntherization of metal sites [1,4], this may be possible due to their lower Pd dispersion, which allows an easy deactivation mechanism [1,3,4].

**Table 2.** Response in reaction conditions.

Catalyst	X <sub>HMF</sub> (%)	Y <sub>DMF</sub> (%)	S <sub>DMF</sub> (%)
PdKL	39,0	24,1	61,1
PdNaY	97,5	10,4	10,7
PdHL	98,4	94,7	96,5
PdHY	98,1	14,4	14,6

The PdHL catalyst with a higher Pd dispersion than PdHY has shown more activity in the production of DMF because it has more active sites exposed in the surface and pores to carry out the hydrogenation under the reaction conditions throughout time. The study suggests that regulated acidity [4] and low pore sizes [5] are necessary to restrain secondary reactions which produce organic byproducts that can polymerize and deposit as carbon [4].

### Significance or Main Conclusions

High acidity zeolites can produce deactivation by degradation of HMF or by-products by deposition of carbon, decreasing the yield of DMF. The PdHL catalyst has shown the highest production of DMF due to its adequate acidity, higher dispersion, lower particle size, and pore volumes. Also, Butanol is a suitable solvent to stabilize the DMF. This zeolite/solvent system will be used to optimize operational conditions looking to design a continuous flow process.

### References

- [1] Y. Roman-Leshkov, C. Barrett, Z. Liu, J. Dumesic, et al; Nature, 447 (2007) 982-986.
- [2] M. Chidambaram, A. Bell; Green Chem, 12 (2010) 1253-1262.
- [3] A T. Hoang, S. Nizetic, A L. Olcer, H C. Ong; Fuel 286 (2021) 119337.
- [4] L. Esteves, M. Brijaldo, E. Oliveira, J. Martinez, H. Rojas, et al; Fuel 270 (2020) 1175242.
- [5] C. Naimeng, Z. Zhiguo, M. Haikuo, et al; Molecular Catalysis 486 (2020) 110882.

## Valorization of glycerol by esterification reactions

Bruno Dalla Costa<sup>1</sup>, Hernán Decolatti<sup>1</sup>, Maira Maquirriain<sup>1</sup>, María Laura Pisarello<sup>1</sup>, Lucas Tonutti<sup>1</sup> and Carlos Querini<sup>1\*</sup>

<sup>1</sup>INCAPE, Colectora RN 168 – CCT CONICET Santa Fe, Santa Fe 3000 (Argentina)  
\*querini@fiq.unl.edu.ar

### Introduction

Biodiesel production from vegetable oils generates glycerol as a side-product, which has led to an excess of it in the market; therefore, several processes have been proposed to obtain chemicals of higher value from it [1]. Esterification of glycerol with acetic acid produces mono-, di- and triacetylglycerol (MAG, DAG, TAG, respectively), which, among other uses, can be added to biodiesel to improve its anti-knocking properties [2]. Alternatively, esterification of glycerol with fatty acids (FFA) from residual streams can produce second generation oils which can be further processed to yield biodiesel. Furthermore, the interesterification reaction between vegetable oils (Triglycerides, TG) and ethyl acetate (EA) allows to simultaneously obtain biodiesel and TAG without generating a residual glycerol stream. These reactions, apparently similar, pose different requirements to the catalysts. Series of different mesoporous materials were synthesized, tuning their porosity, acid/basic behavior and hydrophobicity. They were characterized and assayed in reaction, comparing their performances with those of blank tests and homogeneous catalysts.

### Materials and Methods

Mesoporous zeolites were prepared from commercial MFI by alkaline treatment, followed by a restoration of their acidic character. SBA-15 silicas were synthesized hydrothermally. Acidic and hydrophobic functions were provided by propylsulfonic and trimethylsilane groups, incorporated by co-condensation. Basic properties were provided by impregnation with  $\text{Ca}(\text{NO}_3)_2$  and  $\text{Ba}(\text{NO}_3)_2$  followed by calcination. Characterization included sorptometry, XRD, SAXS, ED-XRF, TEM, TPD, FTIR, TGA and titrations, among others. Reaction tests were performed in batch reactors, under reflux or vacuum, and samples were analyzed by GC. For comparison, blank tests have been performed, as well as tests with sulfuric acid (SA), *p*-toluenesulfonic acid (PTSA), methanesulfonic acid (MSA) and sodium methoxide (MeONA).

### Results and Discussion

Esterification of glycerol with acetic acid is a monophasic reaction. There, mesoporous zeolites performed close to a blank test, due to a lack of accessibility to the active sites. Contrarily, sulfonic SBA-15 catalysts were as active as homogeneous acids at equal proton equivalents per mol of reagents (Figure 1 A) [3,4]. Moreover, reusability tests showed a preservation of activity for 3 cycles.

On the other hand, esterification of glycerol with fatty acids is a biphasic reaction. Therefore, catalysts with affinity for the interphase are more favorable. In consequence, for the homogenous catalysts the order of activity was SA < MSA < PTSA [5]. Although sulfonic SBA-15 was active, it was not as active as the aforementioned acids. An improvement in reaction rate was achieved when hydrophobic groups were also incorporated, obtaining a partially

hydrophobic catalyst which was located preferentially at the interphase. The phase where the catalyst was initially dispersed was also relevant. Better performance was achieved when the hydrophobic catalyst was initially added to the oil phase. On the contrary, sulfonic SBA-15 without hydrophobic groups performed better when first incorporated to glycerol (Fig. 1 B). The level of activity in the solids was also preserved for 3 cycles [6].

Interestesterification of TG and EA is rather slow in the presence of acids, but it is favored under basic catalysis. MeONA as a reference catalyst provides good performance but its recovery is not as easy as in transesterification reactions, since no aqueous phase is formed in this case. Thus, supported superbasic catalysts were proposed. Studies are in early stages and, opposed to solid acids, basic materials are more sensitive to storage conditions and their sites are more difficult to probe.

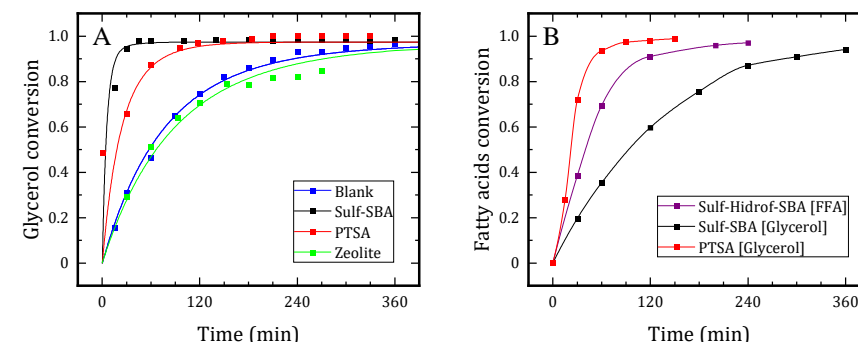


**Figure 1.** Catalytic activity for the esterification of glycerol with acetic acid (A) and with fatty acids (B). Brackets indicate the phase where the catalyst was initially added.

### Significance or Main Conclusions

Catalysts were designed according to the characteristics of the different reacting systems, achieving performances comparable to those of homogeneous catalysts commonly employed in industrial scale. Further improvements are being considered regarding hydrophobicity for biphasic systems.

### References

- [1] R. Sedghi, H. Shahbeik, H. Rastegari, S. Rafiee, W. Peng, A-S. Nizami, V. Gupta, W-H. Chen, S. Lam, J. Pan, M. Tabatabaei, M. Aghbashlo, Renew. Sustain Energy Rev. 167 (2022) 112805.
- [2] J. Melero, G. Vicente, G. Morales, M. Paniagua, J. Bustamante, Fuel, 89 (2010) 2011-2018.
- [3] L. Tonutti, H. Decolatti, C. Querini, B. Dalla Costa, Microporous Mesoporous Mater. 305 (2020) 110284.
- [4] L. Tonutti, B. Dalla Costa, H. Decolatti, G. Mendow, C. Querini, Chem. Eng. J. 424 (2021) 130408.
- [5] M. Maquirriain, C. Querini, M. Pisarello, Chem. Eng. Res. Des. 171 (2021) 86-99.
- [6] M. Maquirriain, L. Tonutti, C. Querini, B. Dalla Costa, M. Pisarello, Appl. Cat. A: Gen. 650 (2023) 119014.



## Synthesis and characterization of mesoporous materials with acid properties

Lourdes Vergara<sup>1\*</sup>, Gustavo Mendow<sup>1</sup>, Carlos Querini<sup>1</sup>, Bárbara Sánchez<sup>1</sup>

<sup>1</sup>INCAPE, Colectora Ruta 168 Km 0 Pje El Pozo, Santa Fe 3000 (Argentina),

\*lvergara@fiq.unl.edu.ar

### Introduction

Mesoporous materials functionalized with sulfonic groups are interesting for use in biomass valorization reactions. These types of reactions generally involve bulky reagents and/or products and also require different levels of acidity to be catalyzed. The solids studied in this work can be modified according to the requirements of the reaction: they have the particularity of allowing the type of acid (Brønsted and/or Lewis) anchored to the surface and the density of the sites to be varied. This study presents the most important results of the synthesized mesoporous materials, which were characterized with various techniques with the aim of correlating the textural and structural properties, chemical composition and acidity of the catalysts.

### Materials and Methods

The synthesized mesoporous materials were KIT-6, FDU-12, Silica Nanotubes (NTS), SBA-15, SBA-15 large pore, SBA-16, mesoporous SnO<sub>2</sub> and MCM-48 silicas. In all cases, Tetraethylorthosilicate (TEOS) was used as silicon source, and mercaptopropyl-trimethoxysilane (MPTMS) as a precursor of the sulfonic groups. In some materials the Pluronic P-123 copolymer was used as template, and in others Pluronic F-127 and CTAB. The synthesis conditions (temperature, hydrothermal treatment) were different for each support, following procedures published in the literature.

For the incorporation of propylsulfonic groups with the objective of generating acidity, three alternatives were explored:

- (i) Co-condensation 1 (C1): Functionalization with mercapto groups (-SH) during the synthesis and subsequent oxidation to sulfonic groups (-SO<sub>3</sub>H) [1].
- (ii) Co-condensation 2 (C2): Functionalization with -SH groups and oxidation to -SO<sub>3</sub>H in the same step [2].
- (iii) Grafting (G): Functionalization with -SH groups post-synthesis followed by oxidation [3].

With the three methods, catalysts with different contents of functional groups were prepared: 10 and 15%, expressed as %mol/mol S/Si.

Textural properties were determined by N<sub>2</sub> adsorption-desorption isotherms. The specific surface area was estimated by BET method and the pore size distribution was calculated using the Broekhoff-de Boer (BdB) method for adsorption branches. The S/Si ratios on the silicas were measured by energy dispersive X-ray fluorescence (XRF) (EDX). Acidity measurements were made by potentiometric titration with butylamine using acetonitrile as solvent. The efficiency of the mercapto groups oxidation treatment was evaluated with

thermogravimetric analysis (TGA) and qualitatively, by N<sub>2</sub> stripping at programmed temperature.

### Results and Discussion

In general, it was observed that all of the catalysts had good levels of acidity, but those synthesized by co-condensation showed better efficiency in the oxidation of mercapto to sulfonic groups, compared to those prepared by grafting method, which had lower oxidation efficiency. As a counterpart, in the latter, the mesoporous structure of the starting solid was better preserved. As the sulfonic groups content increases, the acidity increases and the BET area and pore diameter decreases.

The FDU-12(C2)-15% catalyst reported very good textural properties. The structure of the starting mesoporous solid was preserved, decreasing the BET area from 602 m<sup>2</sup>/g for the non-functionalized support to 395 m<sup>2</sup>/g, with a pore diameter of 5.5 nm. In addition, the highest acidity of the series of catalysts prepared was obtained and the -SH groups were totally oxidized. In comparison, for the NTS(C1)-15% catalyst, only 33% of the incorporated groups were completely oxidized to sulfonic, while for the KIT-6 support functionalized with the same method, this value was 63%. For those materials in which the oxidation was not complete, a two stages oxidation treatment was explored, achieving an improvement in the final acidity.

The effectiveness in the incorporation of sulfur was evaluated by means of the FRX technique, which allows determining the % S/Si that was actually incorporated, defining effectiveness as the ratio between the measured value and the theoretical or nominal value. It was found that for all of the catalysts it was between 0.7 and 1. However, the lower values correspond to the catalysts prepared by grafting. This is consistent with the result obtained by TGA.

KIT-6 catalysts synthesized by the three methods were particularly studied in the esterification reaction of glycerin with free fatty acids (FFA). It was found that with the KIT-6(C2)-15% catalyst, at 180 min of reaction, a FFA conversion of 93% was achieved, and 80% selectivity, calculated as the sum of mono, di and triglycerides (products of interest). This is a good result considering what has been reported in the bibliography for this reaction, using heterogeneous catalysis and similar reaction conditions.

### Significance or Main Conclusions

More than nine mesoporous supports functionalized with sulfonic groups to generate acidity were synthesized. It should be highlighted that these solids have been little explored in the literature and therefore, they were characterized by several techniques and evaluated in different reactions in which the presence of acid sites and mesoporosity are required. The catalysts were evaluated in the esterification reaction of glycerin with free fatty acids, in the obtention of 5-ethoxymethylfurfural from fructose and in the C-C coupling reaction of hydroxyalkylation-alkylation of furfural with 2-methylfuran.

### References

- [1] W.D. Bossaert, D.E. De Vos, W.M. Van Rhijn et. al.; J. Catal 182 (1999) 156-164.
- [2] D. Margolese, J.A. Melero, S.C. Christiansen et. al.; Chem. Mat, 12 (2000) 2448-2459.
- [3] K. Niknam, D. Saberi, M.N. Sefat; Tetrahedron Lett, 50 (2009) 4058-4062.



## Effect of ethylene glycol functionalization on a CeO<sub>2</sub>-SiO<sub>2</sub> support for Ni catalysts applied in the ethanol steam reforming

Marcela Jaramillo-Baquero<sup>1\*</sup>, John F. Múnera<sup>1</sup> and Laura M. Cornaglia<sup>1</sup>

<sup>1</sup>INCAPE, Santiago del Estero 2829, Santa Fe 3000 (Argentina)

\*jaramillob.marcela@gmail.com

### Introduction

Hydrogen is considered the future energy vector due to its great electricity generation potential. In this context, the steam reforming of ethanol could play a key role due to the multiple advantages, such as low cost, ease of transportation, and the possibility of producing hydrogen in relatively mild conditions, with high efficiency [1]. The increasing interest in the use of hydrogen demands the development of active, stable, and selective catalysts at moderate temperatures (723 K – 873 K).

Catalysts based on non-noble metals like Ni are considered an interesting alternative as an active phase in the steam ethanol reforming (SER) reaction since they have high catalytic activity and low cost compared to other metals. Nevertheless, the main cause of deactivation in this catalyst type is carbon deposition [2]. To improve the catalytic properties, it has been suggested to use supports that provide a higher interaction with the active phase, a high specific surface, and promote the oxidation of carbonaceous deposits [3]. Furthermore, it has been reported that increasing the concentration of Si-OH sites by treating silica with ethylene glycol (EG) allows the formation of smaller supported metal particles with high reducibility [4]. Thus, in this work, the EG-modified Ni/CeO<sub>2</sub>-SiO<sub>2</sub>(EG) catalyst was synthesized and compared with the unfunctionalized material in the ethanol steam reforming reaction for hydrogen production.

### Materials and Methods

The catalysts were prepared by the successive incipient wetness impregnation (IWI) of 10 wt% CeO<sub>2</sub> and Ni (5 wt%) onto SiO<sub>2</sub> (Aerosil 200 m<sup>2</sup>/g) support using Ce(NO<sub>3</sub>)<sub>3</sub>·6H<sub>2</sub>O and Ni(CH<sub>3</sub>COO)<sub>2</sub>·4H<sub>2</sub>O as precursor salts. After each impregnation, the materials were dried in air at 353 K for 12 h and then calcined at 823 K for 6 h. In the functionalized catalyst, the silica support was pretreated with ethylene glycol at room temperature for 1 h.

The catalytic test was performed in a quartz tubular reactor. The catalytic bed was heated in Ar flow until the reaction temperature (773 K); then, the catalysts were reduced in flowing H<sub>2</sub> for 2 h. A mixture with a water/ethanol ratio equal to 5 was fed, with Ar as the carrier gas. All products and reagents were analyzed by gas chromatography. The catalysts were characterized using X-ray diffraction (XRD), Raman spectroscopy. In addition, other techniques such as X-ray photoelectron spectroscopy (XPS), transmission electron microscopy (TEM), and programmed temperature oxidation (TPO) were employed.

### Results and Discussion

By XRD analysis of the calcined catalysts, the reflections corresponding to NiO were not observed; this could indicate a very small crystallite size. By TEM of the reduced catalysts, it

was determined that the functionalization with EG allows obtaining a smaller particle size, being 2 nm for Ni/CeO<sub>2</sub>-SiO<sub>2</sub>(EG) and 6 nm for Ni/CeO<sub>2</sub>-SiO<sub>2</sub>.

On the other hand, the XPS results (Table 1) showed that Ce/Si ratio for the EG-modified material was at least double compared to the unmodified catalysts. This indicates that cerium is more dispersed on the surface, generating higher contact with the Ni nanoparticles, increasing the reducibility of the cerium surface.

Table 1. XPS results of the reduced catalysts.

Catalyst	Ce/Si		Ni/Si		%Ce <sup>+3</sup>	%Ni <sup>0</sup>
	Calc.	Nom.	Calc.	Nom.		
Ni/CeO <sub>2</sub> -SiO <sub>2</sub>	0.035	0.039	0.037	0.059	21	67
Ni/CeO <sub>2</sub> -SiO <sub>2</sub> (EG)	0.074	0.042	0.059	0.059	44	66

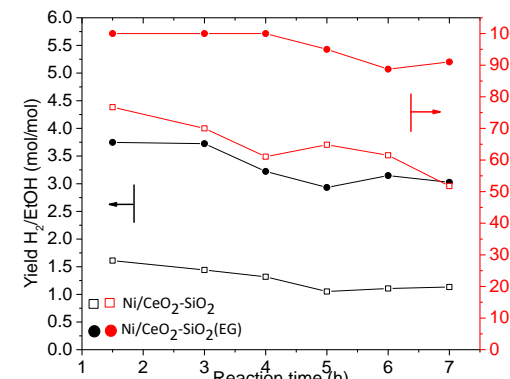


Figure 1. Catalytic results. Reaction conditions: 773K, 101.3 kPa, W/F = 4.9 x 10<sup>-3</sup> g h L<sup>-1</sup>, R = 5.

### Significance

This work reports a novel and simple functionalization of the silica supports with ethylene glycol to develop Ni-based catalysts, providing high performance towards hydrogen production via ethanol steam reforming reaction, with less formation of carbonaceous deposits.

### References

- [1] V. Palma, C. Ruocco, E. Meloni, R. Antonio, Catalysts 7 (2017) 1-16.
- [2] M. Greluk, W. Gac, M. Rotko, G. Slowik, J. Catal 393 (2021) 159–178.
- [3] M. Konsolakis, Z. Ioakimidis, T. Kraia, G. Marnellos, Catalysts 6 (2016) 1-27.
- [4] B. Wang, Jian-Feng, C. Zhang, Y. Zhang, RSC Advances 3 (2015) 10715–10722.

## Comparison of batch and continuous operating mode of the reactor for C-O hydrogenolysis of erythritol on Ir-Re catalysts

Emanuel Virgilio, Ludmila Chorvat, Cristina L. Padro and María E. Sad\*  
Catalysis Science and Engineering Research Group (GICIC), INCAPe-(UNL-CONICET)  
Santiago del Estero 2654, (3000) Santa Fe, Argentina  
\*mesad@fiq.unl.edu.ar

### Introduction

New processes starting from biomass derivatives are replacing the traditional synthesis of numerous chemicals involving sources of fossil origin. As a disadvantage, the biomass-derived molecules typically contain excess of oxygen that must be removed to render valuable chemicals. C-O hydrogenolysis is a key reaction for the conversion of polyols and sugar alcohols to platform molecules because it allows the removal of oxygen while preserving the number of carbon atoms of the starting molecule. Erythritol ( $C_4H_{10}O_4$ , ERY) is commercially produced through fermentation of glucose and sucrose from chemically and enzymatically hydrolyzed wheat and corn starches. It is considered as a platform molecule and then, susceptible to participate in attractive chemical transformations, such as C-O hydrogenolysis, conducting to valuable products like butanediols (BDO) which are important chemicals used in the industry of synthetic rubber and polymers, among many other uses.

The direct hydrogenolysis of ERY to produce butanediols was previously reported [1] using 4 wt.% Ir-ReO<sub>x</sub>/SiO<sub>2</sub> catalyst (Ir/Re=1); the selectivity to butanediols reached was 48% at 74.2 % conversion at 100°C and  $P_{H_2}=80$  bar after 24 h of reaction. Some more recent research have been developed in order to improve to BDO yield by changing the noble metal (Ir, Rh, Pt), the oxide promoter (Re, W, Mo) and the support [2,3] but only batch reactors were used for ERY reactions. The goal of this work is to compare the catalytic activity of two Ir and Re bimetallic catalysts with different physicochemical and acidic properties in the reaction of ERY to BDO using a batch and a continuous reactor.

### Materials and Methods

Ir-Re/TiO<sub>2</sub> and Ir-Re/Al<sub>2</sub>O<sub>3</sub> (2%wt.Ir, Ir/Re=1) were prepared by successive incipient wetness impregnation using an aqueous solution of H<sub>2</sub>IrCl<sub>6</sub> and HReO<sub>4</sub> on supports previously treated in air flow at 523 K. The catalysts were characterized by N<sub>2</sub> physisorption, CO chemisorption, TPR, TPD of NH<sub>3</sub>, XPS and TEM. Prior reaction, both catalysts were reduced in order to ensure the total reduction of Ir while Re remaining partially oxidized. Both catalysts were tested in the ERY hydrogenolysis at 453 K in both batch and continuous reactors. Catalytic results reported here for the con system continuous taken after a stabilization period (about 100 min), these values remained invariant during 6 h on stream. Condensable products were collected and analyzed using HPLC (RI detector, Aminex HPX-87 column) whereas gaseous products were analyzed using a GC.

### Results and Discussion

ERY may react in presence of H<sub>2</sub> through four main routes: C-O hydrogenolysis (CO), C-C bond cleavage (CC), dehydration (DH), and isomerization (ISO). The primary products

from C-O scissions from ERY are the butanetriols that can be converted into BDO by a second C-O hydrogenolysis; the over-C-O hydrogenolysis is, however, undesirable because butanols and butane may be formed and transferred to gas phase.

Catalytic results from batch and continuous reactor are display in the Figure 1. In batch process, the ERY conversion to liquid products was similar on Ir-Re/TiO<sub>2</sub> and Ir-Re/Al<sub>2</sub>O<sub>3</sub> but the TiO<sub>2</sub> catalyst favored the C-O scissions more than Al<sub>2</sub>O<sub>3</sub>-based catalyst that promoted dehydration reactions. At these conditions, ERY conversion to gas products and gaseous products distribution were similar on both catalysts. The main difference between these two solids was the higher acidity of alumina, as well as the presence of slightly reduced Re species, and lower accessibility of Ir on Ir-Re/Al<sub>2</sub>O<sub>3</sub>. In addition, the catalysts were tested in a continuous reactor at the same temperature. For this operating mode, the ERY conversion was almost total on both catalysts. However, only Ir-Re/TiO<sub>2</sub> favored the C-O hydrogenolysis to render liquid products such as BDO (XL≈ 70% and 56% of products from C-O hydrogenolysis within liquid) whereas the high acidity of Ir-Re/Al<sub>2</sub>O<sub>3</sub> clearly promoted dehydration reactions with 1,4-anhydroerhyritol as main compound and also formed high amounts of products from C-C scissions in gas phase (mainly methane). ISO (threitol formation) was negligible compared to batch reactor due to the high conversion reached.

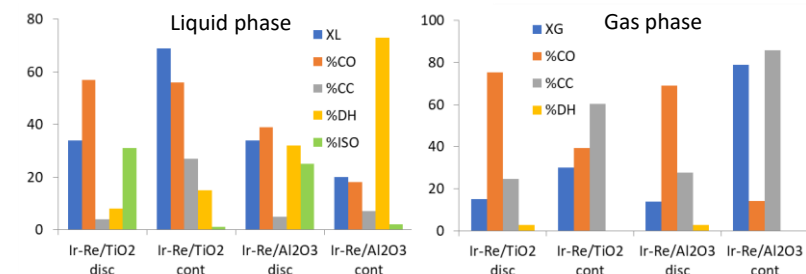


**Figure 1.** Liquid and gaseous ERY conversion (XL and XG) and products distribution on Ir-Re bimetallic catalysts [disc: 453K, 25 bar H<sub>2</sub>, 0.4M ERY, 8 h; cont: 453K, 18 bar, 0.1 mL/h 0.4M ERY].

### Significance

Catalyst acidity and the operating mode influence on the activity and selectivity to different routes during ERY reactions. The highest BDO productivities were achieved on Ir-Re/TiO<sub>2</sub> (60 and 80 mmol/g<sub>Ir</sub>.h for batch and continuous reactor respectively).

### References

- [1] Y. Amada, H. Watanabe, Y. Hirai, Y. Kajikawa, Y. Nakagawa, K. Tomishige; ChemSusChem 5 (2012) 1991-1999.
- [2] E. Virgilio, C. Padro, M.E. Sad; ChemCatChem 13 (2021) 3889-3906.
- [3] K. Tomishige, Y. Nakagawa, M. Tamura; Green Chemistry 19 (2017) 2876-2924.

## Synthesis and modification of MgO-based sorbents for the CO<sub>2</sub> capture during the water gas shift reaction at intermediate temperatures

Carlos F. Imbach-Gamba<sup>1\*</sup>, Laura Cornaglia<sup>1</sup> and John Múnera<sup>1</sup>

<sup>1</sup>INCAPE, Santiago del Estero 2829, FIQ-UNL, Santa Fe 3000 (Argentina)

\*cfimbachi@fiq.unl.edu.ar

### Introduction

The development of different materials which could replace the Cr-Fe catalysts employed in the water gas shift reaction (WGSR) is widely studied. According to different studies, catalysts based on non-noble metals such as Ni, Co, and Cu supported on CeO<sub>2</sub> are the best candidates for the reaction. These materials have high stability, selectivity to hydrogen, and catalytic activity in the reaction. At the same time, it is well known that the WGSR not only produces hydrogen but also carbon dioxide, suggesting that if a free or low CO<sub>2</sub> emissions process is required, it is necessary to eliminate the CO<sub>2</sub> in the effluent of the process [1].

Industrially, CO<sub>2</sub> is captured in an external unit, using amine-based sorbents. An alternative proposed is to incorporate a solid sorbent in the same reactor where the WGSR is carried out to capture the CO<sub>2</sub> *in situ*. In this case, for the CO<sub>2</sub> capture at temperatures between 300 and 400°C, MgO-based materials have good performance when doped with alkaline molten salts (AMS) of Na, K, or Li in loads between 20-60%wt [2].

In this work, we propose to modify the MgO via hydration-dehydration processes to enhance its CO<sub>2</sub> capture capacity, reducing the required AMS content and testing its performance in the WGSR conditions.

### Materials and Methods

MgO obtained by precipitation of Mg(NO<sub>3</sub>)<sub>2</sub> with K<sub>2</sub>CO<sub>3</sub> was selected as the reference. The solid was mixed in deionized water at 45°C and 80°C for 5h. Then, the hydrated MgO was dried and calcined at 400°C for 1h. Samples were called MgO Mod. (45°C) and MgO Mod (80°C), respectively. The samples were characterized by XRD, N<sub>2</sub>-sorptometry, SEM, and CO<sub>2</sub>-TPD. Previous to the capture capacity test, all samples were impregnated with a mixture of NaNO<sub>3</sub>-NaNO<sub>2</sub> (18%wt) through the incipient wetness impregnation technique. With the AMS-loading the samples were called AMS-MgO, AMS-MgO Mod. (45°C), and AMS-MgO Mod (80°C), respectively. The CO<sub>2</sub> capture tests were carried out in a TGA, the capture temperature was 350°C with 40 mL/min of pure CO<sub>2</sub> flow. The weight gain by the samples was followed to determine the maximum CO<sub>2</sub> capture capacity.

### Results and Discussion

XRD confirms the formation of the periclase phase of MgO. After the hydration, the crystal phase of the solid was completely converted into Mg(OH)<sub>2</sub>; after dehydration, the modified materials recovered the MgO phase. Table 1 shows that after the hydration-dehydration there was a reduction in the crystallite size of the MgO. At the same time, the modified samples have better S<sub>BET</sub> and pore volume compared with the MgO. Figure 1a shows that, initially, the MgO possesses a rod-like morphology; however, after the treatments, the particles look like sheet aggregation. The new morphology could be related to the increase in

the specific surface area and surface defects in the modified materials. Previous reports [3] suggest that the modification could increase the surface defects of the MgO, necessary for CO<sub>2</sub> sorption. Capture capacity tests followed by TGA are presented in Figure 1b and the maximum capture capacity is exhibited in Table 1. The results show that modified samples have a higher CO<sub>2</sub> capture capacity and a higher capture rate than the unmodified MgO sample.

**Table 1. Textural properties, crystallite size, and capture capacity of the samples.**

Sample	S <sub>BET</sub> (m <sup>2</sup> /g)	V <sub>total(0.98)</sub> (cm <sup>3</sup> /g)	D <sub>Sch</sub> <sup>a</sup> (nm)	Capture capacity (mmolCO <sub>2</sub> /g) <sup>b</sup>
MgO	20	0.05	7.47	11.77
MgO Mod. (45°C)	110	0.50	4.25	16.86
MgO Mod. (80°C)	150	0.60	4.58	17.06

<sup>a</sup> Crystallite size calculated by the Scherrer equation.

<sup>b</sup> Calculated at 80 min of test over the AMS-doped samples.

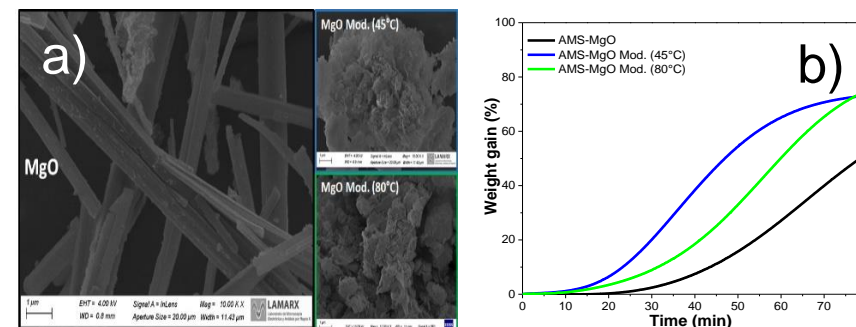


**Figure 1.** a) SEM images for unmodified and modified MgO samples and b) CO<sub>2</sub> capture tests followed by TGA of the AMS-doped unmodified and modified MgO samples.

### Significance

This work reports the development of MgO-based materials which are good candidates to be used as sorbents for the *in situ* removal of CO<sub>2</sub> during the water gas shift reaction. The modification proposed for the MgO enhances the maximum CO<sub>2</sub> capture capacity and its capture rate compared with the AMS-MgO sorbent.

### References

- [1] D. Pal, R. Chand, S. Upadhyay et al; Renew. Sust. Energ. Rev., 93 (2018) 549–565.
- [2] M. Dunstan, F. Donat, A. Bork et al; Chem. Rev., 121 (2021) 12681-12745.
- [3] A. Fan and H. Gao; Process Saf. Environ. Prot., 156 (2021) 361-372.

## Gasification of cannabis waste

Paula Saires\*, Melisa Bertero and Ulises Sedran

*Instituto de Investigaciones en Catálisis y Petroquímica "Ing. José Miguel Parera" INCAPe (UNL-CONICET). Colectora Ruta Nacional Nº 168 Km 0, S3000AOJ, Santa Fe, Argentina.*

\*psaires@fiq.unl.edu.ar

### Introduction

Biomass gasification involves its partial thermal oxidation leading to the production of gaseous and solid products, as well as tar. It is a highly flexible technology to produce clean energy, with lower NO<sub>x</sub> and SO<sub>x</sub> emissions than those of combustion. The gaseous products can be used to generate energy and they are also raw materials to produce liquid biofuels and green chemicals.

Lignocellulosic biomass is a promising energy source given its neutrality in the CO<sub>2</sub> cycle, high availability and sustainability; moreover, forest and agro-industrial wastes do not compromise food provision [1].

A particular case of residual biomass is that from the obtention of therapeutical products from cannabis, that is, wastes from cropping and conditioning the plants and extracting the active components. The important and persistent social demands in Argentina about those products and the increasing scientific and industrial interest, as reflected by Laws 27350 and 27669, position our country as a feasible producer of cannabis products. Wastes from cannabis utilization, which include cellulose, hemicellulose and lignin, as well as some other components (e.g. proteins, lipids and inorganic compounds), represent about 80 to 90 %wt. of the plants [2]. These characteristics make them very promising to be used as raw materials in thermochemical processes.

It is interesting, then, to study the gasification of cannabis wastes as a valorization approach, as the final disposition of those wastes is regulated by legislation given their content of phytocannabinoids, particularly tetrahydrocannabinol THC, the most powerful psychoactive component in the plants.

### Materials and Methods

The raw biomass in the experiments was a mixture of wastes from the extraction of therapeutical cannabis oil (RC) including leaves and branches (18 %wt.), and exhausted flowers (82 %wt.). The mixture was composed by 4.5 %wt. cellulose, 11.1 %wt. hemicellulose, 7.0 %wt. lignin, 16.7 %wt. lipids, 22.6 %wt. proteins, 12.7 %wt. ash and 16.1 %wt. of other components, having 9.3 %wt. humidity. The higher heating value was 16.2 MJ kg<sup>-1</sup>.

The gasification was performed in a batch, moving bed laboratory reactor, its operation simulating the process in a continuous downdraft gasifier with four reaction zones (drying, pyrolysis, oxidation and reduction). Fifteen experiments were performed following the combination of three operating parameters: equivalence ratio (ER), which is the relationship between the amount of air used and the stoichiometric amount of air, biomass residence time (t<sub>R</sub>) and temperature (T). The values were ER 0.2, 0.3 and 0.4, t<sub>R</sub> 30, 50 and 70 min and T 750, 800 and 850°C. The amount of biomass in each experiment was about 70 g. Gases

were analyzed in a Agilent 6890N gas chromatograph with a GS-CARBONPLOT capillary column and TCD detection. The lower heating value (LHV) and the gasification efficiency (EG), that is, the relationship between the energy content of the gases and that obtained in biomass combustion, were also calculated.

### Results and Discussion

The gas yields were from 51 to 65 %wt., the composition of the gaseous products in the most relevant experiments being shown in Figure 1.

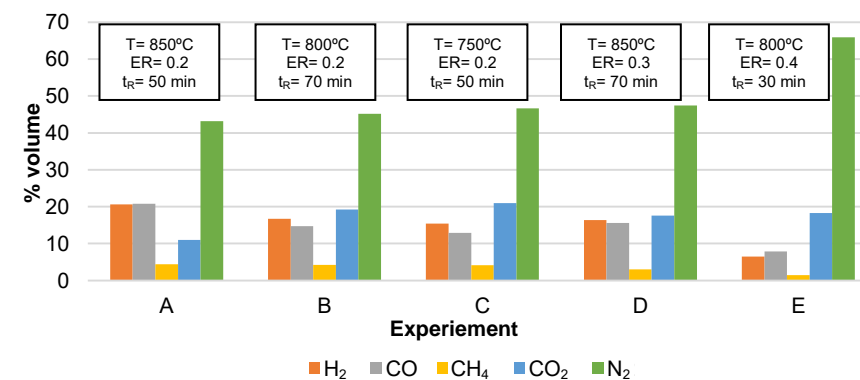


Figure 1. Composition of the gaseous products in the gasification of cannabis waste.

Char and tar yields were from 23 to 42 %wt. and 4 to 16 %wt., respectively.

The highest LHV (1401.5 kcal Nm<sup>-3</sup>) was obtained in the experiment at 850°C, ER 0.2, and t<sub>R</sub> 50 min, leading to EG of 70.4 % and gas yield of 51 %wt. The highest EG was 77%, obtained in the experiment at 850°C, ER 0.3 and t<sub>R</sub> 70 min, LHV being 1050.5 kcal Nm<sup>-3</sup> and gas yield 63 %wt.

It can be observed that the best combination of operating parameters allows the generation of gases with LHV higher than 1000 kcal Nm<sup>-3</sup>, EG being higher than 50 %.

### Significance or Main Conclusions

The observations in the experiments of cannabis waste gasification show that it is feasible to use gasification technologies to valorize them. Gas yields were higher than 50 % and LHV were important. Most importantly, this option is very attractive and positive to obey legislation about cannabis wastes.

### References

- [1] C. Ciliberti et al. Processes 8 (2020) 1567.
- [2] G. Suurkuusk. Doctoral dissertation, Master Thesis, University of Tartu, Faculty of Science and Technology Institute of Chemistry, Estonia (2010).



## Oxidative dehydrogenation of propane for the production of propylene using VO<sub>x</sub>/Al<sub>2</sub>O<sub>3</sub> catalysts

Francisco J. Passamonti<sup>1</sup>, Silvana A. D'Ippolito<sup>1</sup>, Catherine Espel<sup>2</sup>, Florence Epron<sup>2</sup>, Carlos L. Pieck<sup>1</sup>, Viviana M. Benítez<sup>1\*</sup>

<sup>1</sup>INCAPE, Colectora RN 168, km 0 Paraje El Pozo, Santa Fe 3000 (Argentina),

<sup>2</sup>Institut de Chimie des Milieux et Matériaux de Poitiers (IC2MP), Université de Poitiers, CNRS, 4 rue Michel Brunet, TSA51106, 86073 Poitiers Cedex 9, (France)

\*vbenitez@fiq.unl.edu.ar

### Introduction

The oxidative dehydrogenation of hydrocarbons process (ODH) uses propane and/or ethane as raw material to produce propylene and/or ethylene, key components in the chemical industry due to their multiple applications. It presents as advantages with respect to conventional steam cracking: high theoretical conversion to olefins, low energy consumption and little or no coke formation.

Currently the petrochemical industry demands more propylene than ethylene. This work studies the conversion of propane using VO<sub>x</sub>/Al<sub>2</sub>O<sub>3</sub> catalysts. The selectivity, activity and stability of VO<sub>x</sub> supported catalysts can be modified by the vanadium oxide content, the support, the reaction temperature and the oxidizing agent. These variables are considered in the development of this research.

### Materials and Methods

VO<sub>x</sub>/Al<sub>2</sub>O<sub>3</sub> catalysts were prepared by wet impregnation from a NH<sub>4</sub>VO<sub>3</sub> solution on the γ-Al<sub>2</sub>O<sub>3</sub> support (60°C/2h/stirring), then dried for 12 h at 120°C and subsequently calcined at 500°C for 4 h. Vanadium concentrations were varied from 1 to 11%w. They were characterized by different usual analytical techniques for this type of catalysts.

The evaluation of the catalytic activity was carried out in a fixed bed tubular reactor at atmospheric pressure. Propane was fed along with a stream of N<sub>2</sub> and O<sub>2</sub> (which acted as an oxidizing agent). The experiences were carried out in a range of 300 < T [°C] < 550 temperature, a constant C<sub>3</sub>H<sub>8</sub>/O<sub>2</sub> ratio of 2.5, a C<sub>3</sub>H<sub>8</sub> flow of 30 cm<sup>3</sup>/min and 100 mg of catalyst mass. Additionally, experiments were carried out, under same reaction conditions, with γ-Al<sub>2</sub>O<sub>3</sub> to establish the reference of the support used. The reaction products were analyzed by gas chromatography.

### Results and Discussion

Figure 1 shows the average conversion of propane as a function of temperature and vanadium content; Figure 2 shows the yield to propylene, under the same conditions as Figure 1. In both figures, the experimental results are represented by dots while that the surface shows the trend.

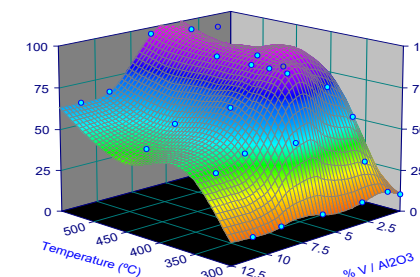


**Figure 1.** Conversion of C<sub>3</sub>H<sub>8</sub> as a function of temperature and V/Al<sub>2</sub>O<sub>3</sub> load

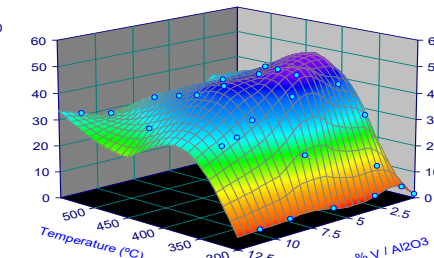


**Figure 2.** Performance of C<sub>3</sub>H<sub>8</sub> as a function of temperature and V/Al<sub>2</sub>O<sub>3</sub> load

The following reaction products were mainly obtained: C<sub>3</sub>H<sub>6</sub>, CO and CO<sub>2</sub>; CO and CO<sub>2</sub> formed mainly by consecutive oxidative reactions of propylene. In addition, C<sub>2</sub>H<sub>6</sub>, C<sub>2</sub>H<sub>4</sub>, CH<sub>4</sub> and oxygenated compounds (acetaldehyde and acetic acid) were found in very small amounts. The high propylene yield, which remained constant during the reaction, strongly depends on the temperature, reaching a maximum of 375°C, for all catalysts; this is because at higher temperatures the yield of CO<sub>x</sub> and cracking products is increased.

It is observed that the increase in propylene yield is proportional to the load of V until reaching 6%V, then it decreases according to the increase in load (6 <%V < 11). This behavior is related to the fact that the vanadium density on the surface determines the degree of polymerization of the VO<sub>x</sub> species, evidence observed in the characterization analyzes performed on the catalysts.

The results obtained allowed establishing criteria to continue with the line of research, using V catalysts, in different proportions, on SiO<sub>2</sub> and different SiO<sub>2</sub>-Al<sub>2</sub>O<sub>3</sub> supports (with variable SiO<sub>2</sub>/Al<sub>2</sub>O<sub>3</sub> ratio).

### Main Conclusions

Vanadium catalysts supported on alumina show very good activity in propane ODH. The reaction temperature and the vanadium load on the catalyst strongly influence its behavior, this is due to the type of VO<sub>x</sub> species that are formed on the surface. It was found that the 6%V/Al<sub>2</sub>O<sub>3</sub> catalyst at 375°C presented the best performance, obtaining a 51% yield of propylene with a propane conversion of 90.5%.

## Co-processing of sugarcane bagasse pyrolytic tar and vacuum gas oil under FCC conditions

Leandro Emanuel Dietta\*, Mariana Rodriguez, Juan Rafael García, Marisa Falco, Ulises Sedran

<sup>1</sup>Instituto de Investigaciones en Catálisis y Petroquímica (INCAPE)  
Colectora Ruta Nac. N° 168 Km 0 - Paraje El Pozo - (3000) Santa Fe - Argentina  
\*ldietta@fiq.unl.edu.ar

### Introduction

Currently, energy is mainly produced from non-renewable fossil sources, which generates, on the one hand, a growing need for developing new and renewable energy sources and, on the other hand, significant efforts to control CO<sub>2</sub> emissions [1]. Multiple factors have created a driving force for decarbonizing refining processes, such as pressure from society, regulations and investors. One of the areas of particular interest for many refiners is the processing of bio-based feedstocks in existing operating units, including the fluid catalytic cracker (FCC) which is the main catalytic conversion process within refineries [2]. This work proposes the FCC cracking of mixtures of vacuum gas oil and tar from the pyrolysis of sugarcane bagasse, a non-conventional source of renewable origin.

### Materials and Methods

Four feedstocks were used in the experiments; a vacuum gas oil (VGO), and its mixture with 5, 10 and 20%wt. of tar from the pyrolysis of sugarcane bagasse.

The experiments were performed in the CREC Riser Simulator [3], a laboratory batch fluidized bed reactor with internal recirculation. An equilibrium FCC catalyst of the octane-barrel type was used for the experiments. The VGO was obtained from a local refinery and the tar fraction (tarry liquid) of pyrolysis products was produced in the laboratory from sugarcane bagasse [4]. The experimental conditions were 550°C, contact time of 45 seconds and different catalyst/oil ratios in the range of 4 to 8. The gas and liquid reaction products were analyzed by on-line gas chromatography (HP-1 column and FID detector). The coke on catalyst was determined by temperature programmed oxidation and subsequent methanation of the carbon oxides. Conversion was defined as the sum of the mass yields of dry gas (DG, C1-C2), liquefied petroleum gas (LPG, C3-C4), gasoline (C5-216°C), light cycle oil (LCO, 216°C-340°C) and coke.

### Results and Discussion

Figure 1 shows the product distributions observed in the cracking of VGO and its mixtures with different percentages of tar at iso-conversion (conversion ≈ 70 %wt.). The mixtures VGO-tar yielded more dry gas and coke than VGO alone. Given the high content of coke precursors (phenolic compounds, cyclic ketones and furans) in the sugarcane bagasse tar, a higher coke formation is to be expected if compared with VGO alone. However, the coke yields are within the typical range in the commercial process and, therefore, changes in the global heat balance of the unit are not to be expected. The yields of gasoline were lower after the incorporation of

tar to the VGO. Nevertheless, the increase in the amount of tar was not proportional to the gasoline yield decrease, the lowest yield being observed in the 5%wt. tar mixture. The addition of 5%wt. of tar yielded more gases (DG and LPG) and less LCO if compared with VGO alone, while the opposite behavior (less gases and higher LCO production) was observed when 10%wt. and 20%wt. of tar were added.

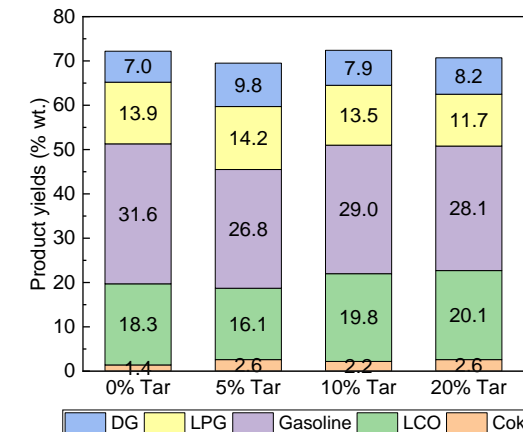


**Figure 1.** Product yields in the cracking of VGO and its mixtures with different percentages of tar (conversion ≈ 70 %wt.).

### Significance or Main Conclusions

These results, while preliminary, suggest that it is possible to co-process biomass-derived liquid streams (such as plant biomass pyrolysis tar) together with typical FCC feedstocks without major changes to unit configuration or operating conditions. In this way, a positive contribution would be made to mitigate the environmental impact of refining and to partially decrease the energy dependence on fossil resources.

### References

- [1] R. Pujio, J. R. García, M. Bertero, M. Falco, U. Sedran; Energy and Fuels, 35 (2021) 16943-16964.
- [2] B. Riley, S. Brandt, and K. Bryden; Decarbonization Technol. Powering Transition to Sustain. Fuels Energy (2022) 55-59.
- [3] H. de Lasa; US Patent 5.102.628 (1992).
- [4] M. Bertero, J. R. García, M. Falco, U. Sedran; Waste and Biomass Valorization 11 (2020) 2925-2933.



## Study of the sorption properties of a Li<sub>4</sub>SiO<sub>4</sub>-based sorbent in the presence of water and low CO<sub>2</sub> concentration

Diana Peltzer<sup>1\*</sup>, Betina Faroldi<sup>1</sup>, John Múnica<sup>1</sup>, and Laura Cornaglia<sup>1</sup>

<sup>1</sup> INCAPE-FIQ, Santiago del Estero 2829, Santa Fe 3000 (Argentina)

\*djpeltzer@fiq.unl.edu.ar

### Introduction

Among human activities which generate greenhouse gases (GHG), energy production accounts for around 75% of the total shares [1], and CO<sub>2</sub> is considered the largest source of GHG in this category. In this context, diverse strategies for low carbon-energy production have been raised. Between these technologies, CO<sub>2</sub> capture at high temperatures can be used in power generation systems to decarbonize post-combustion gases or can be coupled to H<sub>2</sub> production from fossil fuels to generate blue H<sub>2</sub>, a less carbon-intensive variation of grey H<sub>2</sub>.

The sorbents for CO<sub>2</sub> capture at high temperatures retain the CO<sub>2</sub> by means of the reversible carbonation reaction. Therefore, significant efforts are being made in the development of sorbents with high cyclic stability, reaction kinetics, and capture capacity. The most studied sorbents include CaO, alkaline zirconates, and silicates, though other materials have also been explored. In our group, we have developed a Li<sub>4</sub>SiO<sub>4</sub>-based sorbent which have proved good kinetics and capture properties in dry conditions and high CO<sub>2</sub> concentrations [2]. Hence, this contribution aims to study the capture properties of this sorbent in conditions similar to the reforming or post-combustion systems, including the presence of low CO<sub>2</sub> concentration and a variable amount of water.

### Materials and Methods

The sorbent with a Li/Si molar ratio of 4.1 (LiSi), was prepared by wet impregnation, using LiNO<sub>3</sub> as a lithium precursor. The silica source was obtained by a thermally controlled treatment of rice husk. After impregnation, the sample was dried at 80 °C for 24 h and calcined in air flow at 650 °C (heating rate of 1.75 °C/min) for 6 h. XRD patterns were obtained in a PANaliticcan Empyrean with Cu K $\alpha$  radiation at 45 kV-45 mA. Capture properties were evaluated through Temperature Programmed Desorption (TPD), with isothermal capture steps at 550 °C and different gas feedings; and regeneration steps in N<sub>2</sub>, heating up to 700° C (10 °C·min<sup>-1</sup>) and maintaining the temperature for 10 minutes. Later, the stream was fed to a methanation reactor and then analyzed online in an FID chromatograph (Shimadzu GC-8a).

### Results and Discussion

Table 1 shows the sorption capacity of LiSi under different conditions. Capture steps were performed during 60 minutes (long cycles) with 15% CO<sub>2</sub> and 0, 10, 20, and 30% H<sub>2</sub>O. It can be observed an increase in the CO<sub>2</sub> uptake and capture efficiency with the amount of water in the gas feeding, going from 0.10 to 0.19 g CO<sub>2</sub>·g mat<sup>-1</sup> and from 34 to 64%, respectively, between 0 and 20% H<sub>2</sub>O. The incorporation of a higher amount of water (30%) did not produce a variation in the capture capacity. Similar results were obtained in experiments with capture

steps lasting 15 minutes (short cycles), even though for these evaluations the total amount of captured CO<sub>2</sub> was lower (from 0.05 to 0.12 g CO<sub>2</sub>·g mat<sup>-1</sup> between 0 and 30% H<sub>2</sub>O).

Other sorbents based on Li and Na zirconates presented a higher sensitivity to water addition [3], which could be related to a lower reaction kinetic in dry conditions.

The XRD patterns of the “as calcined” sample and after one short capture/desorption cycle with 15%CO<sub>2</sub>-30%H<sub>2</sub>O are presented in Figure 1. In both patterns, Li<sub>4</sub>SiO<sub>4</sub> and Li<sub>2</sub>SiO<sub>3</sub> phases were visualized [2]. Moreover, no significant differences in the phase composition were observed, indicating a good capacity for regeneration.

**Table 1. Capture properties of LiSi in long cycles (60 minutes)**

	Without H <sub>2</sub> O added	10% H <sub>2</sub> O	20% H <sub>2</sub> O	30% H <sub>2</sub> O
Capture capacity <sup>a</sup>	0.10	0.15	0.19	0.19
Capture efficiency <sup>b</sup>	34	52	64	64

<sup>a</sup> gCO<sub>2</sub>·(g mat)<sup>-1</sup>, <sup>b</sup> (measured capture capacity/theoretical capture capacity)\*100

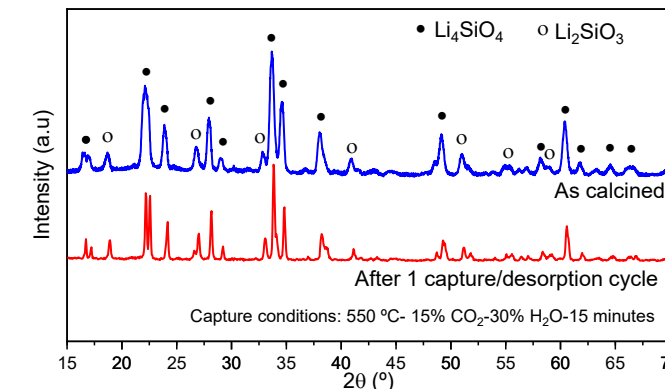


**Figure 1.** XRD Patterns of LiSi “as calcined” and after one short capture/desorption cycle

### Main Conclusions

The capture properties of a Li<sub>4</sub>SiO<sub>4</sub> based sorbent were evaluated with low CO<sub>2</sub> concentration and a variable amount of water. The presence of H<sub>2</sub>O enhanced the capture properties, though no significant effects were observed in the sample structure after one capture/desorption cycle, which resulted interesting in view of its application in real systems.

### References

- [1] IEA, World Energy Outlook 2020, IEA, Paris, 2020.
- [2] L. Salazar Hoyos, B. Faroldi, L. Cornaglia, J. Alloys Compd, 778 (2018) 699-711.
- [3] D. Peltzer, J. Múnica, L. Cornaglia, J. Alloys Compd, 895 (2021) 162419.



## Preparation of Pt-based electrocatalysts supported on hydrothermal rice husk for direct ethanol fuel cell

Maria F. Azcoaga Chort<sup>1\*</sup>, Sergio R. de Miguel<sup>1</sup>, Virginia I. Rodríguez<sup>1</sup>, Natalia S. Veizaga<sup>1</sup>

<sup>1</sup> Instituto de Investigaciones en Catálisis y Petroquímica (INCAPE), Colectora Ruta Nacional 168 Km 0, Santa Fe 3000 (Argentina)

\*fazcoaga@fiq.unl.edu.ar

### Introduction

The use of various materials as support for anode electrocatalysts in direct ethanol fuel cells (DEFC) has been extensively researched, with activated carbon being the most commonly employed. This study explores the use of activated carbon derived from rice husk as a support for mono and bimetallic Pt and PtRe catalysts, which can be utilized for the ethanol electrooxidation reaction.

### Materials and Methods

For the support preparation, the rice husk (CAV) was impregnated with a 23 wt.%  $H_3PO_4$  solution and kept at 200 °C for 24 h in a Teflon autoclave [1]. Then it was dried in air and pyrolyzed under  $N_2$  flow at 750 °C to obtain the appropriate support (CAH). For the synthesis of the catalysts, the polyol method was selected using ethylene glycol (EG) as reducing agent. The carbon was dispersed in a water:EG solution (25:75 %v/v) and ultrasonicated. Then, Pt and Re precursors were added. The mixture was kept under refluxing conditions for 2 h. Finally, it was filtered, washed and dried at 110 °C for 12 h. The nominal Pt loading was 20 wt.% and the Re loadings were 1, 3, 5, and 10 wt.%.

Electrochemical studies were carried out in a potentiostat/galvanostat and a three-electrode test cell at room temperature. The reference electrode was an Ag/AgCl electrode, and the counter electrode was a Pt wire. The working electrode consists of a thin layer of Nafion impregnated catalyst composite cast on a vitreous carbon disk electrode. In CO stripping, the CO was bubbled in the electrolytic solution (0.5M  $H_2SO_4$ ) for 30 min at 200 mV. Cyclic voltammetry (CV) measurements were conducted in a 0.5M  $H_2SO_4$  + 1M  $C_2H_5OH$  solution with a scan rate of 25 mV s<sup>-1</sup>. Chronoamperometric measurements were carried out in a 0.5M  $H_2SO_4$  + 1M  $C_2H_5OH$  solution for 45 min at 350 mV.

### Results and Discussion

The  $N_2$  adsorption-desorption isotherms of CAH correspond to type II isotherms with an H4 type hysteresis loop (IUPAC). The BET area value is 158.3 m<sup>2</sup> g<sup>-1</sup>, presenting micro and mesoporosity. According to thermogravimetric analysis, CAV loses about 70% of its mass while CAH loses only 20% at 900 °C. The mass loss for CAV was attributed to the decomposition of lignin, cellulose and hemicellulose. On the other hand, the mass loss of CAH was assigned to the decomposition of C-O-P groups. In the temperature-programmed reduction (TPR) curve of CAH, a peak was observed in the 550-600 °C zone, corresponding to reducible acid functional groups. The TPR profiles of the catalysts revealed the absence of peaks within the reduction zones of Pt and Re, indicating that these elements exist primarily in a metallic state. The  $H_2$  chemisorption capacities and hence the metallic dispersion of the bimetallic catalysts are significantly higher than those presented by the monometallic catalyst.

Upon comparison of the electrochemical surface area values (ECSA) between the bimetallic and monometallic catalysts, it was discovered that the former exhibited notably greater values. The PtRe(3) formulation showed the highest ECSA (145 m<sup>2</sup> gPt<sup>-1</sup>). Analyzing the values of the CO oxidation onset potential ( $E_{CO,ONSET}$ ), it was found that the addition of Re results in a decrease of these values compared to the one obtained for the monometallic catalyst. Notably, the PtRe(3) formulation exhibited a significantly lower  $E_{CO,ONSET}$  value when compared to both the monometallic catalyst and the other bimetallic catalysts (Table 1).

When comparing the cyclic voltammograms (Figure 1 and Table 1), the PtRe catalysts show higher current values than the monometallic one. This fact is due to the interaction between both metals, which was also evidenced by  $H_2$  chemisorption results. The catalyst that presented the best performance in cyclic voltammetry was PtRe(3)/CAH with an anodic current intensity of 893 mA mgPt<sup>-1</sup> occurring at 816 mV (vs Ag/AgCl).

Time stability measurements were performed through chronoamperometry studies. The PtRe(3)/CAH catalyst reaches the highest steady state current intensity.

**Table 1.** Electrochemical surface area values (ECSA) and CO oxidation onset potential ( $E_{CO,ONSET}$ ) from CO stripping, and anodic potential and current intensity from CV.

Catalyst	ECSA (m <sup>2</sup> gPt <sup>-1</sup> )	$E_{CO,ONSET}$ (mV vs Ag/AgCl)	Anodic potential (mV vs Ag/AgCl)	Current intensity (mA mgPt <sup>-1</sup> )
Pt/CAH	27	572	778	127
PtRe(1)/CAH	105	430	841	340
PtRe(3)/CAH	145	295	816	893
PtRe(5)/CAH	103	437	776	467
PtRe(10)/CAH	73	478	792	510

### Significance or Main Conclusions

Re has a relevant promotion effect on Pt, increasing the metallic dispersion and significantly improving the electrocatalytic behavior. Among the catalysts, the PtRe(3)/CAH was the most promising one.

### References

- [1] F. Quesada-Plata, R. Ruiz-Rosas, E. Morallón, D. Cazorla Amorós; ChemPlusChem 81 (2016) 1349-1359.

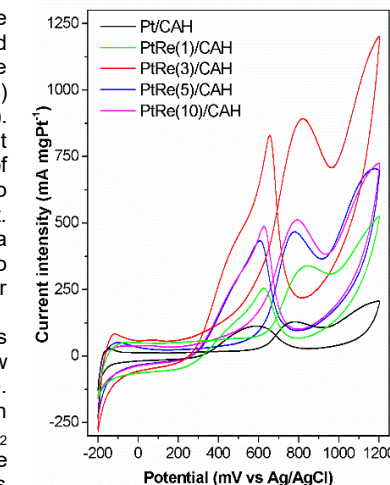


**Figure 1.** Cyclic voltammograms of Pt and PtRe catalysts.

## CsxCo/Na-MOR coating on monoliths for co-adsorption of hydrocarbons mixture and selective catalytic reduction of NO<sub>x</sub>

Inés Tiscornia<sup>1\*</sup>, Leticia Gómez<sup>1</sup>, Ramiro Serra<sup>1</sup>, Milagros Deharbe<sup>1</sup>, Alicia Boix<sup>1</sup>

<sup>1</sup>INCAPE, Santiago del Estero 2829, Santa Fe 3000 (Argentina)

\*itiscornia@fq.unl.edu.ar

### Introduction

The great efforts worldwide to reduce emissions from vehicles continue to advance; a major goal is to reduce NO<sub>x</sub> and hydrocarbons (HCs) emissions during the cold start conditions [1]. An after-treatment technology is to adsorb the harmful gases at a low temperature in a trap and later release and convert them at a higher temperature (light-off temperature). Then, improving the efficiency of post-treatment catalysts requires the design and development of materials. Zeolites have been widely used as support material for HC traps due to their diversity of structure, chemical composition, pore size, and versatility to incorporate different cations to improve adsorption-retention capacity [2].

On the other hand, selective catalytic reduction using HC<sub>s</sub> has been an alternative that allows the use of a mixture of gases similar to those found in the exhaust stream, and which catalysts applying metal-exchange zeolites have been developed. In recent studies, different strategies have been proposed in order to couple adsorption processes and selective catalytic reductions [3]. In this work, Cs<sub>x</sub>Co/Na-MOR coating on cordierite monoliths were evaluated to apply them in the HC<sub>s</sub> mixture adsorption (butane-toluene), as well as in the selective catalytic reduction of NO (SCR) with O<sub>2</sub> excess using that gaseous mixture as reducing agents.

### Materials and Methods

Cobalt (2.9 wt.%) and/or cesium (2 and 7 wt.%) species were incorporated to Na-MOR zeolite by ionic exchange technique. The solids were deposited onto cordierite inner walls by the washcoating method (CoM and Cs<sub>x</sub>CoM samples). HC<sub>s</sub> adsorption-desorption measurements were carried out in a continuous flow system with mass spectrometer; catalytic activity was tested in a fixed-bed flow reactor at atmospheric pressure.

### Results and Discussion

Adsorption and desorption capacities of toluene and butane mixture on the monolithic adsorbents were obtained; while the amount of HC<sub>s</sub> adsorbed at 100°C was determined from breakthrough curves, profiles of temperature-programmed desorption of both gases after co-adsorption were also quantified (100–550°C). Figure 1A shows the retention capacity of butane and toluene reached by the CoM and bimetallic Cs<sub>2</sub>CoM and Cs<sub>7</sub>CoM structures. The parameter is calculated as the desorbed and adsorbed HC quantity ratio, and represents the ratio between the retention capacity above 100°C, with respect to the total amount of adsorbed HC. Cs addition to CoM improved the retention capacity of toluene and butane; while Cs<sub>2</sub>CoM increased the butane and toluene capacity by 2.6 and almost 2 times respectively, with 7 wt.% of Cs the capacity increase was lower for the toluene (1.5 times). This fact could be related to

the steric problems, where an increment of a voluminous cation as Cs<sup>+</sup> hinders the adsorption and desorption of a molecule large. On the other hand, for butane, an increase in Cs concentration increased the retention capacity.

Figure 1B shows the NO to N<sub>2</sub> conversion in the SCR reaction as a function of temperature. Cs<sub>2</sub>CoM and Cs<sub>7</sub>CoM were more active than CoM (about 80 % vs 65 %). It is known that Co<sup>2+</sup> ions are the more active species for this reaction and, on the other hand, alkali metal Cs is promoter of HC<sub>s</sub> adsorption. In this case, the presence of Cs cations close to Co cations increased the hydrocarbons concentration around active sites at high temperature, according to TPD results. These facts could promote the reduction activity of NO.

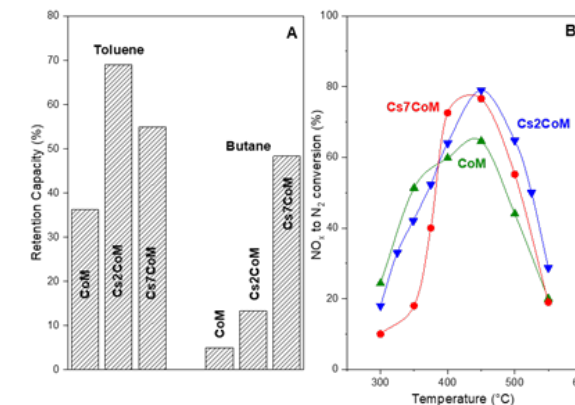


**Figure 1.** A) Toluene and butane retention capacity for HC<sub>s</sub> mixture adsorption on structures; B) NO-SCR by mixture (1000 ppm NO, 250 ppm toluene, 500 ppm butane and 2 vol.% O<sub>2</sub>, He balance).

### Conclusions

By combining Co<sup>2+</sup> and Cs<sup>+</sup> cations in the same zeolitic structure, an efficient material was obtained to adsorb a HC<sub>s</sub> mixture at low temperature and retain them until a medium temperature where the SCR of NO<sub>x</sub> begins to occur. It is possible that the presence of Cs cations close to Co cations increase the HC<sub>s</sub> concentration around active sites, increasing the reducing activity of NO.

### References

- [1] D. Doronkin, V. Casapu; Catalysts 11 1019 (2021) 1-3.
- [2] J. Kim, E. Jang, Y. Jeong, H. Baik, S. Cho, C. Kang, C. Kim, J. Choi; Chem. Eng. J. 430 (2022) 132552.
- [3] M. Azzoni, F. Franchi, N. Usberti, N. Nasello, L. Castoldi, I. Nova, E. Tronconi; Appl. Catal. B Environ. 315 (2022) 121544.



## Biomass Catalytic Valorization: *bio-fuel C15 molecules synthesis by hydrodeoxygenation and condensation reactions of furfural*

M. Soledad Zanuttini<sup>1,\*</sup>, Claudia Neyertz<sup>1</sup>, Lucas Tonutti<sup>1</sup>, Cristián Ferretti<sup>2</sup> and Carlos Querini<sup>1</sup>

<sup>1</sup>INCAPE, RN168 Km 0, Santa Fe 3000 (Argentina)

<sup>2</sup>IQAL, Santiago del Estero 2829, Santa Fe 3000 (Argentina)

\*szanuttini@fq.unl.edu.ar

### Introduction

Due to its abundance and varied chemical composition, lignocellulosic biomass represents an attractive resource for bio-fuel and fine compounds. Among products, the furfural (F) obtained by different biomass treatments and its product, the 2-methylfuran (2-MF), are promising compounds for the synthesis of molecules compatible with diesel fuel, like C12-C15. Our group studies the F transformation to 2-MF by catalytic hydrodeoxygenation (HDO) and the subsequent C-C coupling reaction between both compounds, performed by hydroxyalkylation/alkylation (HAA). We have focused on the selective HDO reaction of furfural in the gas phase at atmospheric pressure with H<sub>2</sub> using Fe-Pt over commercial and synthesized mesoporous amorphous silica with slightly Brønsted acidic properties. On the other hand, the coupling HAA reaction has been studied over mesoporous SBA-15 with propyl sulfonic acid groups. In both reactions, the support has a great influence, due to its porosity and the acid nature of the sites, since they affect the selectivity and stability of the catalyst. In consequence, the structural and acid properties were tuned by adjusting syntheses conditions of the SiO<sub>2</sub>. In similar way, the amount of propyl sulfonic groups and the hydrophobicity of the catalyst were modified for SBA-15 samples in order to optimize the production of the C15 biofuel. Besides, theoretical studies were carried out for a better understanding of the system and the results.

### Materials and Methods

Mesoporous samples of 15%Fe and 5%Fe-0.05%Pt over different silica with low acidities and sulfonic SBA-15 with 3 different loads of acid groups (5, 10 and 15 mol%S/Si) were prepared as previously reported [1, 2]. The samples were characterized by XRF, DRX, BET area, volumetric titration, Py-FTIR, Py-TPD, TGA and TPO. For HDO reaction of F to 2-MF, in situ reduced Fe/SiO<sub>2</sub> were evaluated in a fixed bed reactor with H<sub>2</sub>/N<sub>2</sub> at atmospheric pressure. The HAA reaction of 2-MF with F was carried out in solventless liquid phase in a stirred glass reactor with a reflux system at 40-80 °C for 0.25-4 h varying acid sites/F and F/2MF molar ratio. In both reactions, the compounds were analyzed by GC and FID detector and checked by GC-MS. Studies like the minimum energy geometries, the theoretical IR frequencies and molar volume calculations were determined by DFT and Gaussian 09.

### Results and Discussion

The HDO and HAA reactions are presented in Figure 1. Several catalysts with different support acidity and pore size were analyzed for the gas phase HDO of furfural.

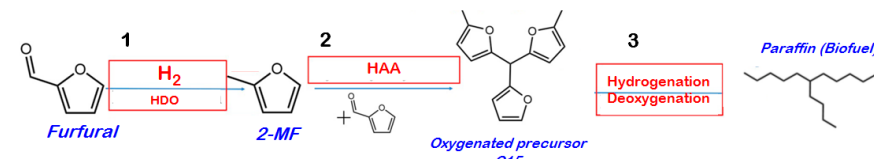


Figure 1. Main reactions involved in the studied process

The presence of iron particles on silica is highly selective for 2-MF at 300°C. An activity and a selectivity of 46% and 97% was obtained at 200 min for a sample with an area of 229 m<sup>2</sup> g<sup>-1</sup>, pore diameter of 17.6 nm and acidity of 0.15 mmol Py g<sup>-1</sup>. While, at the same conditions, a catalyst prepared with the commercial SiO<sub>2</sub> denoted 6.4% and 83% of conversion and selectivity, for 359 m<sup>2</sup> g<sup>-1</sup>, pore diameter 16 nm and 0.08 mmol Py g<sup>-1</sup>. The acid sites are necessary because they catalyze dehydration of F to 2MF. However, since they also catalyze parallel reactions to carbonaceous compounds, an excessive amount of them is not desirable. Hence, the incorporation of Pt and a balance between metallic and acid sites is critical to regulate selectivity, coke formation and stability.

For HAA reaction, the SBA-15 catalyst with more concentration of sulfonic acid sites (S/Si of 7 mol %), acidity of 1.12 mmol g<sup>-1</sup>, 604 m<sup>2</sup> g<sup>-1</sup> and 10 nm of pore diameter, showed the best results. At 60°C with stoichiometric feeding of the pure reagents, the furfural conversion was 99% and the C15 yield was 97% after 2 h. Due to water detrimental effect in the HAA performance, a SB15 catalyst with hydrophobic groups was tested in the same conditions and a 14.5% improvement was obtained for conversion without difference in selectivity. For all the analysis, a catalyst load of 0.7% of the total mass of reactants was employed. This value is compatible with industry catalyst quantities, showing that the process is feasible to be scaled. Moreover, catalyst-recycling studies revealed that samples could be recycled 3 times with a minor activity reduction.

The third step (Figure 1) to transform the oxygenated C15 to paraffin is still unexplored.

### Significance or Main Conclusions

Furfural deoxygenation to 2-MF is feasible over Fe-Pt/SiO<sub>2</sub> with high selectivity. The balance between metallic and weak acid sites is critical to regulate the selectivity and coke formation.

SBA15 silica with sulfonic groups is highly active for C-C coupling of 2-MF with F by hydroxyalkylation/alkylation at low temperature without solvent and under mild conditions. The C15 selectivity was greater than 95%. A synthesis modification by incorporation hydrophobic groups improves C15 yields.

These results with silicas open up opportunities to further catalytic research.

### References

- [1] M.S. Zanuttini, C. Neyertz, G. Mendow, C. Querini. Libro de Resumenes del XXVII Congreso Iberoamericano de Catálisis. México (2020) 2115.
- [2] M.S. Zanuttini, C. Neyertz, C. Ferretti, L. Tonutti, P. Quaranta, C. Querini. 28º Congresso Ibero-Americanico de Catálise. Brasil (2022).



## Selective Hydrogenation of FAME to fatty alcohols on Ru-Sn-B/Al<sub>2</sub>O<sub>3</sub> catalysts.

Cristhian Fonseca Benítez<sup>1</sup>, María Ana Vicerich<sup>1</sup>, María Amparo Sánchez<sup>1</sup>, Carlos L. Pieck<sup>1</sup> and Vanina A. Mazzieri<sup>1\*</sup>,

<sup>1</sup>INCAPE, Ruta Nac. 168 Km 0 - Paraje El Pozo, Santa Fe 3000 (Argentina)

\*vmazzier@fiq.unl.edu.ar

### Introduction

The oleochemical industry tries to obtain products with similar properties that replace the products obtained in petrochemicals. In last years the development of oleochemical processes has increased due to the advantages they present compared to products obtained from petrochemical processes. This is due to their smaller environmental impact, biodegradability and availability from renewable resources [1].

Fatty alcohols are used in the production of detergents, in cosmetic emulsions to provide consistency, and in industrial emulsions as co-surfactants or solubilizers. Fatty alcohols may be produced through the hydrogenation of fatty acids or their esters derived from vegetable oils. In previous works we studied the selective hydrogenation reaction of methyl oleate and oleic acid to oleic alcohol using Ru-Sn-B and Rh-Sn-B catalysts supported on Al<sub>2</sub>O<sub>3</sub>, SiO<sub>2</sub> and TiO<sub>2</sub>. The catalysts supported on Al<sub>2</sub>O<sub>3</sub> were found to have good activity (conversion of 80-100%) and selectivity to oleic alcohol 45% and stearyl alcohol 11% with Ru-Sn-B [2] and selectivity to oleic alcohol 88,5% and stearyl alcohol 5% with Rh-Sn-B [3]. As biodiesel has a high content of fatty esters it was interesting to study their transformation into fatty alcohols. In order to obtain catalysts capable of processing feeds similar to industrial ones, studies the activity and selectivity to fatty alcohols using Ru-Sn-B/ Al<sub>2</sub>O<sub>3</sub> and Rh-Sn-B/ Al<sub>2</sub>O<sub>3</sub> catalysts and biodiesel as feed.

### Materials and Methods

**Catalyst preparation:** γ-Al<sub>2</sub>O<sub>3</sub> was used as support. The catalysts were prepared according to the method described by Shoenmaker-Stolk et al. After the impregnation step the metal precursors (RuCl<sub>3</sub>, RhCl<sub>3</sub> and SnCl<sub>2</sub>) were reduced with a sodium borohydride solution. Finally, the catalysts were activated by reduction in hydrogen at 300 °C for 2 h. The catalysts were named RuSn<sub>x</sub> and RhSn<sub>x</sub>, where x is the nominal percentage of Sn (2 and 4 wt%). The percentage of Ru and Rh was 1 wt%. They were characterized by different techniques, Inductively Coupled Plasma Atomic Emission Spectroscopy (ICP/AES), Specific surface area (BET), XPS, FTIR-CO, TPR, CO chemisorption, cyclohexane dehydrogenation, and TEM.

**Hydrogenation of FAME:** The experiments were carried out in a stainless-steel autoclave type reactor (280 cm<sup>3</sup> capacity). 1 g of catalyst and 20 g of biodiesel were used in all tests. The reagent (biodiesel) was provided by an industry of Santa Fe province (Argentina). The influence of reaction temperature (270, 290 and 320 °C) and hydrogen pressure (2.04, 4.76, 6.12 MPa) were studied. The reagent and the reaction products were analyzed by gas chromatography using a Shimadzu GC-2014 equipment with a Chevron ZB-FFAP column.

### Results and Discussion

In order to analyze the hydrogenation results a simplified reaction scheme is shown in Figure 1.

Figure 2 shows the yield to total alcohols obtained for the different temperatures and pressures studied with the analyzed catalysts. It can be concluded that the optimal reaction conditions for the maximum production of alcohols from biodiesel are: RhSn2 270°C, 4.76 MPa (Yield<sub>TotalAlc</sub>: 56.1%, Yield<sub>OleylAlc</sub>: 48%, Yield<sub>StearylAlc</sub>: 8.1%). RhSn2 290°C 6.12 MPa (Yield<sub>TotalAlc</sub>: 48.9%, Yield<sub>OleylAlc</sub>: 38.7%, Yield<sub>StearylAlc</sub>: 10.2%). At a higher temperature (320) the molar fraction of oleic alcohol has a maximum between 60 and 180 min of reaction. This is due to its transformation to octadecane and stearyl alcohol.

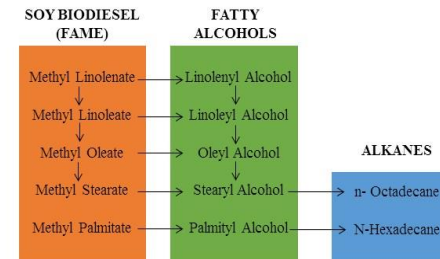


**Figure 1** Simplified reaction scheme. Vertical arrows correspond to C=C hydrogenation and horizontal arrows correspond to C=O hydrogenation.

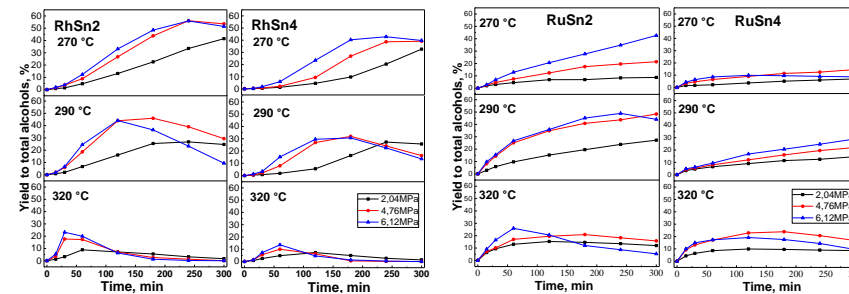


**Figure 2** Yield to Total alcohols (Oleyl Alcohol+Stearyl Alcohol) as a function of reaction time.

### Significance or Main Conclusions

It was found that the most active and selective catalyst for the formation of oleic alcohol by FAME hydrogenation were RuSn2/Al<sub>2</sub>O<sub>3</sub> and RhSn2/ Al<sub>2</sub>O<sub>3</sub> catalyst. This is attributed to an adequate balance between Ru, Rh and Sn. If the amount of Sn is high (4wt%), the catalyst has low activity because Ru and Rh atoms are blocked or electronic disturbed by Sn species, while with a lower amount of Sn (2wt%) a high selectivity for hydrogenating the carbonyl group is observed, thus occurring a higher selectivity to fatty alcohols. It is intended to study the optimal conditions that maximize the production of fatty alcohols in the continuous system. The possible deactivation and regeneration of the catalysts will also be studied.

### References

- [1] R.R. Egan, G.W. Earl, J. Ackerman; J. Am. Oil Chem. Soc. 61 (1984) 324–329.
- [2] M.A. Sánchez, V.A. Mazzieri, M.R. Sad, C.L. Pieck, React. Kinet. Mech. Catal. 107 (2012) 127-139.
- [3] C.A. Fonseca Benítez, V.A. Mazzieri, M.A. Sánchez, V.M. Benítez, C.L. Pieck, Appl. Catal. A, General 584 (2019) 117149.

## Structured catalysts for valorization of biogas to syngas

Francesca Bagioni<sup>2</sup>, Silvia Maina<sup>1</sup>, Patricia Benito<sup>2</sup>, Sonia Bocanegra<sup>1</sup> and Adriana Ballarini<sup>1\*</sup>

<sup>1</sup> INCAPe, Universidad Nacional del Litoral, Col. Ruta Nac, 168, Santa Fe 3000 (Argentina)

<sup>2</sup> Dip. Chimica Industriale e Materiali Toso Montanari, University of Bologna, Alma Mater Studiorum, viale Risorgimento 4, Bologna, 40136 (Italy).

\*aballa@fiq.unl.edu.ar

### Introduction

H<sub>2</sub>, besides its applications in the chemical industry, is considered to be the major energy carrier of the future, whereas syngas (CO and H<sub>2</sub>) can be used for chemical, fuel and power production. Dry reforming of Methane (DRM) has been proposed as one of the most promising technologies for harnessing these greenhouse gases and has turned out to be a good alternative. The importance of structured catalysts is increasing and is due to the advantages derived from good mass transfer and heat transfer that increase energy efficiency and heat recovery. The work reports the study of structured catalysts based on Rh-CeO<sub>2</sub>, Rh/ZnAl<sub>2</sub>O<sub>4</sub> and Rh/Al<sub>2</sub>O<sub>3</sub> supported on NiCrAl open cell metallic foams using two different techniques as washcoating and electrodeposition. The objective is to compare the two techniques used to cover the foams, evaluating their effect with respect to the activity and stability of catalysts synthesized, determining in particular the formation of carbon and the resistance of the layers in the DRM reaction. The effect of support and the active metal loadings on physical-chemical properties and catalytic activity was studied.

### Materials and Methods

Synthesis of catalysts by: 1) Electrodeposition (Rh3Ce97 and Rh8Ce92): They were performed in a flow cell at three electrodes (NiCrAl foam, the saturated calomel electrode (SCE) as a reference and the counter electrode is a Pt wire) and two compartments. Electrolytic solutions contain Rh/Ce nitrates (Molar ratio Rh/Ce: 3:97 and 8:92). The samples were dried and then calcined at 750°C. 2) Whascoating (Rh/Al<sub>2</sub>O<sub>3</sub> and Rh/ZnAl<sub>2</sub>O<sub>4</sub>): consists in the deposition of bohemite on NiCrAl foams by 3 immersions consecutive in the gel, increasing its concentration from 5% to 15%. To synthesize the γ-Al<sub>2</sub>O<sub>3</sub> layer, the samples were calcined at 450°C. Instead, to form a coating of ZnAl<sub>2</sub>O<sub>4</sub>, the bohemite-coated foams are impregnated with a solution of Zn(NO<sub>3</sub>)<sub>2</sub> and were calcined at 900°C. The deposition of the active phase (1%) was carried out by impregnating a solution of Rh(NO<sub>3</sub>)<sub>3</sub>, oven dried and calcined at 350°C.

The catalytic tests were performed at 750°C, atmospheric P, CH<sub>4</sub>:CO<sub>2</sub> ratio 1:1, 135 min reaction time. In order to study the catalyst stability, the catalyst displaying the best catalytic performance, additional experiments were performed for longer reaction times (5 h). XPS and SEM-EDS characterizations were carried out on fresh, calcined and reduced catalyst samples.

### Results and Discussion

Regarding the study carried out on the DRM reaction, all catalysts were found to be catalytically active and the tests carried out on the components of the catalysts allowed better identify their different contributions (Fig. 1 and 2). The support contribution (NiCrAl foam) turned out to be of little influence, despite the presence of the active metal in the reaction of the Ni(0),

as detected in the XPS analysis. The characterization of the surface of the Rh-CeO<sub>2</sub> catalyst by SEM-EDS showed that the coatings were well produced and the XPS data revealed the presence of Rh(0). The results obtained from the tests demonstrate that the CeO<sub>2</sub> alone was active, but the incorporation of Rh in the foams favored the increase of the activity and catalytic stability in the reaction, in agreement with the studies on the mechanism of the DRM catalyzed by noble metals. It was observed that increasing the Rh content in the Rh8Ce92 catalyst did not substantially improve the catalytic performance. A study of the reaction to longer times of reaction of the catalyst Rh3Ce97 gave as result a very good catalytic stability. Rh/Al<sub>2</sub>O<sub>3</sub> catalyst showed a performance catalytic in line with that of the Rh-CeO<sub>2</sub> catalysts while the Zn spinel affected negatively to catalytic performance (Fig. 2). Regarding the H<sub>2</sub>/CO ratio, it is similar for all the catalysts, varying between 0.6 and 0.7. H<sub>2</sub>/CO ratio, less than 1 indicates the presence of competing reactions, such as the WGS reverse, the Boudouard reaction, and the CH<sub>4</sub> decomposition, which produce water, CO, and carbon.

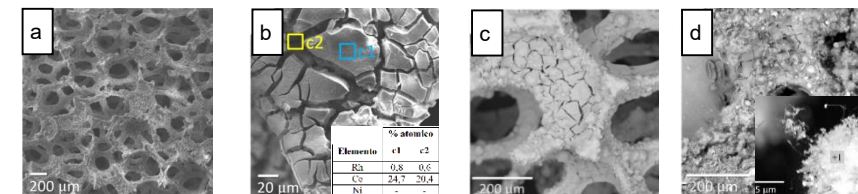


Figure 1. SEM images of NiCrAl foam (a), Rh3Ce97 (b), Rh/Al<sub>2</sub>O<sub>3</sub> fresh (c) and used (d). The EDS analysis was carried out in the area

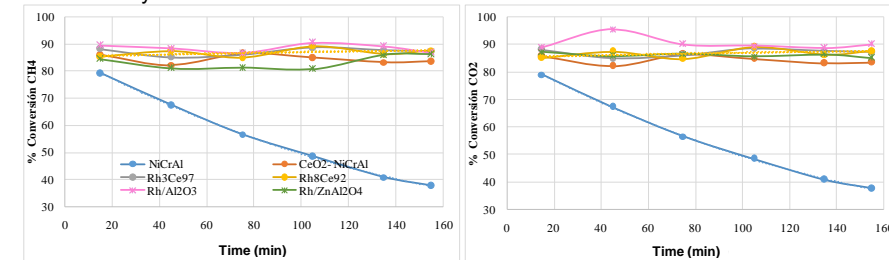


Figure 2. CO<sub>2</sub> (a) and CH<sub>4</sub> (b) conversions for the samples evaluated: NiCrAl foam, Rh3Ce97, Rh8Ce92, Rh/Al<sub>2</sub>O<sub>3</sub> and Rh/ZnAl<sub>2</sub>O<sub>4</sub>.

However, regardless of the synthesis technique used, the support oxide and the amount of active phase, all catalysts have developed amounts of nanometric filamentary carbon, which led to disintegration and loss of part of the coating, which will be improved (Fig. 1c).

### Significance or Main Conclusions

All the catalysts turned out to be catalytically active in the DRM reaction. Electrodeposition is an effective and fast technique to cover the foams, with a homogeneous and constant composition, although the fast speed of deposition is supported by the large preliminary study. On the other hand, to improve the layer deposition by washcoating, more studies are needed.

## Direct dehydrogenation of n-butane to n-butenes on Pt-based bimetallic catalysts supported on carbon nanotubes and vulcan carbon. Study of the promoting effect of Sn and In.

Gustavo Ramos Montero<sup>1\*</sup>, Adriana Ballarini<sup>1</sup>, Sergio de Miguel<sup>1</sup>, Sonia Bocanegra<sup>1</sup> and Patricia Zgolicz<sup>1</sup>

<sup>1</sup> INCAPe, FIQ-UNL-CONICET, Santa Fe 3000 (Argentina)

### Introduction

Studies on direct non-oxidative dehydrogenation of paraffins constitute one of the main lines of research in our research group. Unsaturated hydrocarbons can be obtained by selective dehydrogenation of paraffins, which is one of the raw materials required for the manufacturing of compounds such as detergents, solvents and polymers. Dehydrogenation of n-butane by non-oxidative catalysis can be a selective process. It is nevertheless constrained by thermodynamic limitations. In order to achieve good conversions, high temperatures are needed [1]. This causes lateral reactions to occur, including coke production, hydrogenolysis, isomerization, and cracking. As a result, effective supported metal catalysts with a high support surface, high degree of dispersion, and favorable metal-support interactions are required.

The addition of a second metal enhances the stability and selectivity of monometallic catalysts since these are frequently quite active but not very selective. These promoters could alter the catalytic metal phase, through geometric and/or electronic effects, resulting in a dilution of the Pt surface. This could then result in the formation of alloys and/or an intermetallic phase, which would avoid catalyst deactivation by preventing undesirable reactions [2].

Regarding the support, nanostructured mesoporous carbonaceous materials have certain features that make them suitable for dehydrogenation reactions. For instance, their surface ensures stronger electronic interactions with metals than conventional supports [2], which would prevent metallic particle agglomeration, and their high surface area and mesoporous structure could improve mass transfer and prevents intraparticle transfer [3]. Despite this, it is important to highlight that there is a limited amount of literature on non-oxidative direct dehydrogenation of light paraffins using catalysts supported in carbon materials, moreover, there are no publications with bimetallic catalysts supported in nanostructured carbonaceous materials for this type of reactions. The aim of this research is to study the effect of Sn and In in Pt catalysts supported in nanostructured carbon for the direct dehydrogenation of n-butane.

### Materials and Methods

Multi-walled carbon nanotubes (CNP, Sunnano MWCN, purity after purification >99%) and carbon black (CV, Cabot Corp. Cabot Corp. Vulcan carbon XC-72, purity >99%) were used as supports. To obtain 0.3% wt. of Pt, the supports were impregnated using an  $H_2PtCl_6$  aqueous solution. Bimetallic samples were obtained by impregnating the monometallic catalysts with  $SnCl_2$  or  $In(NO_3)_3$  aqueous solutions, to obtain 0.176% wt. of In and 0.06% wt. of Sn. The n-butane dehydrogenation was carried out in a continuous flow reactor at 530 °C, with a mixture of  $H_2/C_4H_{10}=1.25:1$ . Prior to the reaction, each catalyst was reduced in  $H_2$  flow by 2 h at 530 °C. The reaction products were analyzed in a gas chromatograph with a FID detector.

### Results and Discussion

The results of the n-butane dehydrogenation reaction are depicted in Figure 1. Pt catalysts are active, but both are deactivated throughout the course of a reaction. Coke production is the primary factor in the deactivation of monometallic catalysts, whereas cracking and isomerization reactions could be cause for the lower selectivities of monometallic catalysts [3]. Compared to its analogue supported in CNP, Pt/CV catalysts show higher activity but the lowest selectivity; this is presumably due to a different dispersion, particle size and/or metallic phase. The presence of Pt sites supported mainly in mesoporous materials, such as nanotubes and Vulcan carbon, guarantees a very good catalytic performance. The structure of nanostructured and semi -structured graphite carbons, CNP and CV, may encourage improved access for reagents to active sites without being constrained by mass transfer restrictions.

In general, the promoters addition to Pt catalysts improved the selectivity and stability of catalysts while reducing cracking and isomerization products as well as coke formation. The positive effect of the promoters addition may be associated with an electronic modification of the Pt. In the case of catalysts supported on CNP, the support would also contribute to the increase in electronic density around Pt metal particles, this could decrease the probability of coordination of C=C links due to repulsion, which also increases the activity and selectivity of reaction. Likewise, this could be related to the decrease in the assemblies required for the formation of coke by a geometric effect of blocking and/or dilution

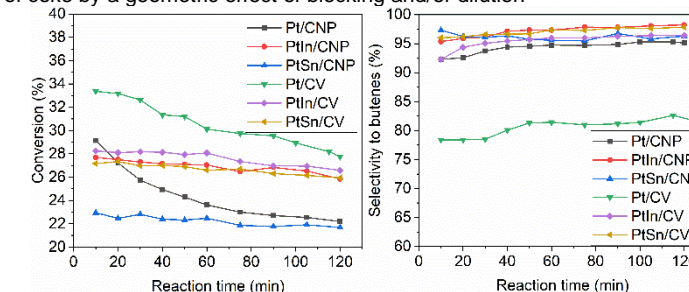


Figure 1. Results of n-butane dehydrogenation reaction: conversion and selectivity to butenes vs the reaction time for all catalysts.

### Significance or Main Conclusions

The monometallic catalysts supported on CNP showed good catalytic behaviors due to their high surface area, strong metal-support interactions, favorable reagent accessibility and product desorption. The promoters addition caused a formation of modified metal phases that decrease the concentration of assemblies that favor unwanted parallel reactions.

### References

- [1] S. Bocanegra, A. Ballarini, P. Zgolicz, O. Scelza, S. de Miguel; Catal Today 143 (2009) 334.
- [2] S. de Miguel, A. Ballarini, S. Bocanegra, S. de Miguel; Appl Catal A Gen 590 (2020) 117315.
- [3] A. Ballarini, S. Bocanegra, J. Mendez, S. de Miguel, P. Zgolicz; Inorg Chem Commun 142 (2022) 109638



## Effect of reduction temperature on ruthenium catalysts supported on biochars from rice husk for the hydrogenation reaction of levulinic acid to $\gamma$ -valerolactone

Virginia Rodríguez, Gustavo Mendow, Bárbara Sánchez, M. Florencia Azcoaga Chort, Juan Rafael García, Richard Pujo, Sergio de Miguel and Natalia Veizaga\*  
INCAPE, Ruta 168 km 0, Santa Fe 3000 (Argentina)

\*nveizaga@fiq.unl.edu.ar

### Introduction

Levulinic acid (LA) is one of the most important biomass platform molecules because it can be chemically converted to many secondary derivatives. Among the possible ones, the synthesis of  $\gamma$ -valerolactone (GVL) from LA by hydrogenation has attracted much attention due to the wide application of GVL in the production of solvents, polymers, and especially as fuel additives [1]. Supported Ru nanoparticles are active and selective catalysts due to their satisfactory ability to activate the C=O bond in the LA molecule [2]. Besides that, the preparation of high-performance activated carbon from biomass residues is promising and low-cost. The main objective of the work will be aimed at the synthesis of activated carbon from a biomass residue capable of being used as catalytic support, and on the other hand to find an optimal reduction temperature of Ru that leads to a high selectivity towards GVL.

### Materials and Methods

For the synthesis of the hydrothermal carbon (HTC), the rice husk from *Oryza sativa* L. (VRH) was dispersed in an aqueous solution of  $H_3PO_4$  (23 wt%) and kept at 200 °C for 24 h in a Teflon autoclave. Then, the solid was air-dried for 48 h and the carbonization stage was carried out under  $N_2$  flow with a heating rate of 6 °C min<sup>-1</sup> until 750 °C, which was held for 2 h. Finally, the charcoal was washed with distilled water at 65 °C in three stages.

The preparation of the catalysts with 2% Ru was carried out by the wet impregnation method, using HTC as support. Subsequently, the reduction of the catalyst was carried out in  $H_2$  flow and temperature (100, 150, 200, 275, or 350 °C) for 2 h. The hydrogenation reactions were carried out in a Parr autoclave. The reactor was charged with 100 mg of catalyst, 33 mL of distilled water, and 2.3 g of LA. The system was heated to 70 °C, with constant  $H_2$  pressure equal to 218 psi and stirring maintained at 1500 rpm. The reaction time was 2 h. The reactant and product concentrations were determined by gas chromatography.

The elemental composition (CHON) was determined with the aid of a LECO CHN 628 Series Elemental analyzer. The textural properties of VRH and HTC were determined by  $N_2$  adsorption-desorption at -196 °C. The acidic properties were determined using temperature-programmed desorption (TPD) of pyridine. After metal deposition, catalysts were reduced by using a reductive mixture (10 mL min<sup>-1</sup> of  $H_2$  (5 vol%)- $N_2$ ) in a flow reactor. Samples were heated at 6 °C min<sup>-1</sup> from 25 to 800 °C to obtain TPR signals.

### Results and Discussion

As can be seen from the elemental analysis, the carbon content for VRH is close to 40 %, making it viable for use as a carbonaceous support. From the analysis of the  $N_2$  adsorption-desorption isotherms, it is observed that VRH and HTC correspond to a type II isotherm with a hysteresis loop of type H4, according to IUPAC. HTC presents micro and mesoporosity. The BET area of the VRH has a value of 6 m<sup>2</sup> g<sup>-1</sup> and after activation with  $H_3PO_4$ , the HTC presents a BET area of 158.3 m<sup>2</sup> g<sup>-1</sup>. The acidity analysis showed that when the catalysts are treated with temperature, their acidity decreases with respect to the original sample (HTC). It is observed that the catalysts after being impregnated with the metallic precursor ( $RuCl_3$ ) and reduced at 150 and 200 °C present a lower acidity (87.2 - 87.8 umol Py g cat<sup>-1</sup>), regarding those treated with other temperatures such as 100, 275 and 350 °C, where the acidity values are 111.7, 97.6 and 103.7 umol Py gcat<sup>-1</sup>, respectively.

The TPR profiles are characteristic of supported Ru catalysts. Two very close peaks can be observed (120 and 178 °C). The first peak is attributed to the reduction of chlorinated species of Ru, while the one at a higher temperature corresponds to the reduction of ruthenium oxychloride. As reported in the literature, the hydrogen consumption that is visualized between 300 and 400 °C corresponds to the methanation of carbon by  $H_2$ . This peak is negligible for catalyst whose reduction temperature is above 200 °C.

When hydrogenating AL, it can be noted that the Ru reduction temperature has an optimum at which the selectivity towards GVL and levulinic acid conversion has a maximum (Figure 1). At 100 and 150 °C the conversion increases with increasing temperature and so does the selectivity. At 200 °C, the peak of maximum levulinic acid conversion (82%) and selectivity to the desired product (90%) is presented. When the temperature increases to 275 and 350 °C, it is observed that the conversion drops sharply to values below 30 %, while the selectivity drops more slowly for 275 °C, but at 350 °C no selectivity to the desired product is observed.

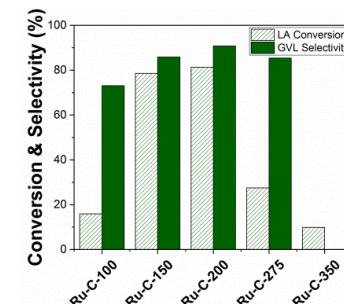


Figure 1. LA conversion (full bars) and GVL selectivity (dashed bars) for Ru supported on biochar catalysts reduced at different temperatures (Ru-C-temp).

### Significance or Main Conclusions

Ru catalysts supported on biochars obtained by hydrothermal treatment of rice husk were evaluated in the hydrogenation reaction of levulinic acid to  $\gamma$ -valerolactone. A relationship was found between acidity and reduction temperature with conversion and GVL selectivity results. These results showed that the catalyst with the best performance was the one whose Ru reduction temperature was 200 °C, which presented the lowest acidity.

### References

- [1] D. Albani, Q. Li, G. Vilé, S. Mitchell, N. Almora-Barrios, P.T. Witle, N. López, J. Pérez-Ramírez, Green Chem. 19 (2017) 2361-2370.
- [2] S. Li, Y. Wang, Y. Yang, B. Chen, J. Tai, H. Lui, B. Han, Green Chem. 21 (2019) 770-774.

## Wheat bran biorefinery. Fractionation, characterization and catalytic dehydration.

Lucas E. Retamar<sup>1\*</sup>, Federico Piovano<sup>1</sup>, Alicia V. Boix<sup>1</sup>, Soledad G. Aspromonte<sup>1</sup>

<sup>1</sup>Instituto de Investigaciones en Catálisis y Petroquímica (INCAPE, CONICET), Facultad de Ing. Química, Universidad Nacional del Litoral (Argentina).

\*lretamar@fiq.unl.edu.ar

### Introduction

Biorefineries emerge as a new technological system that allows the use of renewable raw materials, such as biomass, in order to obtain high value-added products [1]. This work proposes the revaluation of a by-product of agricultural production such as wheat bran (WB) to obtain compounds of commercial interest, like furans (HMF and furfural) and lactic acid (LA). This process involves WB fractionation, characterization of both, raw material (WB) and different fractions obtained, and the catalytic evaluation in polysaccharides dehydration.

### Materials and Methods

Fractionation: WB grain was fractionated, obtaining an extract (WBE) rich in C6 sugars and a residual solid (RS). This process consisted of a hydrothermal extraction at 90 °C with continuous stirring and microwave-assisted heating (MWH). Procedure was carried out with a concentration of 0.033 g/ml (g WB/ml H<sub>2</sub>O) for 15 min. Aqueous phase was centrifuged to obtain a residual solid (RS). The WBE fraction was obtained from ethanol precipitation.

Characterization: WB and different fractions were characterized, determining the contents of sugars, starch, protein, cellulose, hemicellulose, lignin, ashes and moisture, with techniques such as FTIR, TGA, UV-Vis, Elemental Analysis (CHONS) and XRF.

Catalytic evaluation: Fractions obtained (WB Extract and RS) were catalytically evaluated in dehydration with a stirred batch reactor at 180 °C, 30 atm of N<sub>2</sub> and 120 min. In the catalytic process, a mesoporous hydrous zirconia (ZrO<sub>2</sub>) catalyst synthesized by Sol-Gel method assisted by Pluronic P123 as surfactant was used. Reaction products were identified and quantified by HPLC using UV-Vis and Refraction Index (RI) detectors.

### Results and Discussion

Characterization and Hydrothermal Extraction: WB showed protein, starch and ash contents of 17.25 %, 19.1 % and 5.8 %, respectively (Table 1).

**Table 1. WB and RS characterization, H: hemicellulose, C: cellulose and L: lignin.**

Raw Material	Protein %	Starch %	Ash %	H %	C %	L%
WB	17.25	19.1	5.8	18.89	5.66	2.49
RS	20.04	-	-	27.65	10.49	3.67

The RS fraction presented a higher protein content than that found in the original biomass, indicating that the proteins are not extracted and remain in the RS. Insoluble polysaccharide contents were determined, i.e., hemicellulose, cellulose and lignin fractions are shown in Table 1. As can be seen, these fractions are concentrated after the extraction process in the RS, so it is the soluble portion is likely to separate in the extraction process. Furthermore, Figure 1 presents the DTG profiles obtained for WB, WBE and RS. A peak below 100 °C is linked with

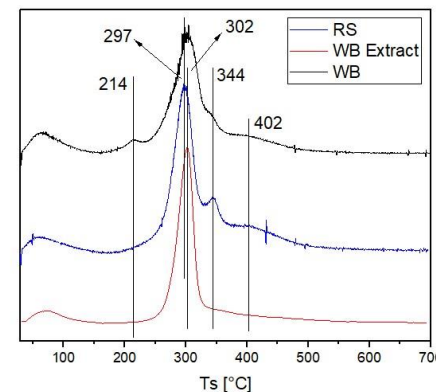


**Figure 1.** DTG profiles of extracted

water loss. WB shows a peak at 214 °C associated with a soluble fraction that is lost in the extraction process. It also presents a predominant signal close to 300 °C related to cellulose and starch contents. Two peaks are presented at 344 °C and 402 °C due to the presence of hemicellulose and lignin, respectively. RS has a predominant peak at 297 °C associated with a high cellulose content and also, shows the hemicellulose and lignin signals mentioned above. WB extract only shows a prominent peak at 302 °C related to a high starch content. In this way, it is highlighted that during the hydrothermal extraction with microwaves, an extract rich in starch is obtained.

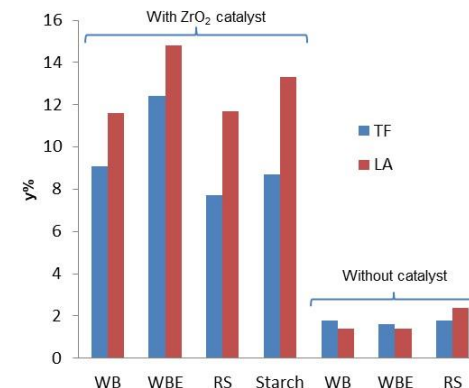


**Figure 2.** Catalytic results.

### Significance or Main Conclusions

A starch-rich extract was obtained from a real biomass source, obtaining yields of 12.4% and 14.8 % for TF and LA, respectively. The results obtained are promising and motivate to continue with the optimization of the fractionation processes to improve the mass yields obtained.

### References

- [1] Bajpai, P., Recycling and Deinking of Recovered Paper, Elsevier insights, Cap. 16: Uses of recovered paper other than papermaking (2014) 283–295.

## Synthesis and characterization of bimetallic catalysts for COPrOx reaction

Leticia E. Gómez\* and Alicia V. Boix  
FIQ-UNL, INCAPe, Santiago del Estero 2829, Santa Fe 3000 (Argentina)  
\*legomez@fiq.unl.edu.ar

### Introduction

Hydrogen has emerged as a promising energy vector that is both environmentally friendly and sustainable. The use of fuel cells, which are powered by H<sub>2</sub>, offers numerous desirable properties that make them attractive for a variety of applications. However, when H<sub>2</sub> is produced through the reforming of hydrocarbons and alcohols, a significant amount of CO remains in the H<sub>2</sub>-enriched stream. To avoid damage to the anode of the fuel cell, it is necessary to reduce the CO content to less than 10 ppm. One effective means of achieving this objective is through the Water Gas Shift reaction, which reduces the CO content to 1%. Then, CO Preferential Oxidation (COPrOx) is a promising alternative for eliminating the CO content [1]. Nobel metals and promoted noble metals have surged as promising catalysts for this reaction [2]. In this work, bi-metal exchanged zeolites were prepared to be used in the COPrOx reaction. A series of different techniques were employed to characterize the active phase.

### Materials and Methods

Catalyst Preparation: The powder catalysts PtCo-Mor (1wt.%Pt, 3wt%Co) and PtCu-Mor (1wt%Pt, 3wt%Cu) were synthesized via the ionic-exchange method with commercial Na-mordenite. In both cases, Pt was incorporated first, followed by the addition of Co or Cu metal. On the other hand, CoPt-Mor and CuPt-Mor were prepared with a similar procedure, but with a different order of incorporation of the cations. The resulting catalysts were dried and calcined in air flow.

Catalyst Evaluation: The catalysts were evaluated in a flow system under the following conditions: 1% CO, 1% O<sub>2</sub>, 40% H<sub>2</sub> and He. Before reaction, the catalysts were in situ reduced at 300 °C.

Characterization: The prepared catalysts were characterized using various techniques, including X Ray Diffraction (XRD), Temperature Programmed Reduction (TPR), Transmission Electron Microscopy (TEM), and X-ray Photoelectron Spectroscopy (XPS).

### Results and Discussion

The catalytic results of the study are presented in Figure 1, which displays the CO conversion curves of various powder catalysts. The findings demonstrate that cobalt-based catalysts exhibit higher activity compared to their copper-based counterparts. Specifically, CoPt-Mor and PtCo-Mor catalysts achieved maximum CO conversion rates of 94% at 120 °C and 92% at 135 °C, respectively. In contrast, CuPt-Mor and PtCu-Mor catalysts reached their maximum CO conversion values only slightly above 50% in the 100-120 °C temperature

range. All curves of selectivity of O<sub>2</sub> to CO<sub>2</sub> reaction (not showed) presented a decreasing trend.

Regarding the characterization of the catalysts, X-ray diffraction analysis indicated that all the catalysts presented dominant diffraction patterns of mordenite, and no peaks associated with Pt, Co, or Cu species were detected, indicating good dispersion of the metallic species in the support. TPR analysis showed that Co species were predominantly present as Co<sup>2+</sup> in exchange positions of the mordenite channels, in CoPt-Mor and PtCo-Mor catalysts. On the other hand, the temperature profiles of reduction in CuPt-Mor and PtCu-Mor catalysts suggested that Cu species were mainly present as CuO. Surface catalyst analyses conducted by XPS confirmed that cobalt species were primarily present Co<sup>2+</sup> in exchanged positions, whereas the binding energy measured for Cu 2p region indicated the presence of Cu<sup>2+</sup> and Cu<sup>+</sup> species. Regarding platinum, the analysis of the Pt 4d region suggested the coexistence of metallic platinum species and partially oxidized Pt in all samples. Further, TEM images showed that the PtCo-Mor particles had an average size of 2.1 nm, while the average size of PtCu-Mor particles was 4.1 nm.

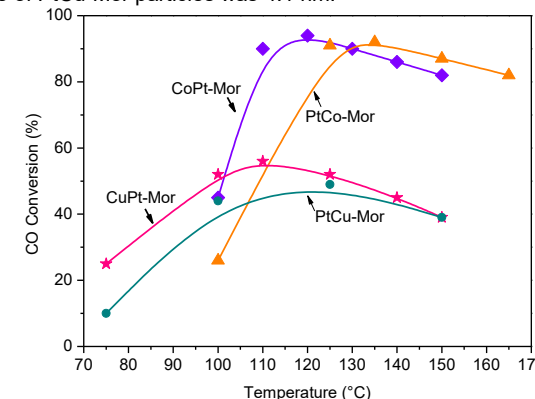


**Figure 1.** CO Conversion curves of bimetallic catalysts. Reaction conditions: 1 % CO, 1 % O<sub>2</sub>, 40 % H<sub>2</sub> and He. W/F: 2.1 mg-min/ mL.

### Conclusions

Catalysts prepared with platinum and cobalt presented promissory catalytic results for the COPrOx reaction. CoPt-M showed 94 % CO conversion at 120°C. The arrangement of cobalt cations within the zeolite in conjunction with Pt centers demonstrated superior catalytic performance respect Cu-based catalysts.

### References

- [1] N. Bion, F. Epron, M. Moreno, F. Mariño, D. Duprez, V. Top Catal 51 (2008) 76–88.
- [2] K. Liu, A. Wang, T. Zhang, ACS Catal. 2 (2012) 1165–1178.

## Facile preparation of Co and Ce oxide nanoparticles by an aerosol method and their catalytic evaluation for diesel soot abatement

María L. Godoy\*, Ezequiel D. Banús, Eduardo E. Miró and Viviana G. Milt  
INCAPE, FIQ - UNL, Santiago del Estero 2829, Santa Fe 3000 (Argentina)  
\*mgodoy@fiq.unl.edu.ar

### Introduction

Internal combustion engines are currently the most widespread used propulsion system in road and non-road transport. Among them, diesel engines are used for light and heavy-duty vehicles, agricultural and construction machinery, ships and industries because of their low consumption rate, high fuel economy and strong durability throughout time. Nevertheless, the associated increased particulate matter (PM) emissions during incomplete combustion of diesel engines are of global concern, as human health, our environment and global climate are all affected. Thereby, worldwide restrictive exhaust emission limits have been imposed in order to improve urban air quality. Current commercial solutions combine different operations performed in different compartments, thus increasing the size and cost of this aftertreatment technology. Consequently, there is a substantial interest in novel approaches that involve more abundant or discarded elements with high efficiency and stability, combined with low-cost technology. Catalyzed diesel particulate filters (CDPFs) have been proven to be effective in reducing PM in diesel engines. In order to reduce the production costs of the CDPF catalysts,  $\text{CeO}_2$  and  $\text{Co}_3\text{O}_4$  oxide particles were synthesized by precipitation from microdroplets of Ce and Co nitrate precursor solutions generated using a nebulizer and two different precipitating agents. This method was selected due to its simplicity and low cost. Both synthesized particles were characterized and tested for the catalytic removal of carbonaceous particles. This is a first step towards achieving cobalt oxide particles recovered from spent lithium-ion batteries [1] and depositing them in stacked wire mesh monoliths [2].

### Materials and Methods

$\text{CeO}_2$  and  $\text{Co}_3\text{O}_4$  particles were obtained from the precipitation of 0.5 mol/L  $\text{Ce}(\text{NO}_3)_3$  and  $\text{Co}(\text{NO}_3)_2$  solutions in concentrated  $\text{NH}_4\text{OH}$  and  $\text{NaOH}$  solutions respectively, using a nebulizer an aerosol microdroplet generator. The resulting suspensions were filtered and washed with distilled water six times and then once more with ethanol. They were then oven-dried at 70 or 130 °C for 24 h, calcined at 600 °C for 2 h and named Ce(S) and Co(S). It was necessary to use a thermostatic bath at 25 °C in the case of the synthesis of Ce particles due to the endothermicity of the process.

The morphology of synthesized samples was determined by Transmission Electron Microscopy (TEM). The particles were also analyzed by X-Ray Diffraction (XRD) to determine the formation of the different crystalline oxides, along with the crystallite size, and these studies were complemented with Laser Raman Spectrophotometry (LRS).

Catalytic evaluations were carried out by incorporating diesel soot into synthesized particles (1/20 soot/catalyst ratio) via wet impregnation using *n*-hexane. The reactor was fed with 20 ml/min of a mixture composed of NO (0.1%) and O<sub>2</sub> (18%), He balance, 5 °C/min from room temperature to 600 °C.

### Results and Discussion

TEM images are shown in Figure 1. In the case of Ce(S) sample, non-spherical cube-shaped particles 8 nm average size were observed whereas for Co(S) sample, larger, rounded-

edged particles in the form of spheres and nanorods, 37 nm average size, were observed (Table 1). Diffraction patterns off the prepared samples Ce(S) and Co(S) indicated the presence of the fluorite-type ceria cubic phase and cubic spinel phase of  $\text{Co}_3\text{O}_4$  respectively, in agreement with LRS analysis. The average size of the nanocrystallites was also estimated (Table 1) using the Debye–Scherrer equation, and it was found to be 8.4 nm for Ce(S) and 33.1 nm for Co(S), values close to those obtained from the TEM analysis.

Catalytic test on ceria sample showed a broad peak resulting from two contributions, one due to the more intimate soot-catalyst contact and another, at a higher temperature, to the weak soot-catalyst contact. These two types of soot-catalyst contact are a consequence of the method used for the wet impregnation of soot on catalytic particles, which has been adopted as a good simulation of the behavior of a real DPF filter. Curve deconvolution indicated values of maximum soot burning rate temperature ( $T_M$ ) of 387 °C for the intimate contact and  $T_M = 430$  °C for the loose contact. In the case of Co(S) particles, profile is sharper than that observed for ceria catalyst, probably due a better contact originated between soot particles and cobalt oxide nanorods, whereas  $T_M = 358$  °C (Table 1). This improvement in catalytic activity would be related to the morphology of the Co(S) nanoparticles, since their spatial arrangement plays an important role in the solid-solid reactions, with the number of contact points between the soot particles and the catalytic nanofibers being a key factor for the activity [3].

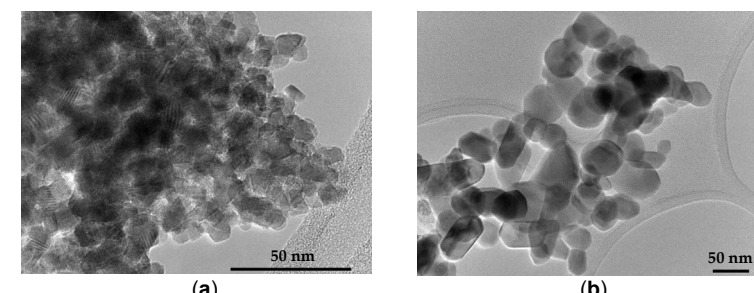


Figure 1. TEM images of synthesized particles (a)  $\text{CeO}_2$  and (b)  $\text{Co}_3\text{O}_4$ .

Table 1. Synthesized  $\text{CeO}_2$  and  $\text{Co}_3\text{O}_4$  particles: characterization and catalytic results.

Catalyst	Average size (nm) <sup>1</sup>	Crystallite size (nm)	$T_M$ (°C)
Ce(S)	8	8.4	387
Co(S)	37	33.1	358

<sup>1</sup>Average values obtained from TEM images (Figure 1).

### Main Conclusions

The facile synthesis route and good catalytic performance of the nanoparticles developed encourages their deposition in structured systems (stacked wire mesh monoliths) for its practical application.

### References

- [1] C. Marcoccia, M. Peluso, J. Sambeth; Mol. Catal. 481 (2020) 110223.
- [2] M. Godoy, E. Banús, O. Sanz, M. Montes, E. Miró, V. Milt; Catalysts 8 (2018) 16.
- [3] M. Stegmayer, M. Godoy, J. Múnera, E. Miró, V. Milt; Surf. Coat. Tech. 439 (2022) 128451.



## Zirconia-based catalysts for hydrothermal conversion of sugars using template-assisted sol-gel method.

Federico A. Piovano\*, Soledad G. Aspromonte and Alicia V. Boix

INCAPE, Colectora Ruta Nac. Nº 168 Km 0 - Paraje El Pozo- (3000) Santa Fe - Argentina  
\*fpiovano@fiq.unl.edu.ar

### Introduction

Catalytic hydrothermal conversion of saccharides is an attractive green chemistry process, since reactants can be obtained by hydrolysis of lignocellulosic biomass. Lignocellulose is an abundant and low-cost resource from agricultural and forestry residues. Depending on the catalyst employed, this process allows producing valuable platform molecules, such as lactic (LA), glycolic, formic, acrylic and levulinic acids, furfural and 5-hydroxymethylfurfural (HMF) [1]. Among them, LA has extensive applications in cosmetics, pharmaceutical and food industry. In addition, it is the chemical precursor of polylactic acid (bioplastics) and alkyl-lactates (biosolvents). LA can be obtained from sugars by retro-aldol condensation route using alkaline catalysts [2]. However, a more selective and efficient process demands a catalyst with a suitable balance of Lewis and Brønsted acid sites. Furthermore, catalysts require aqueous medium stability, high surface area and a porous structure that allows diffusion of bulky molecules involved. The aim of this work is the synthesis of high surface porous catalysts based on zirconia for their application in the hydrothermal conversion of sugars towards LA. The impact of certain parameters, such as the synthesis medium and template removal method, on the physicochemical properties was determined.

### Materials and Methods

Synthesis of catalysts was carried out by template-assisted sol-gel method. Zirconium n-propoxide and non-ionic copolymer Pluronic P123 ( $\text{PEO}_{20}\text{PPO}_{70}\text{PEO}_{20}$ ) were used as metallic precursor and template, respectively. Isopropanol (I), ethanol (E) and water (W), were studied as synthesis mediums. In addition, two template removal procedures were employed: calcination in airflow at 673 K (Cal) and refluxing extraction with ethanol at 353 K (Ex). Physicochemical characterization of materials was performed by means of  $\text{N}_2$  absorption-desorption isotherms at 77 K, XRD, FTIR, TGA/DTA, TEM and potentiometric titration with n-butylamine. Catalytic evaluation was carried out in a stainless steel batch reactor (45 mL) under a  $\text{N}_2$  pressurized atmosphere and test reaction was the hydrothermal conversion of a monosaccharides solution. Reaction products were analyzed by HPLC using UV-Vis and RI detectors.

### Results and Discussion

Table 1 shows main physicochemical characterization results for synthesized catalysts. Materials treated by refluxing extraction resulted in high surface areas ( $S_{\text{BET}}$ ), pore volumes ( $V_p$ ) and amount of acid sites ( $A_s$ ), especially for those synthesized in alcoholic medium. Non-aqueous medium allowed a better control of hydrolysis/condensation rate of the metal precursor during the oxide/hydroxide network formation. Additionally, the synthesis medium strongly affected  $A_s$ , finding the order I > E > W. On the other hand, heat-treated catalysts

underwent a significant reduction in all parameters, with the exception of the one synthesized in ethanol and calcined (E-Cal), which maintained an equally high  $V_p$ .  $\text{N}_2$  ads.-des. isotherms (not shown) of first group can be classified as intermediate between type I and IV, indicating the presence of micro- and mesoporosity, while the calcined materials showed a more defined type IV isotherm. E-Cal consists of regular shape crystals (500-700 nm) with a disordered wormhole-like porous structure (13 nm average pore diameter), as can be seen in Figure 1. In agreement with the physicochemical properties, the extraction-treated materials reached the highest conversions and selectivities towards LA during the hydrothermal conversion of sugars. The most outstanding catalyst was "I-Ex", which achieved a mass yield of 42.8 %. The calcined materials showed higher selectivities towards furans but significantly lower conversion.

**Table 1. Main physicochemical characterization and catalytic evaluation results.**

Catalyst	Physicochemical properties			Conversion (%)	Selectivity (%)	
	$S_{\text{BET}}$ ( $\text{m}^2/\text{g}$ )	$V_p$ ( $\text{cm}^3/\text{g}$ )	$A_s$ ( $\mu\text{mol/g}$ )		LA	Fur
I-Ex	326	0.22	270	90.2	38.6	13.9
I-Cal	109	0.10	50	65.6	26.8	25.1
E-Ex	367	0.43	156	84.6	34.4	15.1
E-Cal	133	0.40	30	66.1	31.7	23.2
W-Ex	186	0.11	67	78.2	31.5	17.7
W-Cal	47	0.05	26	56.4	25.0	26.5

Reaction conditions: 453 K, 90 min, 30 bar, 70 mg of catalyst, 18 ml of reactant solution (xylose 0.04 M, arabinose 0.02 M and glucose 0.01 M). LA: lactic acid, Fur: total furans (furfural and 5-hydroxymethylfurfural).

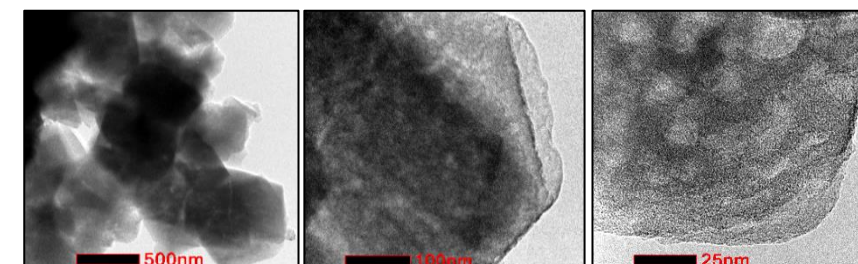


Figure 1. TEM images of mesoporous  $\text{ZrO}_2$ -based catalyst E-Cal (JEOL-2100 plus microscope operated at 200 kV).

### Significance or Main Conclusions

Instead of heat treatment, template removal by reflux extraction avoids the destruction of internal microporous structure, which confers high surface area, and preserves a larger number of acid sites. Among the synthesized materials, the I-Ex catalyst obtained the best performance in the conversion of an aqueous solution of sugars towards LA.

### References

- [1] F.A. Piovano, S.G. Aspromonte, A.V. Boix; Biomass Conv. Bioref. (2022).
- [2] L. Yang, J. Su, S. Carl, Applied Catalysis B: Environmental 162 (2015) 149–157.

## Catalytic performance of structured substrates based on synthesized Co,Ce oxide nanoparticles for particulate matter combustion

Maria L. Godoy\*, Eduardo E. Miró, Viviana G. Milt and Ezequiel D. Banús  
INCAPE, FIQ - UNL, Santiago del Estero 2829, Santa Fe 3000 (Argentina)  
\*mgodoy@fiq.unl.edu.ar

### Introduction

Diesel engines have stood out for their high performance, with the disadvantage of emitting particulate matter. Diesel particulate filters (DPF) are an after-treatment system implemented to prevent their release into the atmosphere. Cordierite ceramic monoliths are currently widely used as DPFs. In order to develop systems that can be technologically applicable, the production costs of structured catalysts must necessarily be reduced. To this end, it was proposed to develop Ce and Co oxide particles in the laboratory and deposit them on stacked wire mesh and cordierite monoliths. The developed catalytic systems were evaluated for diesel soot combustion.

### Materials and Methods

Ce and Co oxide particles were developed from the precipitation of 0.5 M  $\text{Ce}(\text{NO}_3)_3$  and  $\text{Co}(\text{NO}_3)_2$  solutions in concentrated  $\text{NH}_4\text{OH}$  and  $\text{NaOH}$  solutions, correspondingly, using a nebulizer. Synthesized particles were named Ce(S) and Co(S), respectively and were deposited onto metallic and ceramic monoliths by immersing the structures into  $\text{CeO}_2$  or Co,Ce equimolar suspensions during 1 min. Four suspensions were prepared, as seen in Table 1, containing commercial  $\text{CeO}_2$  nanoparticles (Nyacol®, Ce(Ny)) and polyvinyl alcohol (PVA).

AISI 304 stainless steel monoliths (16 mm diameter and 30 mm height) were assembled as described by Godoy et al. [1], calcined at 900 °C, and here referred to as "M". Cordierite monoliths (100 mm<sup>2</sup> frontal area and 20 mm height) were prepared according to Stegmayer et al. [2], washed and dried in an oven at 130 °C overnight and designated as "m".

Morphology of the catalytic coating obtained on both the surfaces of intermediate wire meshes of metallic monoliths and central channels of cordierite monoliths was studied by Scanning Electron Microscopy (SEM), and its composition by Energy Dispersive X-Ray Spectroscopy (EDS). Samples were analyzed by X-Ray Diffraction (XRD), being complemented these studies with Laser Raman Spectroscopy (LRS).

Catalytic evaluations were carried out by incorporating diesel soot into the catalytic structures from a particulate matter suspension in *n*-hexane (3000 ppm).

### Results and Discussion

$\text{CeO}_2$  and  $\text{Co}_3\text{O}_4$  nanoparticles were obtained by means of the spray-precipitation method, cube-shaped 8 nm and rounded-edged 37 nm average size, respectively. Their deposition on structures substrates produced a homogeneous catalytic layer along the metallic fibers (Fig. 1 a) and cordierite channels (Fig. 1b). In Figure 1a it can be seen that ceria nanoparticles Ce(Ny) cover the metal fibers homogeneously, and the addition of Ce(S) or Co(S) nanoparticles results in micrometric aggregates. For Co(S),Ce(S),Ce(Ny)-M a very homogeneous rough coating of the metal fibers is observed, with aggregates of particles of size 2-3 μm.

In Figure 1b, it is noticed that synthesized particles Ce(S) and Co(S) are deposited on the Ce(Ny) coating as micrometric aggregates, distributed both on the external surface and inside the cordierite macropores. For Co(S),Ce(S),Ce(Ny) catalyst, the image reveals a

homogeneous film covering the external surface and partially filling the macropores. The cubic fluorite-type  $\text{CeO}_2$  and cubic spinel-type  $\text{Co}_3\text{O}_4$  phases were detected by XRD in all structured samples, in agreement with LRS.

Maximum combustion rate temperatures ( $T_M$ ) of structured catalysts are listed in Table 1. It can be noticed that mixed systems containing cobalt and cerium present lower  $T_M$  if compared with systems only containing Ce, because cobalt enhances the ceria oxygen store capacity and hence the catalytic activity of the mixed systems. Among the catalysts tested, the structured systems using ceramic substrates were more efficient.

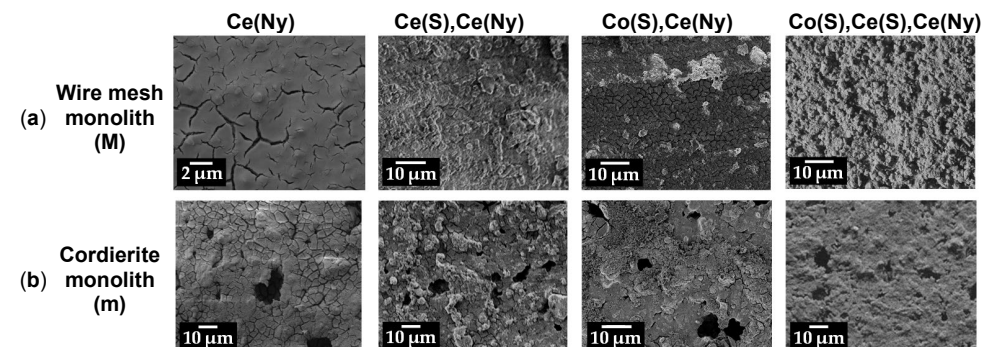


**Figure 1.** SEM micrographs of the central sections of (a) the intermediate wire mesh of metallic monoliths and (b) inner channels of cordierite structures.

**Table 1.** Catalytic activity of structured substrates for soot combustion.

Catalyst incorporated to structured substrates	$T_M$ (°C)	
	Wire mesh (M)	Cordierite (m)
Ce(Ny)	476	444
Ce(S),Ce(Ny)	452	441
Co(S),Ce(Ny)	417	411
Co(S),Ce(S),Ce(Ny)	419	408
Bare substrate	540 [3]	524 [2]

Reaction conditions: 20 mL/min of 0.1% NO, 18% O<sub>2</sub> in He, 5 °C/min from room temperature to 600 °C.

### Main Conclusions

We obtained both metallic and ceramic structured catalysts based on  $\text{CeO}_2$  and  $\text{Co}_3\text{O}_4$  synthesized nanoparticles, with an active layer firmly adhered that showed a good catalytic activity for particulate matter combustion.

### References

- [1] M.L. Godoy, E.D. Banús, O. Sanz, M. Montes, E.E. Miró, V.G. Milt; *Catalysts* 8 (2018) 16.
- [2] M.A. Stegmayer, M.L. Godoy, J.F. Múnera, E.E. Miró, V.G. Milt; *Surf Coat Technol* 439 (2022) 128451.
- [3] M.L. Godoy, E.D. Banús, E.E. Miró, V.G. Milt; *J Environ Chem Eng* 7 (2019) 103290.

## Nanostructured mixed oxide growth on alpacca and their application as microreactors for the CO oxidation

Mayra A. Franco<sup>1\*</sup>, Ana P. Cabello<sup>2</sup>, María A. Ulla<sup>1</sup> and Juan M. Zamalo<sup>1</sup>

<sup>1</sup>Instituto de Investigaciones en Catálisis y Petroquímica INCAPe, Santa Fe 3000 (Argentina)

<sup>2</sup>Instituto de Desarrollo Tecnológico para la Industria Química (INTEC), Santa Fe 3000 (Argentina)

\*mafrancomurcia@fiq.unl.edu.ar

### Introduction

Oxide nanostructures can function as catalysts for oxidation reactions. Our previous work demonstrated that copper-zinc oxides films (CuO/ZnO) grown on metallic substrates had high performance as microreactors for the catalytic CO oxidation reaction [1,2]. The objective of this study is to analyze the in-situ growth of nanostructure films on a trimetallic alloy (copper, zinc, and nickel) called 'German silver or alpacca'. The films were synthesized through a vapor oxidation method and then were studied in a microreactor for the CO oxidation reaction.

### Materials and Methods

Commercial alpacca foils (66%Cu, 20%Zn, 14%Ni) were used as substrate. The oxides films were synthesized on flat alpacca foils (FF) and foils with microchannels (MF) by a vapor oxidation route with equivolumetric mixture of hydrogen peroxide ( $H_2O_2$ ) and ammonium hydroxide ( $NH_4OH$ ). The synthesis was carried out at 25 and 80°C in different times (0,5 – 16 hours). To examine the reproducibility, each synthesis was done in triplicate. Before and after each synthesis, the weight of these samples was determined. The samples were denoted F-T-X, where F: FF or MF the foils type, T: indicates the operation temperature, and X: the synthesis time in hours.

### Results and Discussion

The mass gain increased with the synthesis time for both synthesis temperatures (Figure 1.). As was expected at 25°C, the kinetic of the crystalline growth was lower and then a lower mass gain was obtained. All samples XRD patterns showed  $Cu(OH)_2$ , CuO and ZnO phases. The FF-80-16 sample showed the NiO peak of the (220) plane. In all oxidized samples persisted high XRD intensities of the substrate evidencing a thin thickness of the oxide films.

The SEM analysis of the FF-80-X samples showed that the alpacca substrate was covered with nanostructures having two different morphologies. Some regions were covered with prismatic crystals typical of  $Cu(OH)_2$  and CuO, and these were surrounded by globular aggregates related to ZnO. By increasing the synthesis time up 16 hours, the ZnO crystals grew above the  $Cu(OH)_2$  and CuO structures. By EDS analysis, it was possible to corroborate the presence of NiO only on the FF-80-16 sample.

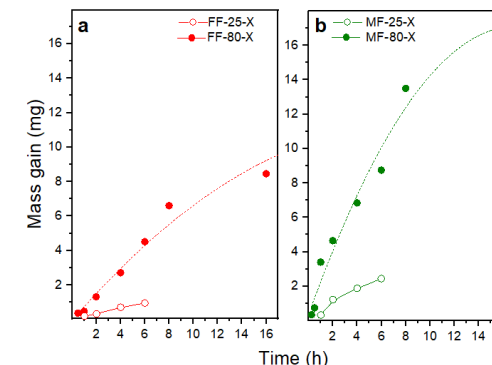


Figure 1. Average mass gain (mg) of alpacca substrates after the syntheses at different times.  
a) FF b) MF

MF showed a comparative higher mass gain because the microchanneled surface. These nanostructure films were evaluated in the CO oxidation reaction. They were highly active reaching full conversion at 175°C. This activity is linked to the strong synergy given the close contact between the nanometric crystals of both oxides. The higher relative activity (Ra) for the MF-25-1 sample was because the thin film of the nanoxide.

Table 1. Catalytic results of nano-oxide microreactors

Sample	Synthesis time	Synthesis Temp.	$mO^a$ (mg)	$T^{50}$ (°C)	$X^{150} b$	$Ra^c$
MF-80-1	1 h		5,9	142	63,6	10,8
MF-80-2	2 h		10	140	67,2	6,7
MF-80-4	4 h	80°C	13,7	142	64,3	4,7
MF-80-6	6 h		17,5	141	63,9	3,7
MF-25-1	1 h		0,45	139	65,9	146
MF-25-2	2 h	25°C±2	2,15	154	43,6	20,3
MF-25-4	4 h		3,6	181	14,1	3,91

a Mass of oxygen incorporated due to oxidation of the foils, b CO conversion at 150 °C, c Relative activity:  $X^{150}/mO$

### Significance or Main Conclusions

It was possible to obtain thin films of well-anchored oxide nanostructures on a ternary alloy substrate such as alpacca. The oxide growths were formed by nanocrystals of  $Cu(OH)_2$ , CuO and ZnO. These catalytic nanofilms were highly active in the catalytic CO oxidation reaction.

### References

- [1] A. Cabello, M. Ulla, J. Zamalo; *Top. Catal.* 62 (2019) 931–940
- [2] A. Cabello, M. Ulla, J. Zamalo; *J.Mater.Sci.* 57 (2022) 12797–12809.



## Catalytic transformation of biomass-derived butanol into light olefins

Cristian A. Fonseca<sup>1</sup>, Pablo J. Luggren<sup>1\*</sup>

<sup>1</sup>Grupo de Investigación en Ciencia e Ingeniería Catalíticas (GICIC), INCAPe (CONICET-UNL), Santa Fe 3000 (Argentina)

\*pluggren@fiq.unl.edu.ar

### Introduction

Nowadays, the fuel industry strongly focuses on biomass-derivate products to reduce its dependence on petrochemical sources and to take advantage of the large amounts of lignocellulosic waste from agro-industrial processes. Due to their properties and availability, oxygenated platform molecules are important feedstock to produce olefins and fuels. In a previous work, this group studied the production of C2-C7 olefins from biomass-derived butyric acid over a series of Zn-Zr mixed oxides of varied molar ratios of Zn/Zr (0.11–0.66), showing 0.25ZnZr the best performance [1].

ABE fermentation is a well-known process to generate alcohols and acetone (Acetone-Butanol-Ethanol, 3:6:1 mass ratio) from biomass [2]. Using the ABE mixture might mean advantages to obtain olefins. However, acetone transformation into hydrocarbons requires higher temperatures. Acetone can be easily removed from the ABE mixture, which improves the process using only the alcoholic phase [2]. Although the olefins from ethanol process has been largely studied [3], the transformation of the ABE alcohol mixture into olefins has been barely developed. In this work, the catalytic transformation of butanol (C4OL) into light olefins is discussed, providing the use of ABE mixture in the future.

### Materials and Methods

A Zn-Zr catalyst (0.25Zn/Zr molar ratio) was prepared by incipient wetness impregnation of a  $\text{Zn}(\text{NO}_3)_2$  aqueous solution on  $\text{Zr}(\text{OH})_4$ , further drying at 373K and decomposition in air at 823K. Acid and base properties of 0.25ZnZr catalyst were investigated, combining TPD of  $\text{NH}_3$  and  $\text{CO}_2$ . The catalytic tests were carried out in a gas-phase fixed bed reactor. C4OL was vaporized in a  $\text{N}_2$  stream to obtain  $\bar{P}_{\text{C4OL}}=0.85 \text{ kPa}$ ;  $\bar{P}_{\text{H}_2}=7.22 \text{ kPa}$ ;  $\bar{P}_{\text{N}_2}=93.23 \text{ kPa}$ . Contact times  $\text{W/F}_{\text{C4OL}}^0$  from 32 to 835 g h/mol were evaluated. Products were identified and quantified by GC-MS.

### Results and Discussion

The Physicochemical properties of simple and mixed oxides catalysts are shown in Table 1. The incorporation of Zn in Zn-Zr mixed oxide improves the surface area and balances the acid-base properties in comparison to the  $\text{ZnO}$  and  $\text{ZrO}_2$  single oxides. The light olefin production from alcohols involves a series of sequential steps comprising dehydrogenation, ketonization, aldol condensation, C-C bond rupture, and deoxygenation reactions, promoted by catalysts with acid-base properties [1,3]. The results obtained in the catalytic experiments performed at different  $\text{W/F}_{\text{C4OL}}^0$  (between 32-835 g h/mol) allow us to postulate the reaction network for the upgrading of C4OL to olefins using 0.25ZnZr mixed oxide. C4OL to olefins reaction might begin from two paths. On one hand, C4OL dehydration produces butene ( $\text{C4=}$ ). On the other hand, dehydrogenation of C4OL leads to the formation of butyraldehyde ( $\text{C4AL}$ ). Then, by combining two molecules of C4AL through a self-esterification reaction (Tishchenko), butyl butyrate can be obtained [4], which gives 4-Heptanone ( $\text{C7K}$ ) through a ketonization reaction. From C7K two different groups of olefins might be obtained [1]: I) McLafferty/aldol condensation pathway ( $\text{C2=}$  + isobutene,  $\text{iC4=}$  +  $\text{C6=}$ ) and II) hydrogenation/ dehydration

pathway ( $\text{C5=}$  +  $\text{C7=}$ , and also including  $\text{C4=}$  as obtained as from C4OL). The yields for these groups of the products obtained on 0.25ZnZr,  $\text{ZrO}_2$  and  $\text{ZnO}$  under at equal conditions are presented in Figure 1A. By comparing these catalysts, it can be observed that  $\text{ZrO}_2$  is active to promote only the initial step of the reaction sequence with high yields of  $\text{C4=}$ ,  $\text{C7K}$  and  $\text{C7=}$  through  $+\text{H}_2/\text{-H}_2\text{O}$  pathway, while both  $\text{ZnO}$  and 0.25ZnZr promote McLafferty/A.C. pathway because of a rapid dehydrogenation of C4OL to C4AL and the final formation of  $\text{C2=}$  and  $\text{iC4=}$ . It can also be observed that Zn-Zr interaction in 0.25ZnZr enhances acid-base properties and favors a higher yield to McLafferty/A.C. derived olefins. In addition, a new experiment on 0.25ZnZr at 723K (Figure 1B) showed that the yield to total olefins reached 52%, and that McLafferty/A.C. pathway was improved.

**Table 1.** Physicochemical properties of the catalysts

Catalyst	SA <sup>a</sup> (m <sup>2</sup> /g)	Acid-base properties	
		$n_b$ <sup>b</sup> (μmol/g)	$n_a$ <sup>c</sup> (μmol/g)
$\text{ZrO}_2$	21	3.3	27.2
0.25ZnZr	61	44.6	136.9
$\text{ZnO}$	18	2.7	2.5

<sup>a</sup>BET surface areas (SA) by  $\text{N}_2$  physisorption;

<sup>b</sup>Catalyst base site number by TPD of  $\text{CO}_2$ ; <sup>c</sup>Catalyst acid site number by TPD of  $\text{NH}_3$ .

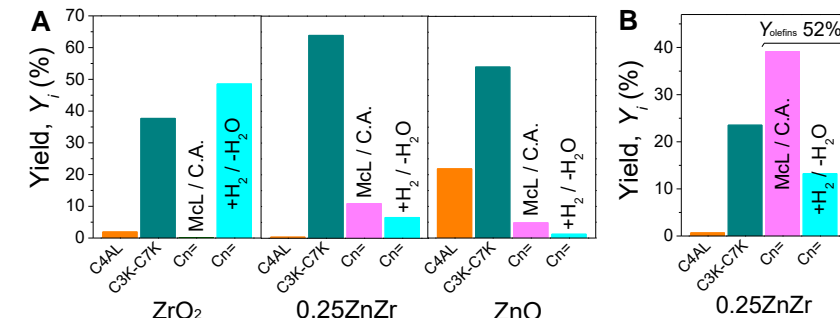


**Figure 1.** Yield of main products ( $Y_i$ ) obtained over: A)  $\text{ZrO}_2$ , 0.25ZnZr, and  $\text{ZnO}$  at  $T=688\text{K}$ , and B) 0.25ZnZr at  $T=723\text{K}$ .  $[\text{W/F}_{\text{C4OL}}^0=322 \text{ h g/mol}; \text{P}=101.3 \text{ kPa}, \bar{P}_{\text{C4OL}}=0.85 \text{ kPa}; \bar{P}_{\text{H}_2}=7.22 \text{ kPa}, \text{X}_{\text{C4OL}}=100\%, \text{balance with N}_2]$

### Significance or Main Conclusions

The highest light olefins yield ( $\text{C2=}$  to  $\text{C8=}$ ) was 52% and was obtained on 0.25ZnZr at 723K and  $\text{W/F}_{\text{C4OL}}^0=322 \text{ h g/mol}$ . The addition of Zn in ZnZr mixed oxide improved both the acid-base properties and the catalytic performance, favoring the obtention of olefins through McLafferty/A.C. pathway.

### References

- [1] P.J. Luggren, L.A. Dosso, J.I. Di Cosimo; Appl. Catal. A: General. 632 (2022) 118474.
- [2] A. Reviere, D. Gunst, M. Sabbe, A. Verberckmoes; J. Ind. Eng. Chem. 89 (2020) 257–272.
- [3] R.A.L. Baylon, J. Sun, Y. Wang; Catal. Today 259 (2016) 446–452.
- [4] W. Shen, G. Tompsett, R. Xing, W. Curtis Conner, G. Huber; J. Catal. 286 (2012) 248–259.

## Synthesis and characterization of Zn-modified MnCO<sub>3</sub> catalysts for application in aromatic alcohol oxidation

Pablo J. Luggren, Juan Zelin, Hernán A. Duarte, Maria E. Sad\*, Verónica K. Díez\*, J. Isabel Di Cosimo

Catalysis Science and Engineering Research Group (G/CIC) – INCAPe (UNL-CONICET)  
Colectora RN 168 km 0 Paraje El Pozo, (3000) Santa Fe, Argentina

\* mesad@fiq.unl.edu.ar, \* verodiez@fiq.unl.edu.ar

### Introduction

Benzaldehyde (B) is an important intermediate widely used in pharmaceutical, dye, food, perfume and agrochemical industries. Traditional synthesis of aldehydes via alcohol oxidation implies methods involving toxic homogeneous catalysts such as chromium(VI)-based reactants or nitric acid and inorganic oxidants (H<sub>2</sub>O<sub>2</sub>, dimethyl sulfoxide, permanganates), with the consequent environmental concerns because of disposal issues. The use of solid catalysts and O<sub>2</sub> overcome the problems associated with traditional processes, the catalyst may be recovered and reused. Both noble and non-noble metal catalysts have been tested in oxidation reactions. In recent years, much attention has been paid to MnCO<sub>3</sub> because of its accessible cost and abundance in nature. Thus, MnCO<sub>3</sub>, MnO<sub>2</sub>, Mn<sub>2</sub>O<sub>3</sub> and Mn<sub>3</sub>O<sub>4</sub> have been shown to be active and selective to aldehyde formation by alcohol oxidation because their redox properties. The catalytic activity of these materials is usually improved by adding promoters such as ZnO, CeO<sub>2</sub>, CuO and Fe<sub>2</sub>O<sub>3</sub>. It was previously reported that the promoter nature as well as catalyst synthesis method can strongly influence the solid particle size and the surface, structural and redox properties of the Mn species [1,2]. In this work, we focus on the synthesis and characterization of Zn-modified MnCO<sub>3</sub> solids. The evolution of the solid physicochemical properties such as Mn oxidation state changes and the development of different surface and tridimensional Mn and/or Zn containing species upon increasing the Zn content was elucidated. The knowledge acquired from solid characterization allowed us to interpret results obtained during selective liquid-phase oxidation of benzyl alcohol (BA) using O<sub>2</sub> as oxidant.

### Materials and Methods

Commercial MnCO<sub>3</sub> was used to prepare a series of Zn modified-MnCO<sub>3</sub> catalysts containing 1.0-22.6 wt.% Zn. Zinc was added to MnCO<sub>3</sub> by incipient wetness impregnation method using aqueous solutions of Zn(NO<sub>3</sub>)<sub>2</sub>.6H<sub>2</sub>O. The impregnated samples were dried at 363 K and then decomposed and stabilized at 573 K in N<sub>2</sub> flow. Catalysts were denoted as xZnMn, where x is the Zn content (x = 1.0, 2.0, 4.3, 8.7, 15.4, 22.6 wt.% Zn). The xZnMn catalysts and pure MnCO<sub>3</sub> and ZnO solids were characterized in their chemical, textural, structural and surface properties using atomic absorption spectrometry, N<sub>2</sub> physisorption, X-ray diffraction, X-ray photoelectron spectroscopy and temperature-programmed decomposition in flowing N<sub>2</sub> techniques. Liquid-phase oxidation of BA with O<sub>2</sub> was carried out at 373 K in a semi batch five-necked glass reactor at atmospheric pressure; toluene was used as solvent. Unreacted BA and reaction products were analyzed by GC technique.

### Results and Discussion

Chemical, textural, structural and surface properties of Zn-modified MnCO<sub>3</sub> catalysts were thoroughly investigated and showed that strongly depend on the Zn content (x). Impregnation

of MnCO<sub>3</sub> with increasing Zn contents from 1.0 to 15.4 wt.% gave rise to an increment in the surface area and pore volume due to the generation of porosity during the catalyst preparation steps. A further increment of x to 22.6wt.% caused a decrease in the textural parameter values due to a partial porous blockage caused by formation of large ZnO crystallites. Structural characterization by XRD and TPN<sub>2</sub> showed that solids investigated consist of different crystalline phases containing Mn and/or Zn species. In these phases Mn oxidation state changes from 2+ toward higher values (3+ and 4+) as x increases entailing the subsequent transformation of MnCO<sub>3</sub> toward ZnMn<sub>2</sub>O<sub>4</sub> spinel and MnO<sub>x</sub> oxides. Furthermore, the Reitveld refinement method allowed to determine that contributions of MnCO<sub>3</sub>, ZnO, MnO<sub>x</sub> and ZnMn<sub>2</sub>O<sub>4</sub> spinel phases also varies with Zn content. The ZnMn<sub>2</sub>O<sub>4</sub>, ZnO and MnO<sub>x</sub> phase fractions increased in detriment of rhodochrosite (MnCO<sub>3</sub>). XPS analysis (Figure 1) confirmed that as Zn loading increases on xZnMn samples, Mn<sup>2+</sup> specie of MnCO<sub>3</sub> is transformed into Mn<sup>3+</sup> and Mn<sup>4+</sup> species.

The application of xZnMn in the conversion of BA to B using O<sub>2</sub> as oxidant showed that all solids resulted active and selective during BA oxidation at 373 K and atmospheric pressure (Figure 2). Contrarily, pure ZnO and MnCO<sub>3</sub> were unable to convert BA. For xZnMn solids, an optimum Zn content of 15.4 wt.% generates a new catalytically active structural composition where the synergistic interaction between Zn<sup>2+</sup> and Mn<sup>4+</sup> gives rise to high B yields in good agreement with the postulated Mars-van Krevelen mechanism. The highest B yield (~70%) was obtained on 15.4ZnMn after 6 h of reaction. The reuse of this sample confirmed the efficiency of the mild regeneration treatment in air at 493K, that restores the B yield to a value similar to that achieved on the fresh catalyst.

### Significance or Main Conclusions

Characterization of Zn-modified MnCO<sub>3</sub> solids with Zn content between 1.0-22.6 wt.% Zn showed that these samples consist of different crystalline phases containing Mn and/or Zn species. The superior catalytic performance of 15.4ZnMn catalyst during the benzyl alcohol oxidation was attributed to a synergistic interaction of both metals (Zn and Mn).

### References

- [1] J. Gao, X. Tong, X. Li, H. Miao, J. Xu, J. Chem. Technol. Biotechnol. 82 (2007) 620-625.
- [2] J. Hu, K. Sun, D. He, B. Xu, Chin. J. Catal., 28(12) (2007) 1025-1027.

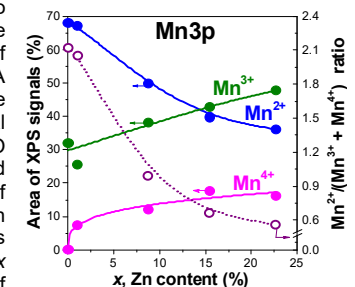


Figure 1. Area of XPS vs x for deconvolutions of Mn species.

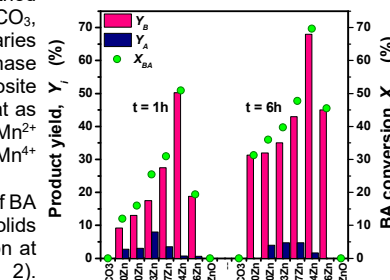


Figure 2. Effect of Zn loading on product yields at 1 and 6 h.



## Co-processing of gas oil and pyrolysis bio-oil in the FCC process. Hydrogen transfer reactions.

Pujro Richard\*, Bertero Melisa, Falco Marisa, Sedran Ulises

Instituto de Investigaciones en Catálisis y Petroquímica "Ing. José Miguel Parera" (INCAPE),  
UNL-CONICET, Colectora Ruta Nac. N° 168 Km 0 – Paraje El Pozo, 3000, Santa Fe,  
Argentina.

\*rpujro@fiq.unl.edu.ar

### Introduction

Limitations of conventional oil resources and environmental regulations drive the search for renewable energy resources and, recently, bio-oils synthesized from residual biomasses became an attractive option in the energy world matrix.

Bio-oils come from the thermal degradation ( $>400^{\circ}\text{C}$ ) of lignocellulosic biomass in absence or with very low oxygen concentration. They form complex mixtures of compounds with high oxygen load in its structure [1]. Their use as a fuel provides an essentially neutral  $\text{CO}_2$  balance, but the high content of oxygenated compounds with acidic nature and the large amounts of water [2], require previous treatments to improve their properties.

The upgrading of bio-oils by means of catalytic processes to eliminate oxygen and transform them into transportation fuels is feasible. Their co-processing in fuel production units such as the Fluidized Catalytic Cracking (FCC) process, require knowing the interaction under actual process conditions between hydrocarbons molecules, typical of fossil feedstocks such as vacuum gas oils, and the oxygenated molecules extensively occurring in bio-oils.

It is the objective of this work to study the hydrogen transfer (TH) reactions in the coprocessing of hydrocarbons and oxygenated compounds under typical conditions of FCC, using model hydrocarbon (tetraline) and oxygenated compounds (aliphatic and aromatic).

### Materials and Methods

An equilibrium commercial FCC catalyst, formulated to maximize the yield of middle distillates, with surface area of  $162 \text{ m}^2/\text{g}$ , zeolite content of 9.83 wt% and cell size unit 2.43 nm, was used. Model reactants were tetraline (Sigma-Aldrich  $\geq 99\%$ ), phenol (Riedel-de Haen 99.5%), syringol (Aldrich 99%), trimethoxybenzene (Aldrich 97%), ethyl acetate (Cicarelli 99.5%), acetic acid (Fluka  $>99.8\%$ ), furfural (Sigma-Aldrich  $\geq 98\%$ ) and methylcyclopentenolone (SAFC 98%). Tetraline/oxygenated compound solutions were prepared with a mass relationship 1.

The co-processing reactions were carried out in a CREC Riser Simulator laboratory reactor [3], with reaction times 3 to 12 s, temperature  $500^{\circ}\text{C}$ , 0.3 g catalyst mass and catalyst to solution ratio 3. The reaction products were identified and quantified by online gas chromatography with FID detection and the coke content was determined by means of programmed temperature oxidation, with methane transformation and quantification in a FID detector.

### Results and Discussion

The distribution of products in the conversion of pure tetraline shows that TH and cracking reactions were the most important ones. In co-processing experiments, tetraline conversion decreased, while oxygenated compounds showed conversions greater than 60% and in some cases total conversions were observed.

The yields of the different product groups were influenced by the presence of oxygenated compounds and their molecular structure. For example, the alkylated aromatic structure of syringol and trimethoxybenzene favored the selectivity to methane, while the compounds of aliphatic base, such as ethyl acetate, increased the production of light gases and LPG, furfural increased gasoline production and methylcyclopentenolone increased LPG yield. In all cases, the yield of compounds in the LCO range was favored. Coke production decreased significantly in co-processing oxygenated aromatic compounds, while it was favored in co-processing aliphatic oxygenates, when compared to coke produced by feeding only tetralin.

The selectivity to TH ( $S_{\text{TH}}$ ) was defined as the relationship of naphthalene production and tetralin conversion. It was observed that  $S_{\text{TH}}$  increased with reaction time, and the co-processing experiments showed selectivities higher than those observed when only tetralin was fed (maximum  $S_{\text{TH}} = 68\%$ ). As an example, figure 1 shows  $S_{\text{TH}}$  at 10 s of reaction.

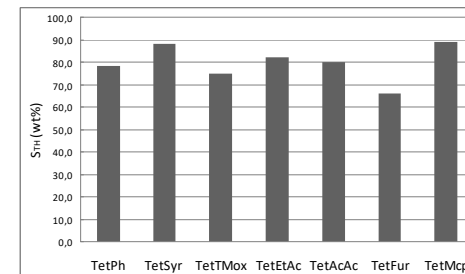


Figure 1. Selectivity to hydrogen transfer reactions in co-processing

### Significance or Main Conclusions

The increase in selectivity to the formation of naphthalene in the co-processing of oxygenated and tetraline, indicates an increase in the ability of tetraline to transfer hydrogen in the presence of oxygenated compounds, and is very important to promote the conversion of oxygenated compounds into hydrocarbons.

### References

- [1] D.K. Ojha, D. Viju, R. Vinu. Energy Convers Manage:X 10 (2021) 100071.
- [2] Y-K. Park, J-M Ha, S. Oh, J. Lee. Chem. Eng. J. 404 (2021) 126527.
- [3] de Lasa, H. I. U.S Patent 5,102,628, 1992.



## Catalytic n-paraffin's dehydrogenation with metallic (Pt, PtSn, PtSnIn, PtSnGa) structured catalysts based on $\gamma$ -Al<sub>2</sub>O<sub>3</sub>, MgAl<sub>2</sub>O<sub>4</sub> and ZnAl<sub>2</sub>O<sub>4</sub>

Adriana D. Ballarini, Patricia Zgolcic, Sergio R. de Miguel and Sonia A. Bocanegra\*  
Instituto de Investigaciones en Catálisis y Petroquímica (INCAPE), Universidad Nacional del  
Litoral, Santa Fe, Colectora RN 168 Km 0 Paraje El Pozo S3000AOJ Argentina  
\*sbocane@fiq.unl.edu.ar

### Introduction

The production of short-chain n-olefins such as ethylene, propene and butenes from n-paraffins by direct catalytic dehydrogenation is a very important industrial process due to the growing global demand for olefins, intermediates in obtaining different products such as alcohols, acids, plastics, etc. The paraffin dehydrogenation reaction is endothermic and have thermodynamic limitations [1,2]. It must be carried out at high temperatures, which leads to problems such as the appearance of side reactions like hydrogenolysis (C-C bond breaking) and the formation of coke that deactivates the catalysts. In relation to this issue, an important advance in the catalytic design is the development of structured supports, where the active phase is supported on a thin layer that coats a generally inert substrate. This arrangement improves mass and heat transfer, which is important because it promote the rapid desorption of olefins once formed, avoiding the polymerization reactions that lead to carbonaceous compounds. Moreover, it prevents the formation of hot spots in the catalysts during the regeneration process for the coke removal [2-4]. In this case, the choice of  $\gamma$ -Al<sub>2</sub>O<sub>3</sub>, MgAl<sub>2</sub>O<sub>4</sub> or ZnAl<sub>2</sub>O<sub>4</sub> to form the thin film on which the metals will be deposited is based on the good metal-support interaction that they present, which can lead to good metallic dispersions [1-3]. Pt was chosen as the active metal, which, accompanied by promoters such as Sn, In and Ga, has demonstrated to be one of the most advantageous in paraffin dehydrogenation due to its good activity and selectivity in the reaction and low hydrogenolytic activity [2-4]. In this work, catalysts of Pt promoted with Sn, In and Ga supported on thin films of  $\gamma$ -Al<sub>2</sub>O<sub>3</sub>, MgAl<sub>2</sub>O<sub>4</sub> or ZnAl<sub>2</sub>O<sub>4</sub> deposited on  $\alpha$ -Al<sub>2</sub>O<sub>3</sub> spheres were studied in the n-butane dehydrogenation reaction for butenes production.

### Materials and Methods

$\alpha$ -Al<sub>2</sub>O<sub>3</sub> spheres (2 mm diameter) provided by SASOL were used as substrate. They were submitted to a pre-treatment with acid [1]. The coating with  $\gamma$ -Al<sub>2</sub>O<sub>3</sub> was carried out starting from a bohemite suspension [1]. The coating with MgAl<sub>2</sub>O<sub>4</sub> or ZnAl<sub>2</sub>O<sub>4</sub> was carried out by two different methods: (i) bohemite-nitrate with purification method (BNAP) [3,4], (ii) citrate-nitrate (CN) [3,4]. From the coated spheres, Pt(0.3 wt%), Pt(0.3 wt%)Sn(0.3 wt%), Pt(0.3 wt%)Sn(0.5 wt%)In(0.3/0.5 wt%) and Pt(0.3 wt%)Sn(0.5 wt%)Ga(0.18/0.3 wt%) catalysts were prepared [1-4]. The supports were characterized by SEM, XRD, measurements of specific surface area and pore volume, and layer stability tests. The catalysts were tested in n-butane dehydrogenation reaction at 530 °C in continuous flow and characterized by TPR, H<sub>2</sub> chemisorption, XPS, TEM and test reactions of metallic phase: CHD and CPH.

### Results and Discussion

The synthesized structured supports showed porous layers coating the  $\alpha$ -Al<sub>2</sub>O<sub>3</sub> spheres with a thickness between 5 and 15  $\mu$ m, which were stable.

A summary of the catalytic results in n-butane dehydrogenation reaction is showed in the Table. The behaviors of the bi and trimetallic catalysts PtSn/Sp-MgAl<sub>2</sub>O<sub>4</sub> (CN) and PtSnIn(0.5)/Sp- $\gamma$ -Al<sub>2</sub>O<sub>3</sub> highlight, showing high yields to butenes between 26 and 29 % and low deactivation between 3 and 9 %.

**Table. Catalytic results: Initial and final n-butane conversion ( $X^0$ ,  $X^f$ ), initial and final selectivity to all butenes ( $S^0$ ,  $S^f$ ), yield to all butenes ( $Y^0$ ,  $Y^f$ ) and deactivation parameter ( $\Delta X = 100*(X^0 - X^f)/X^0$ )**

Catalyst	$X^0$ (%)	$X^f$ (%)	$S^0$ (%)	$S^f$ (%)	$Y^0$ (%)	$Y^f$ (%)	$\Delta X$ (%)
Pt/Sp- $\gamma$ -Al <sub>2</sub> O <sub>3</sub>	31.0	19.6	58.7	62.4	18.3	12.2	37.0
Pt/Sp-MgAl <sub>2</sub> O <sub>4</sub> (BNAP)	25.3	20.7	85.8	96.3	21.7	19.4	18.2
Pt/Sp-MgAl <sub>2</sub> O <sub>4</sub> (CN)	30.5	21.4	55.0	67.4	16.8	14.4	29.8
Pt/Sp-ZnAl <sub>2</sub> O <sub>4</sub> (BNAP)	19.6	17.3	95.0	94.9	18.6	16.4	11.7
Pt/Sp-ZnAl <sub>2</sub> O <sub>4</sub> (CN)	14.8	10.6	97.7	94.3	14.5	10.0	28.4
PtSn/Sp-MgAl <sub>2</sub> O <sub>4</sub> (BNAP)	25.5	22.0	88.6	95.0	22.6	20.9	13.7
PtSn/Sp-MgAl <sub>2</sub> O <sub>4</sub> (CN)	31.0	30.0	93.8	95.2	29.1	28.6	3.2
PtSn/Sp-ZnAl <sub>2</sub> O <sub>4</sub> (BNAP)	21.9	20.2	94.0	96.8	20.6	19.5	7.8
PtSn/Sp-ZnAl <sub>2</sub> O <sub>4</sub> (CN)	27.7	21.5	95.7	95.1	26.5	20.4	22.3
PtSnIn(0.3)/Sp- $\gamma$ -Al <sub>2</sub> O <sub>3</sub>	24.0	21.0	96.0	97.0	23.0	20.0	12.0
PtSnIn(0.5)/Sp- $\gamma$ -Al <sub>2</sub> O <sub>3</sub>	30.0	27.0	96.0	96.0	28.0	26.0	9.0
PtSnGa(0.18)/Sp- $\gamma$ -Al <sub>2</sub> O <sub>3</sub>	24.0	21.5	94.0	97.0	22.0	21.0	10.0
PtSnGa(0.3)/Sp- $\gamma$ -Al <sub>2</sub> O <sub>3</sub>	29.0	26.5	93.0	95.0	27.0	25.0	8.0

Reaction Conditions: 530°C, 1 atm, reactive mixture (n-C<sub>4</sub>H<sub>10</sub> + H<sub>2</sub>, H<sub>2</sub>/n-C<sub>4</sub>H<sub>10</sub> molar ratio = 1.25).

### Significance or Main Conclusions

The preparation of structured supports based on thin films of  $\gamma$ -Al<sub>2</sub>O<sub>3</sub>, MgAl<sub>2</sub>O<sub>4</sub> or ZnAl<sub>2</sub>O<sub>4</sub> was successful, obtaining stable materials suitable for supporting and dispersing metals, and the structured catalysts obtained were active and selective in the n-butane dehydrogenation.

### References

- [1] S. Bocanegra, S. de Miguel , P. Zgolcic , A. Ballarini; Inor. Chem. Comm. 134 (2021) 109033.
- [2] A. Ballarini, P. Zgolcic, S. de Miguel, S. Bocanegra; Can. J. of Chem. Eng. 101 (1) (2023) 1-13.
- [3] S. de Miguel, A. Ballarini, S. Bocanegra; Appl. Catal. A, Gen. 590 (2020) 117315.
- [4] S. de Miguel, I. Vilella, P. Zgolcic, S. Bocanegra; Appl. Catal. A: Gen. 567 (2018) 36– 44.

## Synthesis and characterization of nano-silica from rice husk ash using an alkaline method extraction process

Carlos A. López Vargas<sup>1</sup>, Laura M. Cornaglia<sup>1</sup>, Betina M. Faroldi <sup>1\*</sup>  
INCAPE-UNL-FIQ, CONICET, Santiago del Estero 2829 Santa Fe, Argentina-3000  
\*bfaroldi@fiq.unl.edu.ar

### Introduction

Rice husk is a by-product of crop production which generates significant waste management problems due to its difficulty to degrade and its voluminous load when disposed of [1]. However, interdisciplinary work has allowed for the extraction of useful raw materials, such as rice husk ash, which is mainly composed of silica (75-98%) [2]. Rice husk ash can currently be considered a renewable natural source of SiO<sub>2</sub> in numerous industrial, technological, environmental, commercial, biomedical, and catalytic applications [3]. In this work, we present results of the recovery of amorphous silica with high yields from rice husk ash using hydrothermal extraction with NaOH and precipitation with HCl via sol-gel.

### Materials and Methods

Rice husks were burned in a low O<sub>2</sub> content atmosphere and sieved into three size fractions (100, 149, and 400 µm). Sodium hydroxide solutions with magnetic agitation were used to extract silica. The variables such as NaOH solution concentration, temperature, time, and agitation speed were tested to determine their effect on the extraction process. Vacuum filtration and 3M HCl were used to recover the supernatant and precipitate silica, respectively. A design of experiments was applied to increase the extraction efficiency of silica, and the optimal conditions were determined through an analysis of variance. The initial and residual content of SiO<sub>2</sub> was estimated via TGA and characterized by XRD and FTIR. The SiO<sub>2</sub> yield was obtained by correlating the experimental mass of SiO<sub>2</sub> with the mass of the original ash.

### Results and Discussion

Table 1 shows the experimental design allowed for the identification of the variables with the most interaction with the silica extraction amount. The extraction yielded silica with more than 93% efficiency, the values reported in the literature under similar conditions are low than those reported [3]. The TGA analyses of the ashes before and after the extractions, shown in Figure 1, indicate a mass loss of 53% between 400 and 650 °C, and a remaining fraction of SiO<sub>2</sub> of 47%. Figure 1 also shows that, once the extraction process is carried out, the silica content is substantially reduced. Figure 2 shows the most important bands related to SiO<sub>2</sub>. Nano-silica syntheses at different extraction temperatures are highlighted in the spectrum. Bands (1), (4), and (6) of the figure, in the region of 800 to 1300, 930, and 750 to 800 cm<sup>-1</sup>, respectively, represent Si-O bond stretching and vibration, Si-OH stretching, and Si-O-Si bending [2]. Figure 3 shows the diffractograms of the silica extracted at different times. In all cases, a broad halo is observed in a 2θ range between 15 and 30° with a broad and wide peak centered at 22° indicating the presence of an amorphous material (JCPDS 05-0492)

Factor	[NaOH] M			Temperature °C			Time min		Stirring speed rpm		Particle size µm			% SiO <sub>2</sub> extraction	Result	
Level	0.5	1.0	1.5	RT	40	100	120	80	40	550	1100	0	WS	149	100	
1	-	-	-	-	-	-	-	-	-	+	-	-	-	-	-	63
2	+	-	-	-	-	-	-	-	-	+	-	-	-	-	-	64
3	-	-	-	-	-	-	-	-	-	+	-	-	-	-	-	63
4	+	-	-	-	-	-	-	-	-	+	-	-	-	-	-	82
5	+	-	-	-	-	-	-	-	-	+	-	-	-	-	-	84
6	+	-	-	-	-	-	-	-	-	+	-	-	-	-	-	89
7	+	-	-	-	-	-	-	-	-	+	-	-	-	-	-	90
8	+	-	-	-	-	-	-	-	-	+	-	-	-	-	-	91
9	+	-	-	-	-	-	-	-	-	+	-	-	-	-	-	88
10	+	-	-	-	-	-	-	-	-	+	-	-	-	-	-	90
11	+	-	-	-	-	-	-	-	-	+	-	-	-	-	-	95

Table 1. Optimal extraction conditions design: "+" best extraction condition; "-" worst extraction condition; "—" worst extractor condition per each variable or factor, respectively; RT: Room temperature; WS: without sieve

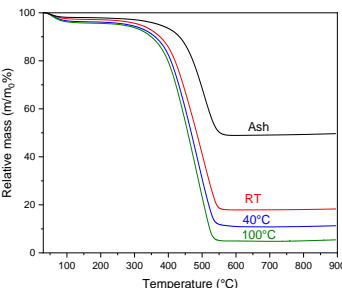


Figure 1. TGA analysis of ash after the extraction at different temperatures; Black: pristine ash

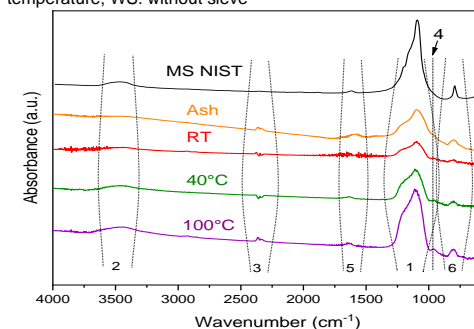


Figure 2. FTIR spectrum of the silicas after extraction at different temperatures Black: NIST amorphous silica spectrum

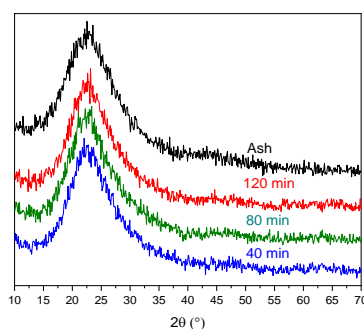


Figure 3. XRD diffractograms of the silica extracted at different times; Black: pristine ash

### Main Conclusions

Rice husk ash was used to synthesize amorphous silica through a simple sol-gel extraction method. Temperature and particle size were the main factors affecting the amount of silica extracted. The results showed yields of 95% under extraction conditions of 1.0 M NaOH, 100 °C, 40 minutes, 550 rpm stirring speed, and 100 µm ash particle size, and complementary techniques confirmed the successful extraction. These materials are promising for their application in the development of new catalysts.

### References

- [1] Informe FAO "Residuos Agrícolas y Residuos Ganadero", <https://www.fao.org/3/bp843s/bp843s.pdf> (2014) 1-40.
- [2] M. Paviotti, L. Salazar Hoyos, V. Busilacchio, B. M. Faroldi, y L. M. Cornaglia, Journal of CO<sub>2</sub> Utilization 42 (2020) 101328-101340.
- [3] A. Gebretatios, A. Kadiri Kanakka Pillantakath, T. Wittoon, J. Lim, F. Banat, C. Cheng, Chemosphere 310 (2023) 136843-136850.

## Eco-friendly chitosan/alginate/carbonate adsorbent for copper and lead removal in water.

Jhonnys D. Guerrero<sup>1\*</sup> and Laura B. Gutierrez<sup>1</sup>

<sup>1</sup>*Instituto de Investigaciones en Catálisis y Petroquímica, INCAPe, (FIQ, UNL-CONICET), Santiago del Estero 2829, S3000, Santa Fe, Argentina.*

\*jguerrero@fiq.unl.edu.ar

### Introduction

The current trend in wastewater treatment is to search for efficient, economical, robust, and stable adsorbents. In this regard, the objective is to produce environmentally friendly materials using natural precursors that are readily available and abundant in nature [1]. Biopolymers such as chitosan (CS) and alginate (SA) are the starting materials of interest, with a focus on the strategic combination of them to enhance intrinsic synergism and adsorption properties. A combination of CS and SA using eco-friendly protocols was proposed, and it resulted a highly feasible way to meet the requirements of a biodegradable, sustainable, and effective adsorbent for wastewater treatment [2, 3].

A resistant biodegradable bio-composite with high adsorption yields of copper and lead ions was obtained by combining alginate and chitosan biopolymers. The influence of carbonates on the material surface was also tested.

### Materials and Methods

The precursors and reagents used were analytical grades: chitosan (CS), sodium alginate (SA), glacial acetic acid, calcium chloride, sodium hydroxide, copper sulfate and lead nitrate. In general, the synthesis protocol started with the solubilization of the starting materials (CS and SA) in a 1:1 (w/w) ratio, mixing of the solubilized precursors (CSA) with constant magnetic stirring, regeneration of the material in  $\text{CaCl}_2$  0,1M/ $\text{Na}_2\text{CO}_3$ / NaOH 1% at room temperature, the obtained gel was filtered, washed, lyophilized (CSALP) and its particle size was reduced by sieving to obtain a size distribution between 420 - 840  $\mu\text{m}$ .

The adsorption tests were performed in batch systems against 200 mg/L copper and lead solutions. The test conditions (1) established in the first instance were: adsorbent dose (d): 0.5 g/L, analysis temperature (T): 25 °C, adsorbent contact time (t): 24 h (it is samples were taken at determined intervals for concentration analysis), and pH 6. In the second stage of experiment (2), the influence of temperature on  $q_e$  was tested. The tests were carried out between 20 – 35 °C, with doses (d = 0.25 g/L) and keeping the other variables of the previous test fixed (1). The material was characterized using FTIR, DRX, optical microscopy and SEM microscopy techniques.

### Results and Discussion

In the first test stage (1), it was evidenced that the equilibrium adsorption capacity ( $q_e$ ) of copper was 361 mg/g at  $t = 360$  min, while in the experiment with lead it was 397 mg/g at  $t = 60$  minutes. In the second stage of experiments, it was possible to verify that the increase in temperature (T) led to higher adsorption speeds (v) of the contaminants, registering at  $T = 35$

°C, maximum adsorption capacities of 376 mg/g at  $t = 360$  min for copper ions and 800 mg/g at  $t = 5$  min for lead ions (Fig. 1a).

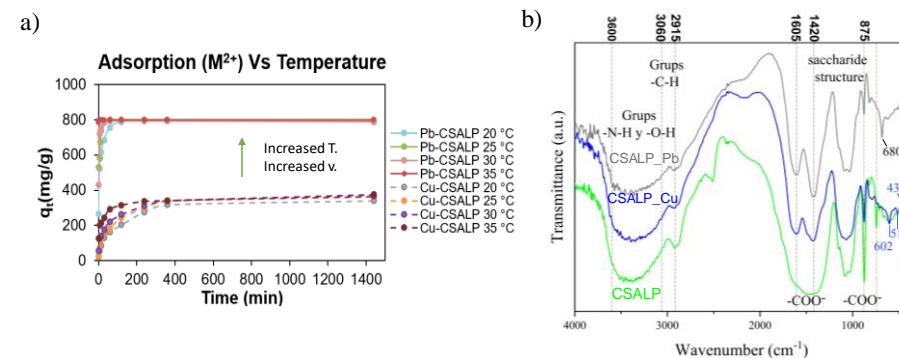


Figure 1. a) Effect of temperature on the Cu<sup>2+</sup> and Pb<sup>2+</sup> adsorption capacity of CSALP.  
b) Fresh CSALP FTIR spectrum and after Cu<sup>2+</sup> and Pb<sup>2+</sup> adsorption process

The materials were characterized by FTIR, XRD, optical microscopy, and SEM. Figure 1b shows the FTIR spectra of the compound prepared fresh and after the adsorption process, identifying shifts and changes in intensity corresponding to the interactions of the metal with the functional groups responsible for the adsorption (COO<sup>-</sup>, OH, and NH). Changes in the pattern of the spectrum and the intensity of the signals are identified around 1605, 1420, and 875 cm<sup>-1</sup> (CSALP Vs CSALP\_Cu and CSALP\_Pb), as well as Cu-O interactions at 602 cm<sup>-1</sup>/516 cm<sup>-1</sup>, Cu-N at 430 cm<sup>-1</sup> and Pb-O at 680 cm<sup>-1</sup> (Fig. 1b). The XRD spectra (not shown) illustrated the changes in the crystallinity of the fresh material and after adsorbing the corresponding metal, observing these changes in greater detail through optical microscopy and SEM (not shown).

### Significance or Main Conclusions

Through a simple synthesis and with environmentally friendly precursors, it is possible to obtain a resistant, economical, biodegradable adsorbent with high copper and lead adsorption capacities for low contact times.

### References

- [1] X. Qi, X. Tong, W. Pan, Q. Zeng, S. You, J. Shen; J. Clean. Prod 315 (2021) 128221.
- [2] C. Zhao, G. Liu, Q. Tan, M. Gao, G. Chen, X. Huang, X. Xu, L. Li, J. Wang, Y. Zhang, D. Xu; J Adv Res 44 (2023) 53–70.
- [3] E. Deze, S. Papageorgiou, E. Favvas, F. Katsaros; Chem. Eng. J. 209 (2012) 537-546.

## Development of catalysts for production of light olefins from methanol

Francisco J. Passamonti<sup>1</sup>, Viviana M. Benítez<sup>1</sup>, Catherine Espeel<sup>2</sup>, Florence Epron<sup>2</sup>, Carlos L. Pieck<sup>1</sup>, Silvana A. D'Ippolito<sup>1,\*</sup>

<sup>1</sup>INCAPE, Colectora Ruta Nac. N° 168 - Paraje El Pozo, Santa Fe 3000 (Argentina),

<sup>2</sup>Institut de Chimie des Milieux et Matériaux de Poitiers (IC2MP), Université de Poitiers, CNRS, 4 rue Michel Brunet, TSA51106, 86073 Poitiers Cedex 9, (France)

\*sildippo@fiq.unl.edu.ar

### Introduction

The production of light olefins through the conversion of methanol (MTO) is presented as an alternative to satisfy the growing demand for propylene and ethylene. Its importance lies in the flexibility to vary the ratio of propylene/ethylene, energy efficiency and low CO<sub>2</sub> emissions compared to the conventional steam cracking process. The commercial catalysts, HZSM5 and SAPO34, present high yields to light olefins. However, they are deactivated by coke deposition and require regeneration. To improve the process initially aluminosilicates with different composition SiO<sub>2</sub>-Al<sub>2</sub>O<sub>3</sub> are proposed.

The present work studies the conversion of methanol to olefins using aluminum-silicates of different percentages of SiO<sub>2</sub> and Al<sub>2</sub>O<sub>3</sub>. It seeks to determine the incidence in the distribution of products of the composition and incorporation of chlorine to these amorphous materials and compare them with commercial catalysts.

### Materials and Methods

The SAPO34 and ZSM5 catalysts were calcined at 550 °C for 8 h (2 °C min<sup>-1</sup>, air, 60 cm<sup>3</sup> min<sup>-1</sup>) and aluminosilicates (indicated Sx, where x=40, 60 and 70 is the number associated with the percentage of SiO<sub>2</sub>) were calcined for 4 h at 450 °C (10 °C min<sup>-1</sup>, air, 60 cm<sup>3</sup> min<sup>-1</sup>). In addition, 1.5 cm<sup>3</sup> g<sup>-1</sup> of HCl (0.2 M) was added to these supports. After standing for 1 h with HCl, it was dried at 70 °C in a thermostatic bath until a dry powder was obtained and left overnight in an oven at 110 °C. Finally, it was calcined in air flow (60 cm<sup>3</sup> min<sup>-1</sup>, 300 °C, 4 h). These catalysts are designated SxHCl. In order to correlate the physicochemical and surface properties of the catalysts with their performance in the MTO reaction different characterization techniques were used.

The MTO reaction was carried out in a fixed bed reactor; conditions: atmospheric pressure, 400 and 450 °C, methanol flow = 0.5 cm<sup>3</sup> h<sup>-1</sup>, space velocity WHSV= 4 h<sup>-1</sup>. Previously, the samples were treated for 1 h in a N<sub>2</sub> flow at 550°C. The products were analyzed by gas chromatography.

### Results and Discussion

The SAPO34 followed by HZSM5 has the smallest pore diameter. The catalysts with 60% SiO<sub>2</sub> have the highest specific surface area and the smallest diameter and pore volume of the aluminum-silicates studied. All the catalysts studied present type IV adsorption/desorption isotherms of N<sub>2</sub>. The incorporation of HCl decreased the surface area, increased the pore size and the total acidity, as well as the number and strength of Brønsted acid sites determined by

FTIR-Py. The SAPO34 catalyst has the lowest acidity of the studied catalysts. It was determined by X-ray diffraction that the HCl modifies the amorphous silica-alumina structure of the 40 and 60% SiO<sub>2</sub> catalysts, HZSM5 has an MFI crystal lattice and SAPO34 CHA structure.

Preliminary experiments were carried out, where the catalytic performance of HZSM5 was evaluated at 350, 400 and 450 °C and different WHSV (1, 2 and 4 h<sup>-1</sup>) to establish the reaction conditions of methanol to olefins. Results obtained were in agreement with the widely accepted double-cycle reaction mechanism for the conversion of methanol to olefins which considers that at low reaction temperatures the aromatic cycle has preponderance while at high reaction temperatures the olefin cycle is favored [1].

Figure 1 shows that at both reaction temperatures the catalysts HSZM5 and SAPO34 achieve the highest conversion. The ethylene/propylene ratio increases with the increase in reaction temperature attributed to the secondary reaction of oligomerization and cracking that are favored when the reaction temperature increases [2]. It can be observed that with the SiO<sub>2</sub>-Al<sub>2</sub>O<sub>3</sub> catalysts higher propylene yields are achieved than those obtained with HZSM5 and SAPO34 even at a lower reaction temperature, except with S40 and S40HCl. The increase in the reaction temperature produces the cracking of propylene and C4+, increasing the formation of ethylene. Ethylene and propylene are formed through different pathways [3]. The highest yield to propylene is obtained with the S60 catalyst at 400 °C. Its better performance can be attributed to adequate acidity, high specific surface area and small pore size.

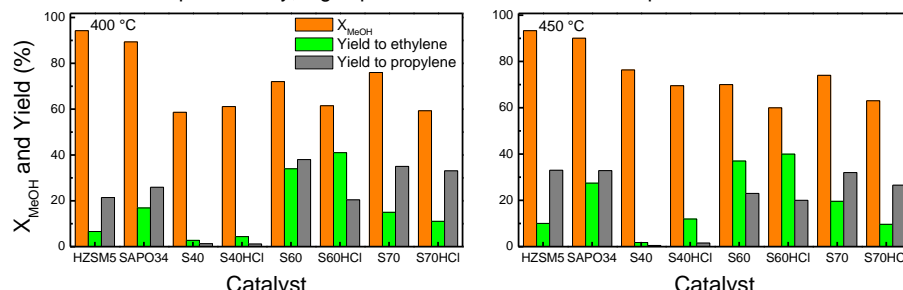


**Figure 1.** Methanol conversion (X<sub>MeOH</sub>) and yield to light olefins at 4 h reaction at 400 and 450 °C obtained with all catalysts.

### Significance

The selection of the support will allow optimization of the catalytic formulations by incorporating Ni and Ce and continue with the study of deactivation and regeneration of the catalysts used in MTO to maximize light olefin yield and minimize catalyst deactivation.

### References

- [1] X. Sun, S. Mueller, Y. Liu, H. Shi, G.L. Haller, M. Sanchez-Sanchez, A.C. van Veen, J.A. Lercher, *J. Catal.* 317 (2014) 185-197.
- [2] X. Wu, M.G. Abraha, R.G. Anthony, *Appl. Catal. A: Gen.* 260 (2004) 63-69.
- [3] M. Bjørgen, S. Svelle, F. Joensen, J. Nerlov, S. Kolboe, F. Bonino, L. Palumbo, S. Bordiga, U. Olfsby, *J. Catal.* 249 (2007) 195-207.

## Ce-based biomorphic fibers for the oxidation of soot and VOCs

Maximiliano Rodriguez<sup>1,2\*</sup>, V.G. Milt<sup>1</sup>, E.E. Miró<sup>1</sup>, E.M. Gaigneaux<sup>2</sup>

<sup>1</sup>INCAPE-Universidad Nacional del Litoral, Facultad de Ingeniería Química, Santiago del Estero 2829, Santa Fe 3000 (Argentina)

<sup>2</sup>Institute of Condensed Matter and Nanosciences (IMCN), Université catholique de Louvain, Place Louis Pasteur 1, 1348, Louvain-la-Neuve (Belgium)

\*mrodriguez@fiq.unl.edu.ar

### Introduction

The world is transitioning into greener and cleaner forms of energy production. In the meantime, we still face the challenge of reducing current emissions which come from conventional energy sources and meeting stringent emission standards. Particulate matter and VOCs are two well-known pollutants regarding air contamination, connected to serious health effects [1]. The most efficient way to achieve regulated values is by catalytic oxidation.

Fiber-based catalysts have gained popularity owing to their intrinsic characteristics such as high aspect ratio, high void fraction and low costs of manufacture [2]. Moreover, fibers can be shaped into countless forms using different materials which provides versatility. A very simple but innovative method of synthesizing fibers is using a biotemplate that transfers a biological structure into inorganic materials, which will retain the morphology of the former.

The objective of this work is to use a plant-based template to produce CeO<sub>2</sub> fibers [3] as active supports of catalysts and use them in two reactions of environmental interests: soot (particulate matter) and benzene (aromatic volatile organic compound, VOC) oxidation.

### Materials and Methods

The catalytic synthesis is sequential. First, commercial cotton (biotemplate) is impregnated with a Ce(NO<sub>3</sub>)<sub>3</sub> solution to obtain pure CeO<sub>2</sub> fibers (Fib Ce), after drying and calcination (600°C) steps. Secondly, different amounts (5-12 % wt.) of Mn (Fib Ce-Mn) and Co (Fib Ce-Co) were deposited on Fib Ce by wet impregnation using Mn(NO<sub>3</sub>)<sub>2</sub> and Co(NO<sub>3</sub>)<sub>2</sub> solutions, drying impregnated fibers at 120°C and calcining for 2h at 600°C. The fibrous catalysts were characterized by SEM, EDX, XRD, FTIR-ATR, LRS, and N<sub>2</sub> physisorption. For soot (Printex U) combustion reaction, a pseudo-real soot-to-catalyst contact was obtained by wet impregnation using n-hexane (1:20). The reaction was only O<sub>2</sub>-assisted with a 30 ml/min feed (20 ml of 5% O<sub>2</sub> in He + 10 ml Ar). CO<sub>2</sub> production was monitored with a MS. For benzene oxidation tests, the feed was 100 ml/min (200 ppm of benzene, 10% O<sub>2</sub> and He balance), S<sub>v</sub>=6000 ml/h.g. Benzene concentration was measured from 50°C until 400°C by a GC with FID detector.

### Results and Discussion

The fibrous morphology was confirmed by SEM imaging. Helicoidal and cylindrical fibers were seen, with different diameters and lengths. FTIR-ATR analysis showed signals corresponding to -OH, H-O-H, NO<sub>3</sub><sup>-</sup>, CO<sub>3</sub><sup>2-</sup>, MnO<sub>x</sub>, and CoO<sub>x</sub> species. No signals from MnO<sub>x</sub> were present in the diffractograms for Fib Ce-Mn samples, but a small shift of CeO<sub>2</sub> main peak suggested the possible insertion of Mn cations into ceria lattice. A similar situation was encountered for Co deposited samples, but at 5% wt. some segregation of CoO<sub>x</sub> was already seen. Raman spectra confirmed the insertion of Mn and Co cations and their segregation,

showing a clear shift of CeO<sub>2</sub> main peak to lower frequencies. An increase of Fib Ce activity for soot combustion was attained for 12% wt. Mn, while not for 5% wt. Mn, showing a possible threshold in Mn quantity. For Co deposition, a similar improvement was seen for both amounts. On the other hand, all combinations of catalysts showed a better performance in benzene oxidation, compared to Fib Ce. The bigger T<sub>50</sub> decrease was reached with 12% wt. Mn and Co samples, being the former the best.

**Table 1.** Textural properties of Mn and Co supported Fib Ce.

Sample	BET [m <sup>2</sup> /g]	Pore volume [cm <sup>3</sup> /g]	Crystallite size of support (CeO <sub>2</sub> ) [nm] *	Crystallite size of supported phase [nm] *	Lattice parameter [Å]
Fib Ce	17	0.105	21	-	5.41
Fib Ce-5Mn	25	0.117	20	-	5.40
Fib Ce-12Mn	21	0.102	22	-	5.40
Fib Ce-5Co	26	0.116	22	-	5.40
Fib Ce-12Co	24	0.107	23	38	5.40

\* Calculated by Scherrer equation.

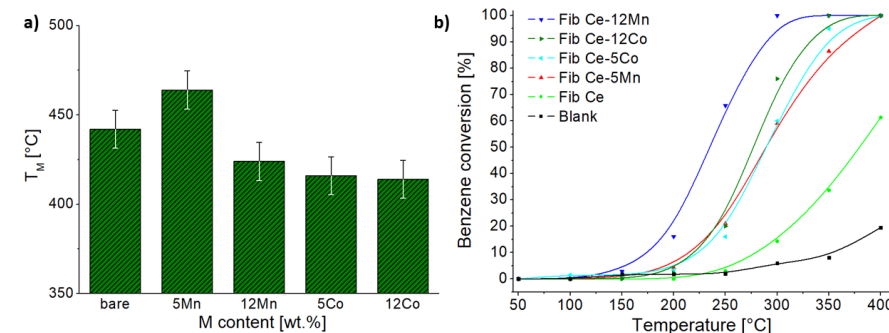


**Figure 1.** a) Maximum combustion rate temperatures (T<sub>M</sub>) in soot combustion tests, b) Half conversion temperatures(T<sub>50</sub>) in benzene oxidation evaluations.

### Significance or Main Conclusions

Biomorphic catalytic fibers were synthesized by a very facile, efficient, and economic technique. An improvement of activity of Fib Ce was achieved in both tested reactions. The boost in activity was ascribed to the insertion of some Mn and Co cations into CeO<sub>2</sub> lattice along with some segregation of MnO<sub>x</sub> and CoO<sub>x</sub> species on top of the fibers.

### References

- [1] H. Reis, C. Reism, A. Sharip et al., Environmental International 114 (2018) 252-265.
- [2] E. Reichelt, M.P. Heddrich, M. Jahn et al., Applied Catalysis A: General 476 (2014) 78-90.
- [3] M.A. Stegmayer, V.G. Milt, E.E. Miró; Catalysis Communications 139 (2020) 105984.

## Production of diesel-type biofuel by conversion of $\gamma$ -valerolactone over noble metal-based bifunctional catalysts

Karla G. Martínez Figueredo, Darío J. Segobia and Nicolás M. Bertero \*  
INCAPE, CCT-Santa Fe, Colectora Ruta Nac. 168 KM 0, Santa Fe 3000 (Argentina)  
\* E-mail: nbertero@fiq.unl.edu.ar

### Introduction

In the last decades approximately 28% of the total energy demand was employed for transportation purposes. However, 92% of this energy was supplied by fossil fuels and this is causing serious environmental problems. Lignocellulosic biomass has been targeted as a promising raw material for the production of biofuels because: 1) is a non-edible biomass; 2) is an abundant and inexpensive form of biomass. The strategy for producing biofuels from biomass comprises: (a) conversion of lignocellulose into platform molecules such as levulinic acid (LA) and  $\gamma$ -valerolactone (GVL); (b) transformation of these platforms into biofuels [1].

Valeric esters have been regarded as attractive biofuels due to their considerably energy density, good volatility-ignition properties and appropriate polarity in comparison with current biofuels and passed satisfactorily a 250,000 km road trial [2]. Particularly, pentyl valerate (PV) has a higher volatility, better cold-flow properties and lubricity than FAME and engine efficiency and emissions are not strongly affected when it is blended with diesel up to 20%.

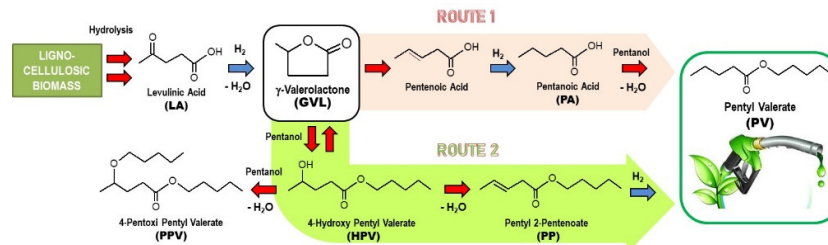


Figure 1. Reaction pathways towards PV from GVL over bifunctional catalysts.

There are two possible routes for obtaining PV from GVL (Figure 1). ROUTE 1 is based on hydrogenation/hydrogenolysis of GVL to pentanoic acid (PA) and subsequent esterification of PA with pentanol (PL), where Brønsted acid sites are required. ROUTE 2 involves the transesterification of PL to the carboxylic group of the GVL to form 4-hydroxy pentyl valerate (HPV), dehydration of HPV to pentyl 2-pentenoate (PP), where Lewis acidity is necessary, and finally hydrogenation of PP to PV. However, other products such as 4-pentoxy pentyl valerate (PPV) and PA can be formed [3]. The aim of this work was to correlate the acid properties of noble metal-based catalysts with their catalytic performance in the PV production from GVL, PL and  $H_2$  following ROUTE 2.

The motivation of this work relies on the necessity of boosting the PV productivity in these batch one-pot processes before considering continuous processes.

### Materials and Methods

Commercial  $SiO_2-Al_2O_3$  ( $Si/Al=7$ ), calcined in air at 500 °C for 2 h and from now on named SA, was used as support. SA-supported catalysts were prepared by incipient-wetness impregnation using chloride aqueous solutions ( $RhCl_3$ ,  $PdCl_2$ ,  $H_2IrCl_6$ ,  $H_2PtCl_6$  and  $RuCl_3$ ). The impregnated samples were dried for 12 h at 100 °C, calcined in air at 5 °C/min to 450 °C for 3 h and activated in  $H_2$  flow for 2 h at 450 °C. Characterization consisted of XRF, XRD, TPR, TEM, TPD of  $NH_3$  and FTIR of adsorbed pyridine. Catalytic tests were performed in batch mode, using PL as reactant/solvent and hexadecane as GC internal standard.

### Results and Discussion

Metal loadings were in the range 0.83-1.00% (Table 1). Textural properties of M/SA samples were between 8 and 15% lower than the values of SA. The pattern for the metal particle size by TEM followed:  $Ru > Ir > Rh > Pd > Pt$ . Values of total acid site density ( $n_A$ ) were between 91% and 146% of the value of SA support. SA support showed a  $L/(L+B)$  ratio of 0.79 degassing at 450 °C and both Ru/SA and Ir/SA showed lower values, whereas  $Rh/SA$ ,  $Pt/SA$  and  $Pd/SA$  had stronger acid sites with a higher Lewis character.

The pattern for the GVL conversion after 8 h was:  $Pd/SA > Pt/SA > Ru/SA \approx Rh/SA > SA \approx Ir/SA$ . SA only produced PP and PPV with minor amounts of HPV. Bifunctional samples hydrogenated PP intermediate to PV shifting the equilibrium towards products and reaching higher values of  $X_{PV}$ . A correlation between the selectivity to desirable products (PP+PV) and the proportion of Lewis nature of the strongest acid sites of bifunctional samples was observed. However, some Brønsted acidity is required to promote dehydration of HPV to PP.

Table 1. Main characterization and catalytic results

Sample	Metal %	$S_g$ ( $m^2/g$ )	$d_{MO}$ (nm)	$n_A$ ( $\mu mol/m^2$ )	$L/(L+B)$ (450 °C)	$X_{PV}$ (%)	$\eta_{PV}$ (%)	$P_{PV}$ ( $mmol.h^{-1}g_M^{-1}$ )
SA	-	460	-	0.59	0.79	58.0	-	-
Ru/SA	0.98	409	7.4	0.52	0.77	60.6	16.0	128
Ir/SA	1.00	413	6.7	0.65	0.69	57.7	11.9	94
Rh/SA	0.94	392	5.6	0.54	0.84	60.5	45.1	376
Pt/SA	0.94	425	2.8	0.86	0.87	69.4	51.0	427
Pd/SA	0.83	397	3.7	0.86	0.89	81.1	70.1	661

Reaction Conditions: 8 h, 250 °C, 10 bar of  $H_2$ , 1.5 ml of GVL, 40 ml of PL and 0.25 g of catalyst.

### Significance or Main Conclusions

Strong Lewis acid sites in SA-supported bifunctional noble metal-based catalysts are critical to promote acid-catalyzed reactions in the production of PV from GVL, PL and  $H_2$  (ROUTE 2). Among these catalysts, Pd/SA has shown the highest PV productivity on batch processes in liquid phase due to its high acidity, high  $L/(L+B)$  ratio and small metal particles.

### References

- [1] S.N. Derle, P.A. Parikh, Biomass Convers. Biorefinery 4 (2014) 293–299.
- [2] J.P. Lange, R. Price, P.M. Ayoub et al., Angew. Chemie - Int. Ed. 49 (2010) 4479–4483.
- [3] C.E. Chan-Thaw, M. Marelli, R. Psaro et al., RSC Adv. 3 (2013) 1302–1306.

## Synthesis of amines from nitrile hydrogenation on Co/SiO<sub>2</sub>: Effect of the substrate structure

Milton Agüero, Dario J. Segobia and Andrés Trasarti \*

INCAPE, CCT-Santa Fe, Colectora Ruta Nac. 168 KM 0, Santa Fe 3000 (Argentina)

\* E-mail: atrasarti@fiq.unl.edu.ar

### Introduction

Nitrogen compounds, and particularly amines, constitute one of the fundamental bases of life. Many neurotransmitters, alkaloids and other active biomolecules are nitrogen compounds. A convenient route for amines production is the hydrogenation of nitriles, due to availability of reagents, low price and high atomic efficiency. This reaction proceeds through hydrogenation/condensation consecutive reactions leading to the formation of a mixture of primary, secondary and tertiary amines. Frequently, a high selectivity to a particular amine is wanted in order to eliminate the cost of product separation process. Increasing research efforts have been devoted to selectively convert saturated nitriles to a given saturated primary (PA), secondary (SA) or tertiary amine (TA). Figure 1 shows the reaction network of nitrile hydrogenation according to currently accepted reaction pathways. There is a general agreement that on metal-supported catalysts the reaction selectivity depends mainly on the nature of the metal component [1], however, operating conditions, catalyst preparation method and the solvent nature have also an important influence on the reaction activity and selectivity. There are very few studies that investigate the effect of the nitrile structure on the reaction activity and selectivity. In the present work we study the effect of the nitrile structure

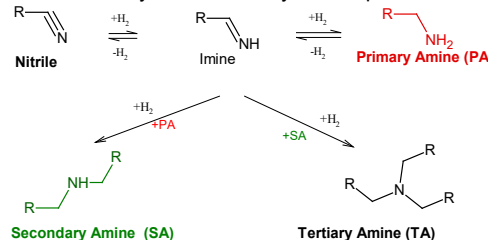


Figure 1. Reaction network

### Materials and Methods

Co/SiO<sub>2</sub> catalyst was prepared by the incipient-wetness impregnation method. The catalyst was characterized by a variety of physical and spectroscopic techniques. The solvent/reagent-catalyst interaction strength was investigated by temperature-programmed desorption (TPD) and calorimetry. The nitriles hydrogenation was studied in a batch reactor.

### Results and Discussion

on the reaction activity and selectivity in solvents of different nature. We discuss the hydrogenation in liquid phase aliphatic (acetonitrile, AN, butyronitrile, BN, isobutyronitrile, IBN) and aromatic nitriles (benzonitrile, BeN and benzyl cyanide, BC) on Co/SiO<sub>2</sub>, using solvents of different chemical nature.

Aromatic and aliphatic nitriles were tested in the hydrogenation reaction in liquid phase at 373 K and 13 bar H<sub>2</sub>. The initial reaction rate, and nitrile conversion and selectivities are presented in Table 1. When ethanol was used as solvent, the activity pattern measured as initial reaction rate followed the order: AN> IBN> BN >BeN> BC. The products distribution was similar for the aliphatic nitriles, obtaining mainly the primary amines; this performance was reduced slightly with the decrease in the length of the chain. BC formed mainly PA, however, the product distribution significantly changed when BeN was used as substrate, giving SA in similar amounts as compared with PA. These effects of nitrile structure on catalyst activity/selectivity may be explained by taken into account that the reagent-metal interaction strength. The molar adsorption enthalpies determined for benzonitrile and benzylamine were higher than the rest of nitriles and primary amines. The higher adsorption enthalpy of BeN and benzylamine favors the condensation over hydrogenation. The solvent nature also plays an important role in the selectivity control. In toluene the selective towards PA was higher than in cyclohexane probably because the strong interaction toluene/Co hampers the readsorption of PA and the consecutive formation of SA. When the reaction is carried out in ethanol, the PA-solvent interaction controls the selectivity.

Table 1. Catalytic results for different structure nitrile hydrogenation

Nitriles	Solvents	Initial rate	Conversion (X <sub>N</sub> , %) and Selectivities (S <sub>i</sub> , %) at the end of reaction			
		r°(mmol/h g)	X <sub>N</sub> (%)	S <sub>PA</sub> (%)	S <sub>SA</sub> (%)	Others
Acetonitrile	Ethanol	26.2	100	67	32	1
Isobutyronitrile	Ethanol	21.6	100	78	16	6
Butyronitrile	Ethanol	20.1	100	80	17	3
Butyronitrile	Toluene	15.4	100	70	28	2
Butyronitrile	Cyclohexane	30.2	100	61	39	-
Benzonitrile	Ethanol	18.6	100	50	42	8
Benzonitrile	Toluene	15.6	100	49	48	3
Benzonitrile	Cyclohexane	19.6	100	46	53	1
Benzyl Cyanide	Ethanol	11.7	100	76	17	7
Benzyl Cyanide	Toluene	4.4	100	69	29	1
Benzyl Cyanide	Cyclohexane	12.4	100	63	35	2

T: 373 K, P=13 bar (H<sub>2</sub>), 800 rpm, V: 150 ml, W<sub>cat</sub>= 1 g, C<sup>0</sup><sub>Nitrile</sub> = 0,16 mol/L.

### Significance or Main Conclusions

The activity and selectivity of Co/SiO<sub>2</sub> for the liquid-phase hydrogenation of nitriles to amines depend on the nitrile structure used as a reagent. Benzonitrile produces a mixture of primary and secondary amines probably due to the strong adsorption of benzonitrile and benzylamine on the metal surface, which favors the condensation over hydrogenation.

### References

- [1] Segobia, D.J., Trasarti, A.F., and Apesteguía, C.R. Appl. Catal. A: Gen. 445, 69 (2012).



## Investigating the Impact of Preparation Method on the Nitrate Reduction and N<sub>2</sub> Selectivity of Alumina-Supported Pd,In Catalysts

Fernanda Miranda Zoppas, Nicolás Sacco, Alejandra Devard, and F. Albana Marchesini\*  
*INCAPE, Santiago del Estero 2829, Santa Fe 3000 (Argentina)*  
\*albana.marchesini@gmail.com

### Introduction

The United Nations aims to provide high-quality drinking water by 2030 as part of its sustainable development goals, but nitrate pollution remains a major concern. Nitrate is the most common chemical contaminant in groundwater [1], caused by excessive fertilizer use and lack of proper waste treatment. Nitrate pollution poses a hazard to human health and the environment as 90% of the world's drinking water comes from groundwater sources.

This work is focused on studying the influence of synthesis steps on the catalytic performance and selectivity of Pd,In-based catalysts for the removal of nitrate from water. Wet impregnation method was used to deposit the catalysts onto alumina, and the catalysts were evaluated for their ability to remove nitrate and produce N<sub>2</sub> as a byproduct. The goal is to find the best conditions for obtaining a catalyst with high activity towards nitrate removal and high N<sub>2</sub> selectivity, to improve the safety and reliability of water supply in the future.

### Materials and Methods

In this work, catalysts were prepared by combining 1 wt.% palladium and 0.25 wt.% indium, which has been studied previously and chosen due to its high activity for nitrate removal from water. The catalysts were prepared using the wet impregnation method, which consists of mixing Pd and In precursor solutions with the support, stirring the mixed solution at 80°C until total evaporation of the liquid phase, drying the solid mixture at 80°C for 12 h in an oven, calcining at 500°C for 4h at a heating rate of 10°C/min, and reducing in hydrazine 0.8 M at 40°C for 1h. The five synthesis sequences were: PACRIR, PACRI, PIACR, PACIR, and PACICR. The catalysts were named according to the order of synthesis steps. The letters represent the following components (P, I, A) and processes (C, R): P: Palladium; I: Indium; A: Alumina; C: Calcination at 500 °C at 10 °C/min, R: Reduction with hydrazine hydrate solution (0.8 M) at 40 °C.

XRF was used to analyze the elemental composition of Pd and In on alumina-supported catalysts, with the elemental quantification being done using a Shimadzu spectrometer equipped with an energy dispersive analytical system (EDX-720).

The catalytic performance of the Pd-In catalysts for nitrate reduction was tested in a 250 mL batch reactor with a catalyst concentration of 2.5 g/L. The reactor was placed on a magnetic stirring system (~800 rpm) to reduce mass transfer limitations. The reaction was performed at room temperature (25°C) and atmospheric pressure. The procedure for catalytic evaluation was as follows: 80.0 mL of deionized water was added to the reactor, and N<sub>2</sub> was injected for at least 20 minutes to purge atmospheric CO<sub>2</sub> and O<sub>2</sub>. The catalyst was then added to the aqueous medium, and H<sub>2</sub> was bubbled. A KNO<sub>3</sub> solution was added to reach 100 ppm of N-NO<sub>3</sub> in the reaction medium (concentrations similar to those found in water

treatment concentrates), and this moment was considered as the initial time (t = 0 min). The pH was controlled by a pH-meter and maintained at 5 using an HCl solution of 0.1 M. The reaction was monitored for 120 minutes, taking aliquots of the reaction medium at fixed time intervals to quantify the nitrite and ammonium production.

The concentration of ions in the solution was determined using a UV-Vis spectrophotometer. The Cd column reduction method was used to analyze nitrate, followed by the Griess method (absorbance at 543 nm). The Griess method was also used to measure nitrite, and the modified Berthelot method (absorbance at 633 nm) was used for ammonium determination.

### Results and Discussion

Table 1 shows the Pd and In atomic percentages obtained by X-ray fluorescence (XRF). The retention percentages of Pd and In were calculated based on the amount added during synthesis and the values obtained by XRF. It was observed that there is deviation from the theoretical values after each synthesis procedure, with a greater proportion of Pd and In retained by the support when calcination occurs after impregnation.

**Table 1. Nitrate conversion (X), N<sub>2</sub> Selectivity and catalysts mass composition.**

Catalyst	X (%) <sub>120 min</sub> (X=90%)	SN <sub>2</sub> (%)	Pd wt. %	In wt. %	Pd retention%	In retention %
PACIR	94.6	84.0	0.45	0.06	45	24
PACRIR	100	94.4	0.40	0.07	40	28
PIACR	100	78.3	0.49	0.06	49	24
PACRI	98.5	87.5	0.41	0.06	41	24
PACICR	98.1	86.7	0.41	0.08	41	32

It is observed by XRF analysis that a low retention of the active phase was obtained in all synthesis variants, which may be attributed to the low interaction between the support and the active phase. Greater metal retention was observed in PIACR, indicating that 2 calcinations do not favor metal retention. It can be seen in Table 1 that all of the Al<sub>2</sub>O<sub>3</sub>-supported catalysts were active in converting nitrate. Conversions close to 100% were achieved, with the PIACR catalyst showing the highest catalytic activity. Regarding N<sub>2</sub> selectivity, for the alumina group, the most efficient was PACRIR, with 94.4% selectivity to N<sub>2</sub>.

### Significance or Main Conclusions

Different procedures of adding the active phase to the support have been implemented in order to investigate how the synthesis procedure affects the performance in nitrate reduction, looking for better selectivity to N<sub>2</sub>. The best compromise between activity and selectivity was obtained with the alumina-supported catalyst, synthesized by the PACRIR method. Catalysts supported onto Al<sub>2</sub>O<sub>3</sub> showed low retention of Pd and In in the bulk. These results suggest that bimetallic In on Pd supported catalysts can reduce efficiently the nitrate content in water, and a sequential synthesis is a powerful tool for improving this capability and to increase selectivity to N<sub>2</sub>.

### References

- [1] S. Ramalingam, A. Subramania, Engineered Science 3 (2021) 80–88.



## Phenol removal from water by advanced oxidation process with Cu-based catalysts.

Nicolás Sacco, Sofia Bidal, Alejandra Devard, Fernanda Zoppas and F. Albana Marchesini\*  
INCAPE, Santiago del Estero 2829, Santa Fe 3000 (Argentina)  
\*albana.marchesini@gmail.com

### Introduction

Water pollution is an important issue that directly affects human health and the environment. Most of the organic pollutants generated during different industrial processes are released directly into the environment, eventually affecting aquatic systems. In particular, phenols and their derivatives are a major focus of attention in the study of environmental pollution due to their toxicity and persistence [1]. The presence of these organic compounds in water involves serious risks to the health of living beings and aquatic environments. Therefore, it has become a necessity to remove them before disposal into the environment.

In the last decade, the use of advanced oxidation processes AOP has been proposed as a complementary step in wastewater treatment plants to address the challenge of wastewater treatment and reuse. Despite the excellent performance in AOP, copper (Cu)-based catalysts present a drawback to be solved which consists in the leaching of the active phase to the reaction solution, which, in addition to deactivating the catalytic system, contaminates the water body being treated]. In this work, the influence of Cu precursors, and synthesis parameters on Cu leaching and phenol removal is studied.

### Materials and Methods

Cu-based catalysts supported on Al<sub>2</sub>O<sub>3</sub> (Puralox ®, SBA 230) were prepared by the wet impregnation method at 80°C using Cu(NO<sub>3</sub>)<sub>2</sub>.3H<sub>2</sub>O as the copper precursor to obtaining a Cu loading of 5 wt%. The suspensions were dried at 120°C and calcined at different temperatures (450, 600, and 900°C) for 4 h at 10°C/min, to evaluate the effect of calcination temperature on catalytic performance and copper leaching. For each of these temperatures, the addition of La or Mn (both at 20 wt%) to the support by wet impregnation and calcined at 900°C, before the addition of the copper precursor, was also evaluated. Catalysts were named: Cu-X/Y-T, where X, represents the support (A: Al<sub>2</sub>O<sub>3</sub>, Mn-A: Al<sub>2</sub>O<sub>3</sub> modified with Mn, and La-A: Al<sub>2</sub>O<sub>3</sub> modified with Lanthanum), Y the Cu precursor (N: Cu(NO<sub>3</sub>)<sub>2</sub> 3H<sub>2</sub>O, C: CuCl<sub>2</sub>H<sub>2</sub>O, O: CuO, and S: Cu(SO<sub>4</sub>)<sub>2</sub>5H<sub>2</sub>O), and T the temperature of calcination (400, 650, or 900°C).

The colorimetric method 5530-D was used to quantify the remaining phenol, proposed by Standard Methods for the examination of water and wastewater using a Cole Parmer 1100 Spectrophotometer. Total organic carbon (TOC) was determined according to ISO 8245 (1999). The copper composition of the catalysts was determined by atomic absorption spectroscopy (AAS).

The catalytic assays were carried out in a glass vessel with continuous stirring and subjected to reflux. 100 ml of 1000 ppm phenol solution was heated up to 70°C, and 100 mg of catalyst was added. Then, the peroxide 100 vol (10 ml) was also added; this moment was considered the beginning of the reaction (*t*<sub>0</sub>).

### Results and Discussion

All catalysts allowed complete phenol conversion within the first minutes of the reaction (between 5 and 25 minutes). Except for the Cu-N/Mn-A-900 catalyst, the other catalysts allowed good mineralization (equal to or greater than 86%). Table 1 summarizes the TOC conversion values after each phenol oxidation reaction with the different catalysts prepared.

The increase of the calcination temperature, both for the catalyst prepared on the unmodified support and modified with La or Mn, allowed a lower loss of catalytic material (less Cu leached) after the 2 h of reaction. For catalysts prepared on unmodified alumina, XPS showed that increasing the calcination temperature generated surface Cu species capable of acting as active sites and with greater resistance to leaching. Regarding the catalysts prepared on the supports modified with La or Mn, for the 3 temperatures it was observed that the presence of both La or Mn promotes a better anchorage of Cu, decreasing the leaching of the active material. Particularly, for the case of the Cu-N-Mn-A-900 catalyst, the abrupt decrease in TOC conversion was associated, in the first instance, with the low-leached copper loading that inhibited the homogeneous phase reaction. On the other hand, by XRD it was seen that the presence of Mn promotes the phase transformation of the support (from gamma- to alpha-alumina) with a considerable decrease of the specific area and consequent decrease of the catalytic performance. Finally, no significant influence of the copper precursor on either variable (both leached copper and TOC conversion) was observed.

Table 1. Phenol and TOC conversion, and leached Cu %.

Catalyst	Leached Cu, %	TOC conversion, %
Cu-N/A-400	64	90
Cu-N/A-650	60	91
Cu-N/A-900	36	86
Cu-N/La-A-400	53	96
Cu-N/La-A-650	53	98
Cu-N/La-A-900	25	86
Cu-N/Mn-A-400	35	96
Cu-N/Mn-A-650	29	94
Cu-N/Mn-A-900	11	56
Cu-O/A-900	40	86
Cu-C/A-900	42	89
Cu-S/A-900	34	86

### Significance or Main Conclusions

Cu-based catalysts show very good performance in the removal of phenol from water by AOPs. A strong influence of their preparation on both catalytic performance and leaching of the active material was observed. An increase in the calcination temperature improves the anchorage of Cu on the support, being further improved by the addition of La or Mn to it.

### References

- [1] A.Septian, A.Venugopal, N.Kumar, A.Sivasankar, J.Choi, I.Hwang, W.Shin. Journal of Hazardous Materials 414 (2021) 125474-125486

## Selective production of 1,2-propanediol by glycerol hydrogenolysis using Cu/Zn/MgAl as catalysts

Matías G. Rinaudo<sup>1\*</sup>, Naila Gómez González<sup>1</sup>, María K. López<sup>1</sup>, Luis E. Cadus<sup>1</sup>, José López Nieto<sup>2</sup>, Marcelo E. Domíne<sup>2</sup>, María R. Morales<sup>1</sup>.

<sup>1</sup>INTEQUI -UNSL Almirante Brown 1455, San Luis 5700 (Argentina)

<sup>2</sup> UPV-CSIC, Avda. de los Naranjos s/n, Valencia46022, (Spain)

\*matirinaudo@gmail.com

### Introduction

Glycerol (GLY) hydrogenolysis is a reaction sensitive to the structure of the catalyst. The main products obtained are acetol, 1,3-propanediol (1,3-PDO) and 1,2-propanediol (1,2-PDO), where the selective production of any of them depends on acid-base features of media and/or catalyst surface and metal-support interactions [1]. In general, supports give acid-base features needed in the reaction while metal sites provide the bond-breaking capacity. This work proposes to evaluate the effect of modifying the acid character of alumina by adding oxides with different acid-base features (MgO and/or ZnO) and thus the interaction of Cu with obtained supports in the selectivity of GLY hydrogenolysis.

### Materials and Methods

Mg-Al<sub>2</sub>O<sub>3</sub> was synthesized according to the method reported by Nuñez et al. [2]. Ultrasound-assisted impregnation was then used to add 10 wt% ZnO and 5 wt% Cu, obtaining the supports MgAl and ZnMgAl; and respective catalysts Cu/MgAl and Cu/ZnMgAl. All systems were characterized by S<sub>BET</sub>, ICP, EPR and isopropanol (2-POH) decomposition test. Each catalyst was reduced and tested under three different reaction conditions: (a) 220 °C; 20 bar H<sub>2</sub> and 0.1 g cat.; (b) 250 °C; 30 bar H<sub>2</sub> and 0.1 g cat. and (c) 250 °C; 30 bar H<sub>2</sub> and 0.2 g cat.

### Results and Discussion

Catalysts were evaluated under GLY hydrogenolysis (Figure 1A), leading to acetol and 1,2-PDO as the only reaction products. Under condition (a), low conversion and selectivity to acetol were achieved but a high selectivity to 1,2-PDO. When increasing temperature and H<sub>2</sub> pressure at condition (b), selectivity was not affected but conversion duplicated, particularly in case of Cu/ZnMgAl. Furthermore, the increase in catalyst mass at condition (c), increased both conversion and selectivity to 1,2-PDO. Cu/ZnMgAl catalyst showed the highest conversion (66%) and selectivity to 1,2-PDO (99%). It has been reported that Cu/Al<sub>2</sub>O<sub>3</sub> catalysts are selective in the production of 1,2-PDO (57%) through acetol hydrogenation, where Al sites (acidic) participate in dehydration step and Cu metal sites in hydrogenation step [3]. In our case, Al<sub>2</sub>O<sub>3</sub> modification by different oxides and a metal with basic character such as Cu, favored its catalytic behavior. Moreover, surface acid-base changes were studied by 2-POH decomposition test (Figure 1B) [4]. Mg and/or Zn incorporation to Al<sub>2</sub>O<sub>3</sub> increased the total number of sites (conversion). The presence of Mg also reduced the acidic character of alumina, while both Zn and Mg generated a completely basic surface. On the other hand, Cu seemed to increase surface basicity. Cu/ZnMgAl showed the highest number of total sites/basic sites

ratio, which could be one of the reasons of its best catalytic performance. EPR was used to investigate the dispersion of Cu<sup>2+</sup> species on the supports. We could observe axially symmetric signals from Cu 1/2 nuclear spin, which means that catalysts have a parallel ( $g_{\parallel}=2.33$ ) and a perpendicular ( $g_{\perp}=2.05$ ) component. Spectra showed a clear presence of hyperfine parallel signals of isolated Cu<sup>2+</sup> species. These components were wider in case of Cu/MgAl, which could be associated to dipole-dipole magnetic interactions with close Cu<sup>2+</sup> species, indicating the aggregation of local species of Cu (bigger sizes and lower dispersion of Cu domains). On the contrary, in case of Cu/ZnMgAl these signals were narrower, indicating smaller and more disperse Cu domains, contributing to the higher conversion and selectivity observed for this catalyst. Additionally, S<sub>BET</sub> values of Cu/MgAl and Cu/ZnMgAl diminished in the range 25-35% respect to the specific surface area of commercial alumina, which could be attributed to thermal treatments applied during synthesis. In addition, Cu experimental amounts were in all cases close to the theoretical value (5 wt%).

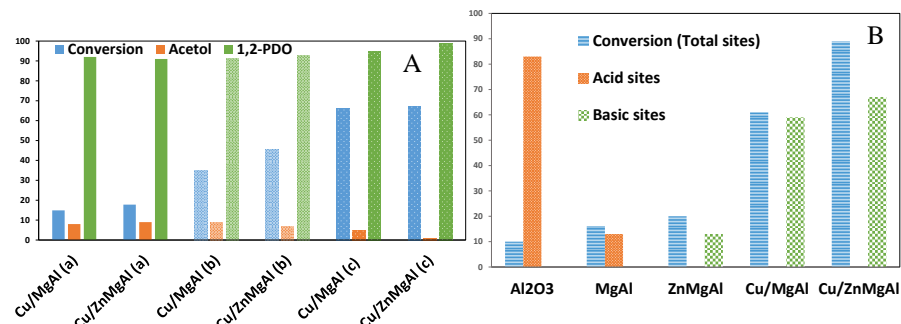


Figure 1. A: Catalytic test and B: 2-POH decomposition test

### Main Conclusions

Cu/ZnMgAl showed a 99% selectivity to 1,2-PDO as a result of its higher basic character, provoked by the incorporation of Zn and Mg to the support, and its higher metal dispersion in smaller metal domains associated to the presence of ZnO.

### References

- [1] J. Beltrán-Prieto, K. Kolomožník, J. Pecha; Australian Journal of Chemistry 66 (2013) 511.
- [2] M. Nuñez, A. Hernández, L. Cadús, F. Agüero; International Journal of Hydrogen Energy 48 (2023) 1337.
- [3] P. Hirunsit, C. Luadthong, K. Faungnawakij; RSC Advances 5 (2015) 11188.
- [4] A. Gervasini, J. Fenyesi, A. Auroux; Catalysis Letters 43 (1997) 219.



## Cu/carbon xerogel catalysts for glycerol selective oxidation reaction

Naila Gómez González<sup>1\*</sup>, Samantha L. Flores<sup>2</sup>, Ana Arenillas<sup>2</sup>, Matías G. Rinaudo<sup>1</sup>, Luis E. Cadus<sup>1</sup> and María R. Morales<sup>1</sup>

<sup>1</sup>INTEQUI-UNSL, Almirante Brown 1455, San Luis 5700 (Argentina)

<sup>2</sup> INCAR-CSIC, Francisco Pintado Fe, 26. 33011 Oviedo (Spain)

\*naila.gomez.gonzalez@gmail.com

### Introduction

Glycerol (GLY) catalytic oxidation is one of the proposed ways to valorize this industrial by-product into high value-added products such as lactic acid (LA) and glyceric acid (GA) [1]. In case of supported catalysts, carbon materials have been widely studied as support, due to their multiple advantages, such as large specific surface area and the possibility to modify the oxygenated functional groups (OFG) present on their surfaces, which can become the active phase in several reactions [2]. Good catalytic performance has been obtained over noble metals [3] while the addition of Cu has been studied to reduce costs. In the present work two carbon xerogels supports with and without Cu were synthesized, characterized and evaluated under glycerol selective oxidation.

### Materials and Methods

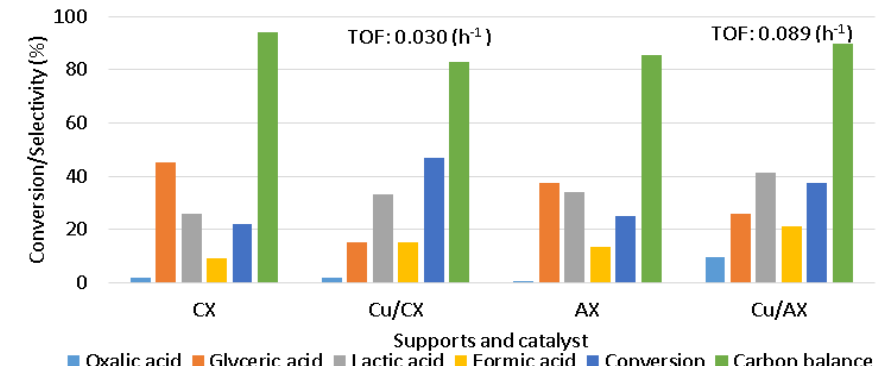
Two carbon xerogels supports were obtained by carbonization at 1000 °C of an organic resorcinol-formaldehyde (RF) gel under two different atmospheres: N<sub>2</sub> (CX) and CO<sub>2</sub> (AX). The Cu precursor was deposited on the xerogels by ultrasound-assisted rotaevaporation impregnation to achieve 3 wt% Cu. The catalysts were named: Cu/CX and Cu/AX. They were characterized by S<sub>BET</sub>, XRD, isopropanol (2-POH) decomposition test, ICP-MS and dissociative chemisorption of N<sub>2</sub>O. The catalytic tests were performed in a Parr-type reactor pressurized with oxygen at 2.5 bar, a constant temperature of 90 °C and 1000 rpm of stirring for 3 h. The reaction products were identified and quantified by HPLC-DAD using an Aminex HPX-87H column.

### Results and Discussion

Different carbonization treatments of the organic gel can lead to structural differences in the carbon xerogels. S<sub>BET</sub> values obtained for CX and AX supports were 607 m<sup>2</sup>/g and 1482 m<sup>2</sup>/g respectively. The use of CO<sub>2</sub> as an activating agent could promote the creation of defects, reaching a higher porosity in AX support than in CX [4]. Cu impregnation decreased the specific surface area in a 15% for Cu/CX and a 9.7% for Cu/AX. The diffractograms obtained for the supports were typical of carbon materials. Diffraction lines corresponding to Cu° (PDF 00-003-1005) were identified on both catalysts and associated to the self-reduction capacity of copper oxide due to the presence of OFG. In Cu/AX catalyst, low-intensity diffraction lines corresponding to CuO species (PDF 00-002-1041) were also identified.

Cu/CX showed a greater amount of highly distributed small Cu domains (dp:1.4 nm – D:73%), compared to Cu/AX (dp:1.8 nm – D:55%) according to the results obtained by N<sub>2</sub>O dissociative chemisorption. The surface acid-base features of supports and catalysts were determined by 2-POH decomposition test. Supports presented an acidic surface and followed a decreasing trend: CX >AX. In contrast, catalysts had a basic surface due to the incorporation

of copper. The metal amount showed the order: Cu/AX (2.2% Cu at. by ICP) >Cu/CX (1.7 Cu at. by ICP). Both catalysts were selective in the production of LA and GA, but particularly for LA (Figure 1). On the contrary, xerogel supports showed a higher selectivity to GA, which could be attributed to the acidic OFG present on their surfaces.



This behavior was associated to the basic surface of the catalysts due to the presence of Cu, promoting the obtention of LA [5]. Turnover Frequency (TOF) values (Figure 1) were in line with the total number of acid-base sites, indicating the strong effect of the acid-base surface features. Furthermore, larger Cu metal domains were more efficient than smaller domains [6]. In addition, Cu<sup>+</sup> and Cu<sup>0</sup> species in Cu/CX could favor conversion and selectivity to LA; whereas large CuO particles in Cu/AX inhibited an increase in GA selectivity, in line with the observations of Zhang et al. [7].

### Main Conclusions

Carbon xerogels supports, both with acidic character, showed higher selectivity to GA in accordance with the amount of total acid-base sites (CX >AX). The addition of Cu increased the basic character of the catalysts and thus directed the reaction towards LA formation. Even though metallic copper phase increases the conversion of the reaction, OFG present on both supports could also act as active sites for glycerol selective oxidation, which may represent an advantage for an industrial scale.

### References

- [1] M. Douthwaite, N. Powell, A. Taylor; ChemCatChem 12 (2020) 107.
- [2] F. Rodríguez-Reinoso; Carbon 36 (1998) 159.
- [3] C. Zhou, J. Beltramini, C. Linet; Catalysis Science and Technology 1 (2011) 111.
- [4] A. ElKhatat, S. Al-Muhtaseb; Advanced Materials 23 (2011) 2887.
- [5] B. Morales, B. Quesada; Catalysis Today 372 (2021) 115.
- [6] N. Dimitratos, J. Lopez-Sánchez, D. Lennon; Catalysis Letters 108 (2006) 147.
- [7] C. Zhang, T. Wang, X. Liu, Y. Ding; Journal of Molecular Catalysis 424 (2016) 91.



## Oxidation advanced processes for dairy phage inactivation

Maria Fiorella Jacob<sup>1\*</sup>, Mariángel Briggiler Marcó<sup>1</sup>, Orlando Mario Alfano<sup>2</sup>, Andrea del Luján Quibroni<sup>1</sup> and María de los Milagros Ballari<sup>2</sup>

<sup>1</sup>INLAIN (UNL – CONICET), Santiago del Estero 2829, Santa Fe 3000 (Argentina)

<sup>2</sup>INTEC (UNL – CONICET) Ruta Nacional No. 168, Santa Fe 3000 (Argentina)

\*fjacob@fiq.unl.edu.ar

### Introduction

Phages infections constitute the main cause of failure of starter cultures during fermented dairy products manufacturing, and can lead to significant technological difficulties and economic losses. Bioaerosols constitute the main dissemination via of phages in industrial environments [1].

The aim of this work was to study diverse oxidation advanced processes as an alternative to reduce the phage concentration in the surface/air.

### Materials and Methods

The following assays were performed in a laboratory scale reactor constituted by two separate compartments, an emission source constituted by seven lamps and an irradiation chamber where phage suspensions were placed for irradiation:

**Photocatalytic paints:** phage suspensions were deposited and dried on the coated plates with photocatalytic paints (0.71 mg modified carbon doped TiO<sub>2</sub> anatase/cm<sup>2</sup>). Inactivation assays were performed for sixteen phages, with a total time of 20 h at 30°C and 80% RH under radiation typically used for indoor illumination ( $\lambda = 360 - 720$  nm) [2].

**Photocatalysis (TiO<sub>2</sub>, UV-A):** drops of phage particles were deposited on plates coated with TiO<sub>2</sub> (0.02 mg/cm<sup>2</sup>). Inactivation assays were performed for seventeen phages under UV-A radiation ( $\lambda = 200 - 400$  nm), for a period of 3 h at 40°C and 89.5% RH [3].

Afterwards, assays were performed in a semi-pilot reactor in order to analyze the inactivation efficiencies in air. The reactor is a close system with recirculation constituted by a chamber where phage particles were nebulized for a total time of 30 min using the 6-jet Collison nebulizer and a photocatalytic reactor with the UV emission system (20 lamps). An axial fan provided a forced air circulation coming from the chamber and a polypropylene tube connected the exit of the photocatalytic reactor with the chamber, allowing phage recirculation. Assays were performed for four phages under UV-A radiation ( $\lambda = 200 - 400$  nm) and presence of photocatalyst (1.77 mg TiO<sub>2</sub>/cm<sup>2</sup>) for a total time of 100 min [1].

For all assays, borosilicate glass plates were used to deposit the catalyst. Phage inactivation as function of time (Log PFU/mL vs time) was evaluated and photonic and quantum inactivation efficiencies were calculated, that is the relations of the inactivation rate per the incident radiation flux and per the rate of absorbed radiation, respectively.

### Results and Discussion

**Photocatalytic paints:** eight phages were completely inactivated within 1.5 and 5 h of treatment, reaching reductions higher than 2.79 log orders, whereas other eight phages reduced their infectivity between 2.33 and 5.88 log orders, within 4 and 20 h. Photonic

efficiencies ranged from  $2.84 \times 10^9$  to  $4.06 \times 10^{12}$  PFU/Einstein and quantum efficiencies ranged from  $6.40 \times 10^9$  to  $9.17 \times 10^{12}$  PFU/Einstein.

**Photocatalysis (TiO<sub>2</sub>, UV-A):** some phages were completely inactivated after 60 - 120 min of treatment, while others maintained their infectivity even after 180 min. Photonic efficiencies ranged from  $3.63 \times 10^9$  to  $4.82 \times 10^{10}$  PFU/Einstein and quantum efficiencies ranged from  $1.03 \times 10^{11}$  to  $1.37 \times 10^{12}$  PFU/Einstein.

**Photocatalytic treatments to airborne phages:** three phages were completely inactivated within 100 min of treatment whereas one was partially inactivated under the same condition. Photonic efficiencies ranged from  $7.65 \times 10^6$  to  $1.59 \times 10^7$  PFU/Einstein and quantum efficiencies ranged from  $2.66 \times 10^7$  to  $5.53 \times 10^7$  PFU/Einstein.

Figure 1 shows the inactivation as a function of time for phage MLC-A using diverse technologies.

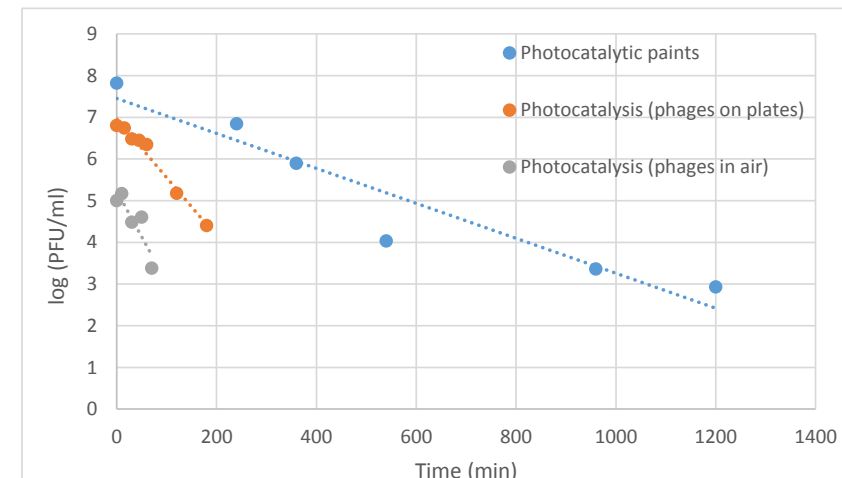


Figure 1. Phage MLC-A inactivation as a function of time using diverse technologies.

### Significance or Main Conclusions

The results obtained demonstrated a phage dependent behavior and the feasibility of oxidation advanced processes (photocatalysis and photocatalytic paints) as simple methodologies that could complement those habitually applied in laboratories and industrial plants handling lactic acid bacteria, in order to reduce the frequency of phage attacks.

### References

- [1] M. Briggiler Marcó et al.; J. Photochem. Photobiol. A Chem. 409 (2021) 987-993.
- [2] S. Zacarías et al.; J. Photochem. Photobiol. A Chem. 364 (2018) 76-87.
- [3] M. Briggiler Marcó et al.; Chem. Eng. J. 172 (2011) 987-993.

## Kinetic Modeling of the Degradation of Water Pollutants in a Photocatalytic Microreactor

Maria L. Satuf<sup>1\*</sup>, Ana.L. Eusebi<sup>1</sup>, Claudio L.A. Berli<sup>1</sup>, Marcela V. Martin<sup>1</sup>

<sup>1</sup>INTEC (UNL-CONICET), Predio CCT CONICET Santa Fe, Santa Fe 3000 (Argentina)

\*mlsatuf@santafe-conicet.gov.ar

### Introduction

Kinetic studies provide essential information to design efficient photocatalytic devices. Nevertheless, reliable parameters are difficult to obtain in conventional reactors. Alternatively, microreactors provide an excellent platform for photocatalytic kinetic studies: laminar flow, short molecular diffusion distances, uniform irradiation, large surface to volume ratio, and accurate control of operation variables. Additionally, small amounts of catalysts and reagents are needed, and results can be obtained employing short assay times. In this study, we present a simple method for obtaining kinetic parameters of the degradation of binary mixtures of pollutants in a photocatalytic microreactor. The degradation of the synthetic hormone 17- $\alpha$ -ethynodiol (EE2) was evaluated in the presence of different amounts of phenol.

### Materials and Methods

Photocatalytic degradation experiments were carried out in a planar, continuous flow microreactor (Fig 1), with an irradiated reactor volume  $V_R$  of 209  $\mu\text{L}$ . The reactor window is a borosilicate glass plate, which was used as support to immobilize the photocatalyst. The reaction chamber was designed to achieve uniform fields of both velocity and radiation throughout the flow domain, as well as negligible diffusive limitations [1].

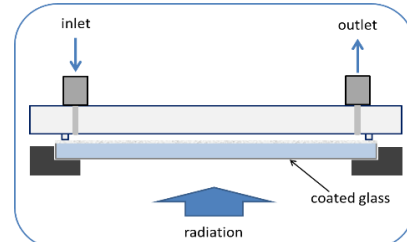


Figure 1. Scheme of the microreactor cross-section.

The photocatalyst, 0.1 % Pd-TiO<sub>2</sub> synthesized by sol-gel method, was immobilized on the glass plate by the dip-coating procedure. [2]. The film thickness was (250 ± 50) nm. Illumination was provided by a solar simulator. The radiation flux incident at the photocatalytic film was 1.04 mW/cm<sup>2</sup> between 300 and 400 nm. Experiments were carried out employing EE2 aqueous solutions at an inlet concentration of 10  $\mu\text{M}$  and two different inlet concentrations of phenol: 50  $\mu\text{M}$  and 25  $\mu\text{M}$ . The flow rates Q used were 40-200  $\mu\text{L}/\text{min}$ . Quantification of the pollutants was carried out by HPLC.

### Results and Discussion

The rate of disappearance of the EE2 is assumed to follow a first-order kinetics with respect to the concentration  $C_i$  [2]. Thus, the volumetric rate of photocatalytic degradation in the reaction cell can be expressed as  $r_i = -k_{a,i}C_i$ , where the apparent reaction rate constant is  $k_{a,i}$ .

The microreactor was designed to work in the operating zone where the characteristic diffusion time is shorter than both residence and kinetic times [1]. The reactant concentration changes principally along the flow direction. For first order kinetics, and considering  $C_{0,i}$  and  $C_{L,i}$  as the reactant concentration at the reactor inlet and outlet, respectively, the variation of the average reactant concentration through the reaction cell results,  $C_{L,i}/C_{0,i} = \exp(-k_{a,i}V_R/Q)$ . This expression quantitatively predicts the conversion as a function of the operating flow rate, for a given kinetic constant. The conversion is controlled by the interplay between the residence time ( $V_R/Q$ ) and the characteristic reaction time ( $1/k_{a,i}$ ). In practice, plots of  $Q/V_R$  vs  $1/\ln(C_{0,i}/C_{L,i})$  allow one to obtain the apparent rate constant  $k_{a,i}$  from the curve slope.

The reactor also enables monitoring the simultaneous degradation of two compounds (i=1,2). In our experiments, we observed that each reactant still follows a pseudo-first-order kinetics, with a kinetic constant  $k_{a,i}^*$  always lower than  $k_{a,i}$ . Therefore, in order to assess the kinetic response of the binary systems, we followed the approach suggested by Turchi and Ollis [3]. Actually, the degradation of the reactants in the mixture is expected to obey the Langmuir-Hinshelwood model, including the effect of the other reactant and the intermediate compounds:  $r_i = -k_{a,i}C_i/(1 + \sum K_i C_i)$ . Nevertheless, if parameters  $K_i$  of the intermediate compounds are fairly similar, they can be simplified to a single constant, and the expressions of the apparent kinetic constants for compounds 1 and 2 in the mixture result, respectively,  $k_{a,1}^* = k_{a,1}/(1 + K_2 C_{0,2})$  and  $k_{a,2}^* = k_{a,2}/(1 + K_1 C_{0,1})$ . In these expressions, the inlet concentration of the companion reactant sums up the influence of all the related intermediates. This approach not only simplifies calculations but also provides easy interpretation of the effects of the governing parameters of the system. The estimated kinetic parameters are presented in Table 1.

Table 1. Kinetic parameters

Compound	i	$k_{a,i} (\text{min}^{-1})$	$K_i (\mu\text{M}^{-1})$
EE2	1	$0.68 \pm 0.02$	0.15
Phenol	2	$0.43 \pm 0.03$	0.028

### Main Conclusions

This work proposes a simple method to analyze the photocatalytic degradation behavior of binary mixtures. Under our experimental conditions, a simplified L-H rate form was adequate to represent the system kinetics. The data processing involves a straightforward linear analysis and thus avoids the implementation of demanding numerical simulations.

### References

- [1] M.L. Satuf, J. Macagno, A. Manassero, G. Bernal, P.A. Kler, C.L.A. Berli; Appl. Catal. B: Environmental 241 (2019) 8-17.
- [2] M.V. Martin, L. Rossi, J.A. Rosso, P.I. Villabril, O.M. Alfano, M.L. Satuf; Photochem. Photobiol. Sci. 22 (2023) 47-58.
- [3] C.S. Turchi, D.F. Ollis; J. Catal. 119 (1989) 483-496.